2007년 2월
박사학위논문

The effect of DNA repair system on the oxidative stress-mediated apoptosis.

조선대학교 대학원

생물신소재학과

윤 차 경

The effect of DNA repair system on the oxidative stress-mediated apoptosis.

DNA 수복효소가 산화성 스트레스에 의한
세포 사멸사에 미치는 영향

2007년 2 월 일

조선대학교 대학원

생물신소재학과

윤 차 경

The effect of DNA repair system on the oxidative stress-mediated apoptosis.

지도교수 유 호 진

이 논문을 이학박사 학위신청논문으로 제출함.

2006 년 10 월 일

조선대학교 대학원

생물신소재학과

윤 차 경

윤 차 경의 박사학위논문을 인준함

위원장 조선 대학교 교수 장 인 엽 인

위 원 조선 대학교 교수 유 호 진 인

위 원 조선 대학교 교수 전 제 열 인

위 원 조선 대학교 교수 전 영 진 인

위 원 조선 대학교 교수 최 석 인

2006 년 12 월 일

조선대학교 대학원

CONTENTS

RESULTS

Ⅰ. hOGG1-deficient fibroblasts undergo p53-dependent oxidative stress-induced apoptosis

Ⅱ. hMTH1 knockdown by small interfering RNA increases oxidative stress-induced cell death and chromosomal instability in human fibroblast GM00637 cells

CONTENTS OF FIGURES

Ⅰ. hOGG1-deficient fibroblasts undergo p53-dependent oxidative stress-induced apoptosis

Ⅱ. hMTH1 knockdown by small interfering RNA increases oxidative stress-induced cell death and chromosomal instability in human fibroblast GM00637 cells

ABSTRACT

The effect of DNA repair system on the oxidative stress-mediated apoptosis.

Youn Cha-Kyung
Advisor : Prof. Ho Jin You Ph.D.
Department of Bio material Engineering
Graduate School of Chosun University

Ⅰ. hOGG1-deficient fibroblasts undergo p53-dependent oxidative stress-induced apoptosis

Human 8-oxoguanine DNA glycosylase (hOGG1) is the main defense enzyme against the mutagenic effects of cellular 8-oxoG. In this study, we investigated the biological role of hOGG1 in response to H_2O_2-derived oxidative stress in human fibroblast GM00637 cells. A large proportion of hOGG1 silencing cells, which were generated by stably introducing small interfering RNA (siRNA), led to a significant increase in apoptotic cell death through the activation of p53-mediated apoptotic pathway, and a range of genomic instability of human fibroblasts in response to H_2O_2 exposure. The hOGG1-depleted cells

lacking p53 did not undergo apoptosis upon treatment with similar H_2O_2 concentrations. The p53-siRNA transfection markedly inhibited the activation of p21, Noxa and caspase-3/7, which were significantly induced by H_2O_2 treatment, resulting in the increased cell viability in hOGG1-deficient cells. The overexpression of p53 in p53-deficient H1299 cells lacking hOGG1 by siRNA transfection significantly caused in the decrease of their cell viability in a H_2O_2 dose dependent manner. The overexpression of hOGG1 in GM00637 resulted a significant increase in the cell viability and a decrease in p53 phosphorylation upon exposure to H_2O_2. These results indicate that hOGG1 plays an important role in protecting cells against p53-mediated apoptosis, and maintaining the genomic stability in response to H_2O_2-induced oxidative stress.

Ⅱ. hMTH1 knockdown by small interfering RNA increases oxidative stress-induced cell death and chromosomal instability in human fibroblast GM00637 cells

Human MTH1 (hMTH1) exhibits oxidized purine nucleotide triphosphatase activity, which repairs oxidized forms of dGTP such as 8-oxo-2′-deoxyguanosine 5′-triphosphate (8-oxo-dGTP) and 2-hydroxy-2′-deoxyadenosine 5′-triphosphate (2-OH-dATP). In this study, we investigated the biological role of hMTH1 in response to H_2O_2-derived oxidative stress using hMTH1-depleted GM00637 cells, which were generated by stably introducing hMTH1-siRNA. The hMTH1 deficient cells caused a significant increase in apoptotic cell death through the activation of p53-mediated apoptotic pathway in response to H_2O_2-oxidative stress. The level of H_2O_2-induced Noxa expression and H2AX phosphorylation (γ-H2AX) was significantly higher in hMTH1 deficient cells than in hMTH1 proficient cells. The cells lacking Noxa and p53 did not undergo cell death in response to the

similar H_2O_2 concentration in hMTH1-depleted cells. Apoptosis of the hMTH1-depleted cells associated with Noxa expression is dependent on p53 phosphorylation. Furthermore, the ablation of hMTH1 protein by hMTH1-siRNA occurred over a range of genomic instability of human fibroblasts in response to H_2O_2-oxidative stress. After the long term culture of the hMTH1-depleted cells, increased intracellular ROS generation and apoptosis. These results suggest that hMTH1 plays an important role in protecting cells against oxidative stress and maintaining the genomic stability caused by H_2O_2-induced DNA damage.

INTRODUCTION

DNA lesions are constantly produced in living cells by the deleterious actions of both endogenous and environmental DNA-damaging agents. In normal cells, several DNA repair pathways remove these lesions to maintain the genomic integrity. According to the class of lesions, two major excision repair pathways are acting in the cell : (i) the nucleotide excision repair(NER) able to detect and remove bulky DNA adducts(like the UV-induced lesions) and (ii) the base excision repair (BER) able to detect and repair non-helix-distorting DNA lesions (like base modifications).

8-Oxoguanine (8-oxoG) is formed by oxidation of the guanine residue by various oxidizing agents such as ionizing radiations, UVA or reactive oxygen species produced through normal oxygen metabolism. 8-Oxoguanine (8-oxoG) is a major oxidized base found in DNA due to endogenous or exogenous pro-oxidant agents. In the absence of repair, this lesion has a high mutation potency giving rise mainly to G;C to A:T transversions. 8-oxoG can pair either with a cytosine(in the anti-conformation) or with an adenine (in the syn-conformation) (Fig1) but disorganization of base pairing in neigh-bouring sequences has been described (1, 2). During replication, DNA polymerases, such as polymerase delta or the translesional polymerase eta, can easily incorporate A opposite 8-oxoG. Thus 8-oxoG is a strong premutagenic DNA lesion in the absence of full repair capacities (3, 4). It's repair deficiency leads to specific G:C to T:A transversions. Indeed, there are three different mechanisms to ensure 8-oxoG detection and removal in human cells (Fig2). The glycosylase hOGG1 removes 8-oxoG when paired with a cytosine through the BER pathway (5) and the glycosylase hMYH remove adenine when mispaired with 8-oxoG, also through BER(6). The hMTH1 gene product is able to sanitize the pool of dGTP(7) from contaminaing 8-oxodGTP. These three pathways are conserved from bacteria to humans (Fig.2).

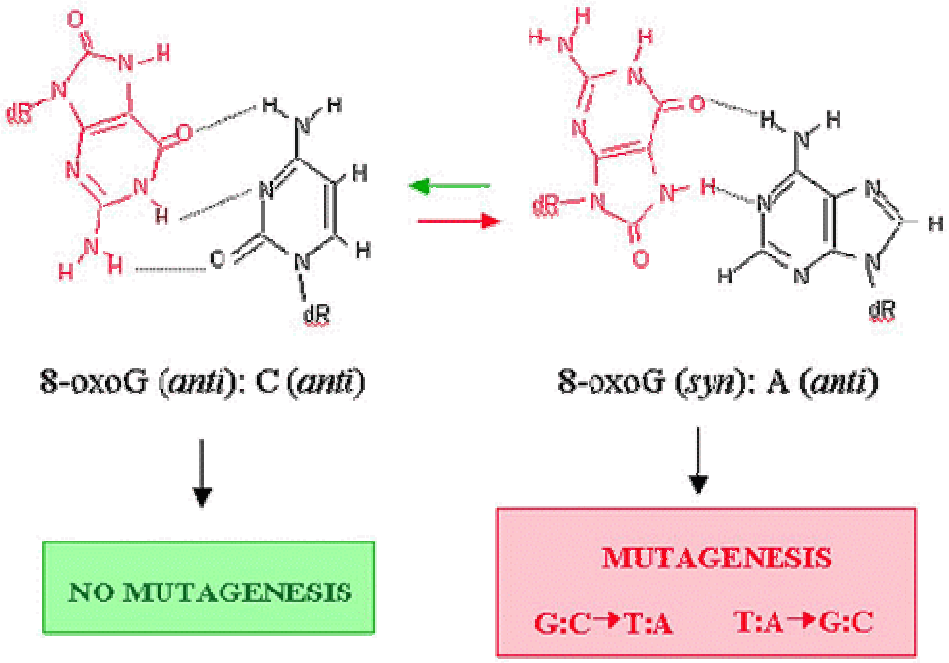

Fig.1. **Structure of 8-oxoG base pairs**. 8-oxoG can pair with C in an anti-conformation or with A in a syn-conformation. Replication of 8-oxoG paired with C by DNA polymerases is a non-mutagenic process. Replication of 8-oxoG paired with A results in GC to TA or TA to GC transversions

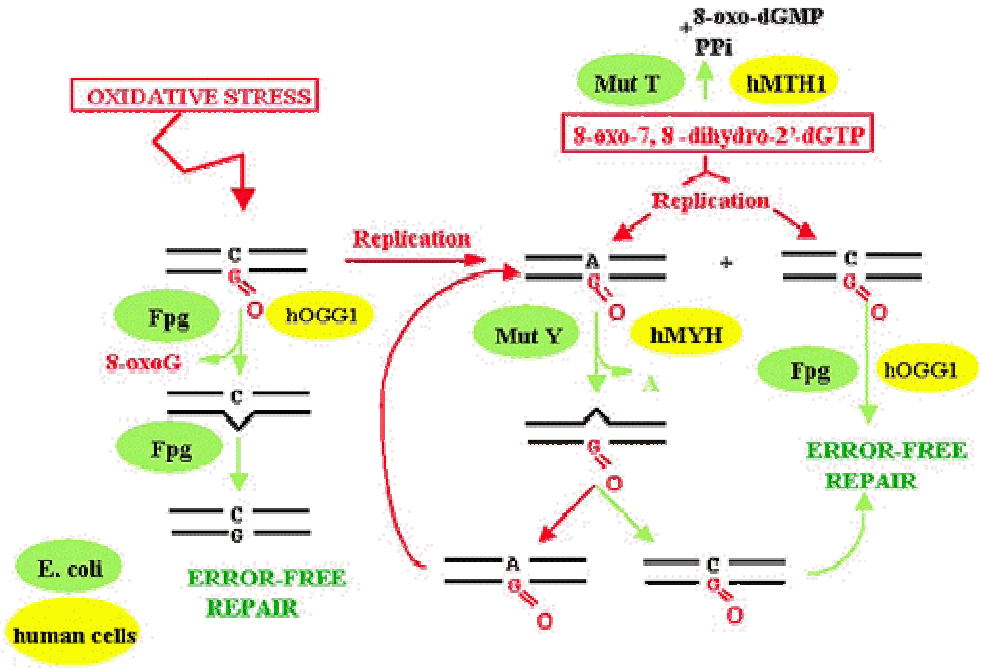

Fig.2. Major pathway for 8-oxoG repair in the global genome. Proteins from bacteria are represented in green. Proteins from humans are represented in yellow. Presence of 8-oxoG in DNA can be due to direct attack of DNA structure of to the oxidation of the pool of guanine nucleotides. In the first case, the lesion can be repaired by Fpg/hOGG1 in a base excision error-free manner. If replication takes place before repairing, 8-oxoG can pair with C and then be repaired by Fpg/hOGG1. When replication machinery incorporates A opposite to 8-oxoG, this mispair is recognized by MutY/hMYH that will excise A, and then A or C can be incorporated. Oxidized guanines from the nucleotide pool can be sanitized by MutT/hMTH1.

Reactive oxygen species(ROS) can damage biomolecules and have been postulated as an important cause of aging, cancer, and various human degenerative diseases(8, 9). The increased amount of ROS in cancer cells may have significant consequenes, such as stimulation of cellular proliferation, promotion of mutations and genetic instability, and alteration in cellular sensitivity to anticancer agents. ROS-mediated DNA lesions and mutations are likely to provide a mechanism through which drug-resistant variants constantly evolve. However, because ROS are chemically active and can inflict severe cellular damage, the very fact that cancer cells are under increased intrinsic ROS stress may also provide a unique opportunity to kill the malignant cells based on their vulnerability to further ROS insults. As such, this biochemical characteristic is likely to have significant therapeutic implicantions. In biological systems, ROS are constantly generated through a variety of pathways, including both enzyme-catalyzed reactions and non-enzyme reactions. During oxidative phosphorylation in mitochondria, electrons are delivered through the respiratory chain, and a proton gradient is established across the inner mitochondrial membrane as energy source for ATP synthesis. One important biochemical event associated with this metabolic process is the production of superoxide. Some electrons may escape from the mitochondrial electron transport chain, especially from complexes I and III, and react with molecular oxygen to form superoxide (10,11,12). It is estimated that about 2% of the oxygen consumed by the mitochondria is reduced by the bifurcated electrons to form superoxide, which is subsequently converted to hydrogen peroxide (13). Because superoxide radicals are constantly generated during respiration and can be converted to H_2O_2 and other reactive oxygen species, mitochondria are considered the major source of cellular ROS(14,15), and are likely to play a significant role in ROS stress in cancer cells. In addition, ROS can also be produced by a family of membrane-bound enzymes such as NAD(P)H oxidases, which seem to affect cell proliferation and apoptosis(16, 17). Induction of gene mutations by endogenous and exogenous free radicals through ROS-mediated DNA damage has long been recognized(18,19). Damage caused

by ROS is considered the most common type of DNA lesion(20). Due to their reactive chemical nature, ROS are capable of attacking various components of DNA, leading to the generation of a variety of ROS-mediated modified products including oxidized bases , DNA strand breaks, DNA intra-strand adducts, and DNA-protein crosslinks (21, 22). The superoxide radicals generated in mitochondria may cause damage not only to mtDNA, but also to nuclear DNA(nDNA) by their conversion to hydrogen peroxide, which is relatively stable and able to travel to the nucleus. In the presence of iron catalyst, hydrogen peroxide can give rise to hydroxyl radical and cause severe damage to nDNA. Oxidative modifications of the DNA bases may result in mutations, largely due to base pair mismatching during DNA replication across the ROS-modified bases or nucleotide insertion(23,24). It should be noted that compared to nDNA, mtDNA is more susceptible to damage by ROS due to its close proximity to the site of ROS generation, its lack of introns and histones, and limited DNA-repair capabilities in mitochondria(14,25). The ROS-mediated damage to mtDNA may cause malfunction of the respiratory chain and further amplify the generation of ROS, which in turn promote mutatins and genetic instability. It has been hypothesized that in normal cells, DNA damage is balanced by multiple pathways for DNA repair to eliminate the genetic errors, whereas in tumor cells this balance may be shifted such that the increased ROS-mediated damage overwhelms the repair capacity, resulting in the accumulation of multiple mutations(26).

One of the most widely used compounds to produce oxidative stress, both in vitro and in vivo biological studies, is hydrogen peroxide(H_2O_2). Unlike other ROS, H_2O_2 is not charged and is therefore freely diffusible within the cell. It can arise spontaneously or be generated from superoxide by superoxide dismutase. More importantly, in the presence of metal ions such as copper or iron, H_2O_2 can undergo Fenton chemistry and give rise to the potent hydroxyl radical. This radical is extremely reactive and can damage different components of the cell(27). The responses of cultured cells to H_2O_2 vary according to cell

type and are known to be both time- and especially, dose-dependent(28). For example, low concentrations (3-15uM) of H_2O_2 were shown to activate a mitogenic response (29), whereas higher doses can have either cytostatic or cytotoxic effects. It was observed that concentrations ranging from 50-150uM promote DNA damage(30, 31) replicative senescence (32-34), sustained p21 levels, cell cycle arrest, transient elevation of p53 protein (35) , and temporary growth arrest followed by increased resistance to subsequent oxidative stress (29, 36). In contrast, H_2O_2 doses of 200uM and higher were demonstrated to induce apoptosis (37), necrosis (37, 38) , protein oxidation (39), as well as lesions in both nuclear and mitochondrial genomes (30, 31).

DNA damage stresses induce apoptotic cell death as well. Senescence and apoptosis, the two irreversible states of cellular life, were frequently shown to be induced by different doses of the same stress. Senescence is induced at subapoptotic doses, suggesting that more severe DNA damage induces apoptotic response, while less severe one causes cellular senescence(40). It appears that p53 protein stands at the center of the complex signal transduction pathways for DNA damage responses. Activated p53 induces a variety of genes whose products, respectively, functions as an executer in DNA repair, G1 check point(p21), apotosis(BaxI, PIG3, p53AIPI, POX, and Fas ligand), and auto-regulation(MDM2)(41). p53 is activated either directly by the ATM/ATR/DNA-PK kinases or indirectly through Chk2, a kinase activated by ATM, and is also regulated by acetylation/deacetylation at lys382(42). Phosphorylation at Ser15, Thr18, and Ser376, and dephosphorylation at Ser392 has been detected in fibroblasts undergoing replicative senescence. p53 activation is likely involved, since p53 induces several known genes involved in ROS generation. Recently, it was reported that p53-induced senescence and ROS generation are subject to an inhibition by Bcl-xL, suggesting Bcl-xL is involved in the ROS generation pathway(43). ROS disrupts the mitochondrial membrane potential, and therefore, have been proposed as an additional route by which p53 induce apoptosis.(44).

Cells in senescence condition, are typified with high level ROS accumulation, transient p53 activation, and sustained p21 expression, while those in apoptosis condition, were devoid of a significant ROS, prolonged p53 and E2F1 upregulation, and lack of p21. Furthermore, it was demonstrated that ATM/ATR activation is an upstream event required for both ROS accumulation and senescence expression(45).

Accumulation of nuclear and mitochondrial DNA damage is though to be particularly deleterious in cells, which cannot be replaced through cell division. Base excision repair(BER) is the main pathway for the removal of small DNA base modifications, which are generated as products of normal metabolism and accumulate with age in various experimental models(46). mtDNA is believed to be particularly sensitive to oxidative agents due to its proximity to the inner mitochondrial membrane, where oxidants are formed, and to the lack of protective histones(47). In addition , oxidative damage to mtDNA in the heart and brain is inversely related to maximum lifespan of mammals(48), suggesting that accumulation of mtDNA damage plays a causative role in the various disorders that are associated with aging, cancer and neurodegeneration.

Once DNA damage has been generated, it is the role of cellular repair systems to prevents its accumulation. However, studies have shown that aging is associated with a general reduction in DNA repair capacity. Overall nuclear BER activity in whole mouse brain extracts, measured using an in vitro uracil-initiated BER assay, was reduced by 85% in old compared with neonatal mice(49). Overall mitochondrial BER activities in rat cerebral cortices were shown to gradually decline with age, reaching 80% lower activity in 30month old rats compared with 17day old rat embryos. They observed a significant age dependent decrease in uracil, 8-oxoG and 5-OH-C incision activities in the mitochondria of all brain regions, whereas variable patterns of changes were seen in nuclei(50).

Ⅰ. hOGG1-deficient fibroblasts undergo p53-dependent oxidative stress-induced apoptosis.

Various cellular metabolites and exogenous DNA-damaging materials routinely induce cellular DNA damage, which, unless promptly and properly repaired, can cause simple base or more complex changes including deletions, fusions, translocations, or aneuploidy resulting in cancer and a variety of genetic disorders (51).

Cellular responses induced by DNA damage include the activation of several distinct biochemical pathways (52-55). First, various DNA repair enzymes are activated to recognize and eliminate the damage. Second, DNA damage stimulates the specific mechanism related to cell cycle checkpoints that arrest cell cycle progression and aid in cellular survival under most circumstances. Third, apoptosis is stimulated by DNA damage to eliminate heavily damaged or seriously deregulated cells. Although these DNA damage-induced biochemical pathways function independently under certain circumstances, there are extensive interactions between these reactions. For example, the regulatory factors in the checkpoints of cell cycle serve not only to delay the cell cycle but also to mediate DNA repair, both directly and indirectly (53-56). However, the precise mechanisms how to access DNA damage both quantitatively and qualitatively so as to choose between mediating DNA repair and apoptosis are not completely understood.

Reactive oxygen species (ROS) are produced as by-products of cellular metabolism as well as through exposure to ultraviolet (UV), ionizing radiation and environmental carcinogens (57). The ROS react with DNA to produce a myriad of cytotoxic and mutagenic base lesions (57). Among the oxidative lesions, 7,8-dihydro-8-oxoguanine (8-oxoG) is the major base damage produced by ROS (53). Unlike normal guanine, 8-oxoG has the propensity to mispair with adenine during DNA replication and thereby gives rise to G:C to T:A transversion mutations (58). Oxidatively modified bases, such as 8-oxoG, are mainly repaired through the base excision repair pathway (BER), the first steps being

the recognition and excision of the damaged base by a specific DNA glycosylase. The major mammalian enzyme for removing 8-oxoG from DNA is 8-oxoguanine-DNA glycosylase (OGG1), which is a bifunctional enzyme with both 8-oxoG excision activity and weak AP-lyase strand incision activity at the abasic sites (59). Following the excision of 8-oxoG by OGG1, the resultant abasic site is further processed in sequential steps by several enzymes to complete repair (52). The OGG1 plays important roles in eukaryotes by preventing the accumulation of oxidative DNA damage, in the nuclear and mitochondrial both genomes, thereby suppressing carcinogenesis and cell death (60).

The suppression of oxidative DNA repair activity has potential drawbacks; one is that the incomplete repair might result in the accumulation of mutagenic lesions in the cellular DNA. This leads to illness, death of cells and unstoppable excessive cell division resulting in cancer and acceleration of aging process (60, 61). The human OGG1 (hOGG1) gene is found on chromosome 3p26.2, and its allelic deletions in this region frequently occur in a variety of human cancers (59). It is somatically mutated in some cancer cells and is highly polymorphic between human population groups (62). The accumulation of 8-oxoG is likely to increase dramatically in patients with various neurodegenerative diseases such as Parkinson's disease (63), Alzheimer's disease (64) or amyotrophic lateral sclerosis (65), which are associated with the progressive loss of cells. The hOGG1 level was also found to be lower in the orbitofrontal gyrus and the entorhinal cortex in Alzheimer's disease patients than in control cases. The accumulation of 8-oxoG increased in a majority of large motor neurons in the amyotrophic lateral sclerosis cases with decreased hOGG1 expression (64). Furthermore, several reports have shown a correlation between the induction of apoptosis by oxidative stress and the repair of oxidative DNA lesions (66-68). Thus, mutations and deletions in the cellular DNA, which could arise from unrepaired oxidative DNA lesions, have been linked to the development of apoptosis. However, the

exact mechanism by which oxidative stress-mediated DNA damage causes cell death is unknown.

In this study, we investigated the effect of hOGG1 in response to H_2O_2-oxidative stress on DNA damage-related apoptotic responses including changes of apoptotic effector caspase activity, p53 phosphorylation and the expression pattern of its up or downstream proteins, together with genomic DNA stability following oxidative DNA damage in human fibroblasts.

Ⅱ. hMTH1 knockdown by small interfering RNA increases oxidative stress-induced cell death and chromosomal instability in human fibroblast GM00637 cells

Reactive oxygen species (ROS) are produced as a by-product of the cellular metabolism as well as exposure to ultraviolet, ionizing radiation and environmental carcinogens (93). The ROS causes a significant harm to DNA including oxidized bases, abasic (AP) sites, strand breaks and DNA-protein cross-links (93). These oxidative DNA lesions cause either spontaneous mutagenesis or cell death. Hence, ROS have been implicated in various age-related diseases such as cancer and neurodegeneration. Among the oxidative DNA lesions, 8-oxoguanine (8-oxoG) is one of the major base lesions formed after oxidative attack to DNA (94). The 8-oxoG is produced by two distinct pathways such as the incorporation of an oxidized precursor, 8-oxo-dGTP into DNA during DNA synthesis, and the direct oxidation of guanine base in DNA (95). Free guanine nucleotides have been shown to be more susceptible to oxidation than guanine in double-stranded DNA (96), and 8-oxo-dGTP can be incorporated into the nascent strand opposite adenine and cytosine in the template with almost equal efficiency (95, 97). Unlike normal guanine, 8-oxoG preferentially mispairs with adenosine during replication giving rise to G:C to T:A

transversion mutation (98). Because of their persistent generation, relative abundance, and potent mutagenicity, 8-oxoG is believed to be a major source of spontaneous mutagenesis in all aerobic cells.

Escherichia coli(E. coli) contains a GO system to prevent the mutagenic effect of 8-oxoG (99). The bacterial GO system consists of three proteins: MutM (also known as the Fpg protein), a DNA glycosylase/lyase that recognizes 8-oxoG:C and catalyzes the excision of 8-oxoG; MutY, which is a DNA glycosylase that recognizes 8-oxoG:A and catalyzes the excision of A; and MutT, a specific phosphatase that cleaves 8-oxo-dGTP. One of potential drawbacks caused by the suppression of oxidative DNA repair is an incomplete repair, which results in the accumulation of mutagenic lesions in the cellular DNA, leading to illness, cell death, cancer, and accelerated aging (100, 101).

Human MTH1 (hMTH1) gene is a homolog of bacterial MutT protein that is found on chromosome 7p22 (102). hMTH1 efficiently hydrolyzes oxidized dGTP, GTP, dATP and ATP such as 2′-deoxy-8-oxoguanosine triphosphate (8-oxo-dGTP) and 2′-deoxy-2-hydroxyadenosine triphosphate (2-OH-dATP) in nucleotide pools (103). The $mutT^{-}$ mutant strain of E. coli have a significantly higher frequency of a point mutation (104). The expression of hMTH1 in $mutT^{-}$ E. coli cells suppresses the elevated level of spontaneous mutagenesis to an almost normal level (102,105). In addition, Mth1-knockout mice showed a significantly more 8-oxoG accumulation in DNA as well as a higher level of spontaneous carcinogenesis particularly in liver, lung and stomach than control mice (106). Therefore, hMTH1 is believed to play an important antimutagenic role in cells by preventing the incorporation of oxidatively modified purine nucleotides into DNA during replication (100).

The accumulation of 8-oxoG is likely to dramatically increase in patients suffering from various neurodegenerative diseases such as Parkinson’s disease (107), Alzheimer’s disease (108) or amyotrophic lateral sclerosis (109), which are associated with the

progressive loss of cells. The hMTH1 level is significantly higher in the substantia nigral neurons of Parkinson's disease patients (110) or in the entorhinal cortex of Alzheimer's disease patients (111) showing the accumulation of 8-oxoG. Moreover, hMTH1 appears to play a role in protecting neurons from oxidative stress (112-114). Recently, several studies also reported a correlation between the induction of apoptosis by oxidative stress and the accumulation of oxidative DNA lesions (115-117), suggesting that oxidative DNA damage derived from oxidized purine nucleotides causes neurodegenerative disease and cancer.

In this study, we examined the effect of hMTH1 on the H_2O_2 oxidative stress-induced DNA damage by analyzing caspase enzyme activities, p53 phosphorylation, Noxa induction, γ-H2AX foci formation and array comparative genome hybridization damage in human fibroblast GM00637 cells. The results indicate that hMTH1 deficient cells exhibit the increased level of H_2O_2-induced cell death through Noxa-dependent pathways, and hMTH1 plays an important role in maintaining genomic stability after H_2O_2-induced DNA damage in GM00637 cells.

MATERIALS AND METHODS

1. Maintenance of Cell Lines

Human fibroblast GM00637 cells (Coriell Institute for Medical Research, Camden, NJ) were maintained in Earle's minimum essential medium supplemented with 10% fetal bovine serum, 100 units/ml of penicillin, and 100 mg/ml of streptomycin (Invitrogen, Carlsbad, CA). Human lung carcinoma H1299 (p53-null) cells were purchased from American Type Culture Collection (ATCC number CRL-5803; Manassas, VA) and grown in RPMI 1640 medium supplemented with 10% fetal bovine serum, 100 units/ml of penicillin, 100 mg/ml of streptomycin (Invitrogen, Carlsbad, CA). The cells were maintained in a humidified incubator in an atmosphere containing 5 % CO_2 at 37 ^{o}C.

2. Plasmid Constructs of hOGG1 and transfection to GM00637 cells

The human OGG1 cDNA was amplified by RT-PCR using the hOGG1 oligo primer: sense 5'-ATGCCTGCCCGCGCGCTTCTGCC-3' and antisense 5'-CTAGCCTTCCGGC

CCTTTGGAAC-3' from human fibroblast GM00637 cells. The amplified hOGG1 cDNA construct was inserted into a pcDNA3.1/ mammalian expression vector driven by the CMV promoter (Invitrogen Life Technologies). After confirming the DNA sequence and orientation, the hOGG1 construct was transfected into cells using the Lipofectamine transfection reagent (Invitrogen Life Technologies) according to the manufacturer's instructions. After transfection, cells were incubated with complete medium containing 200ug/ml G418 for 4 weeks. The cell clones resistant to G418 were isolated and analyzed.

3. hOGG1-siRNA design, synthesis and transfection

Three target sites within human OGG1 genes were chosen from the human OGG1 mRNA sequence (Gene Bank accession number AF003595), which was extracted from the NCBI Entrez nucleotide database. After selection, each target site was searched with NCBI BLAST to confirm the specificity only to the human OGG1. The sequences of the 21-nucleotide sense- and antisense-RNA are as follows: hOGG1-siRNA, 5'-GUACUUCCAGCUAGAUGUUUU-3' (sense) and 5'-AACAUCUAGCUGGAAGUA-CUU-3'(antisense) for the hOGG1 gene (nt 292–312); LacZ siRNA, 5'-CGUACG-CGGAAUACUUCGAUU-3' (sense), 5'-AAUC GAAGUAUUCCGCGUACGUU-3' (antisense) for the LacZ gene. These siRNAs were prepared using a transcription-based method with a Silencer siRNA construction kit (Ambion, Austin, TX) according to the manufacturer's instructions. LacZ siRNA was used as the negative control. Cells were transiently transfected with siRNA duplexes using Oligofectamine (Invitrogen). The siRNA expression vector(pSilencer hygro) for hOGG1 and a control vector were employed. The construction of siRNA-expression plasmid was base on the pSilencer hygro vector(Ambion,Texas,USA). The vector included a human U6 promoter, a hygromycin resistance gene. We purchased synthetic oligo-nucleotides(Xenotech, Korea). After anneling, DNA fragments were ligated into the pSilencer hygro. Cells were transfected with the siRNA vector by using Lipofectamine(Invitrogen. Carlsbad.CA). After transfection with the hygromycin-resistance vector, resistant colonies were grown in the presence of Hygromycin(100ug/ml)(Invitrogen. Carlsbad.CA).

4. Western blot analysis

The cell were washed with phosphate-buffered saline(PBS) and lysed on ice for 10 minutes in the M-PER mammalian protein Extraction Reagent (PIERCE) added protease Inhibitor Cocktail tablet (Roch). After incubation, extracts were vortexed for 5min and

centrifuged at 13000rpm for 15min. The supernatant was diluted with 5X SDS-sample buffer and boiled. After cellular protein concentrations were determined using the dye-binding microassay (Bio-Rad, Hercules, CA), and 20ug of protein per lane were separated by 10% SDS-polyacrylamide gel electrophoresis (SDS-PAGE). After SDS-PAGE, the proteins were transferred onto Hybon ECL membranes (Amersham Biosciences, Piscataway, NJ). After electroblotting, the membranes were blocked by 5% skim-milk in Tris buffer saline containing 0.05% Tween-20(TBST, 10 mM Tris-HCl, pH 7.4, 150 mM NaCl, 0.1 % Tween-20) at room temperature for 2 hours. The membranes were rinsed with TBST and then incubated with appropriate primary antibodies in TBST at 4℃ overnight. All antibodies used in this study are anti-human OGG1 polyclonal antibody (pAb) (Santa Cruz Biotechnology, Santa Cruz, CA); anti-p53 pAb, anti-p53-P(Ser15) pAb, anti-p53-P(Ser20) pAb (Cell Signaling Technology, Danvers, MA); anti-p21 monoclonal antibody (mAb) (BD Phamingen, San Jose, CA); anti-Noxa mAb (Calbiochem, Darmstadt, Germany); anti-b-actin mAb (BD Phamingen, San Jose, CA); anti-a-tubulin mAb (BD Phamingen, San Jose, CA); anti-DNA-PKcs mAb (Santa Cruz Biotechnology, Santa Cruz, CA); anti-DNA-PKcs-P(T2609) (abcam, Cambridge, UK); anti-ATM mAb (Santa Cruz Biotechnology, Santa Cruz, CA); anti-ATM-P (Ser1981) mAb (Cell Signaling Technology, Danvers, MA); anti-Chk1-P (S345) pAb, anti-Chk1 pAb (Cell Signaling Technology, Danvers, MA); anti-Rad51 mAb (Oncogene, San Diego, CA). We followed manufacturer's protocol for dilution of all primary antibodies. The membranes were then washed, incubated with the biotinylated secondary antibodies (1:4,000) in a blocking buffer for 2 hours at room temperature , and washed again. The blotted proteins were developed using an enhanced chemiluminescence detection system (iNtRON, Biotech, Seoul, Korea).

5. Semiquantative Reverse Transcriptase-Polymerase Chain Reaction

RNA extraction was carried out using the RNA-STAT-60 according to the manufacturer's instructions (TEL-TEST, Inc., Friendswood, TX). 2 μg of the total RNA was reverse-transcribed using a M-MLV cDNA synthesis system (Promega, San Luis Obispo, CA), and the reverse-transcribed DNA was subjected to PCR. The profile of replication cycles was denaturation at 94 ℃ for 50 seconds, annealed at 58 ℃ for 50 seconds, and polymerized at 72 ℃ for 1 min. In each reaction, the expression of glyceraldehyde-3-phosphate dehydrogenase (GAPDH) served as the internal control. The primers used for PCR are as follows: hOGG1 forward, 5'-CTG CCT TCT GGA CAA TCT TT-3'; hOGG1 reverse, 5'-TAG CCC GCC CTG TTC TTC-3' designed to amplify a 551-bp region; GAPDH forward, 5'-CCA TGG AGA AGG CTG GGG-3'; and GAPDH reverse 5'-CAA AGT TGT CAT GGA TGA CC-3' designed to amplify a 194-bp region (total number of cycles: 26). The PCR products were resolved on 1 % agarose gels, stained with ethidium bromide, and then photographed.

6. 8-oxoG Glycosylase Activity Assay(Endonuclease Nicking Assay)

The cells at the exponential phase were centrifuged at 800 x g for 5 minutes. The cell pellets (10^6 cells per each assay) were then suspended in 2 volumes of a homogenization buffer (50 mM Tris-HCl, 50 mM KCl, 1 mM EDTA, 5 % glycerol, and 0.05 % 2-mercaptoethanol, pH 7.5) and homogenized. After the supernatants were obtained by centrifugation, followed by dialyzing against the homogenization buffer, they were used for the endonuclease-nicking assay as cell extracts. 8-oxoG-containing 21-mer with the sequence 5'-CAGCCAATCAGTXCACCATTC-3' (X=8-oxoG) along with its complementary strand was chemically synthesized (The Midland Certified Reagent Co., Midland, TX). The synthetic oligonucleotide was 3'-end-labeled using terminal transferase and [a-^{32}P]ddATP (Amersham Biosciences, 3000 Ci/mmol). The end-labeled oligomer was

annealed with its complementary oligonucleotide, and the resulting duplex DNA was used as the assay substrate. The duplex substrate DNA (20 pmol) was incubated with the cell extracts (10 mg of protein) at 37 ^{o}C for 1 hour in 1 ml of reaction mixture (50 mM Tris-HCl, 50 mM KCl and 1 mM EDTA, pH 7.5). The reaction was quenched by heating at 90 ^{o}C for 3 minutes, followed by electrophoresis on 20 % denaturing (7Murea) polyacrylamide gels (DNA sequencing gel). The gels were wrapped in saran wrap and exposed to Kodak film for visualization.

7. Cytotoxicity Assay by trypan blue

The extent of cell death was determined by trypan blue exclusion. Cells were seeded on well plate. After 24 h, cells were treated with H_2O_2(uM). After 24 hours, The floating and trypsin-detached GM00637 cells were collected and washed once with ice-cold PBS. Trypan blue (0.2% in PBS, Invitrogen) was added to the cells. The cell counted using Cedex AS20(INNOVATIS). The cell viability was measured as a percentage of the total cell number that remained unstained.

8. Cytotoxicity Assay by MTT

The cell cytotoxicity was also assessed using a 3-[4,5-dimethylthiazol-2-yl]-2,5-diphenyltetrazolium bromide (MTT)-based colorimetric assay. Cells were seeded on well plate. After 24 h, cells were treated with H_2O_2(uM) for 24 hours. MTT(10mg/ml) was incubated with cells in a plate for 4 h at 37℃. The medium containing MTT was removed, and dimethyl sulfoxide (DMSO) was added. cells were incubated for 15min at room temperature with gentle shaking. The absorbance was read on a scanning elisa reader (BIO-TEK INSTRUMENTS,INC.) using a 540nm filter. Cell viability was calculated from relative dye intensity compared with untreated samples.

9. Flow cytometry by PI staining

The floating and trypsin-detached GM00637 cells were collected and washed once with ice-cold PBS, followed by fixing in 70% cold ethanol for 30minutes at 4℃. The cells were then stained in PBS and PI (50 μg/ml), RNase A (50 μg/ml), and 0.05 % Triton X-100. The DNA content of the GM00673 cells was analyzed by fluorescent-activated cell sorting (FACSort, Becton Dickinson, Franklin Lakes, NJ). At least 10000 events were analyzed, and the percentage of cells in sub-G_1 population was calculated. Aggregates of cell debris at the origin of histogram were excluded from the sub-G_1 cells.

10. Caspase-3/7 activity assay

The caspase-3/7 activity was detected by A Caspase-Glo 3/7 Assay system (Promega) after preincubating the GM00637 cells (1 x 10^6/60-mm plate) with/without 60 μM caspase inhibitor I (CALBIOCAM, La Jolla, CA) for 12 hours, followed by treating with various H_2O_2 concentrations (0 to 70 μM) for another 12 hours. The background luminescence associated with the cell culture and assay reagent (blank reaction) was subtracted from the experimental values. The activity of caspase-3/-7 was presented as the means of triplets for the given cells.

11. p53-siRNA transfection and Cytotoxicity Assay by MTT

The Stealth TP53 RNAi was purchased from Invitrogen(TP53 Validated StealthTM RNAi DuoPak(#45-149), primar accession: NM_000546.2, coding regin: 252-1433). The target sequence of siRNA for p53 is 5'-CCAUCCACUACAAC-UACAUGUGUAA-3'(GC40%) and 5'-CCAGUGGUAAUCUACUGGGACGGAA-3'(GC52%). GM00637 cells were transfected with these double-stranded siRNAs(5pmol) for 48hr by the Lipofectamine RNAiMAX method according to the manufaturer's

protocol(Invitrogen Life Technologies Carlsbad.CA). Cells were treated with H_2O_2(uM) for 24 hours. The cell cytotoxicity was also assessed using a 3-[4,5-dimethylthiazol-2-yl]-2,5-dipheny-ltetrazolium bromide (MTT)-based colorimetric assay.

12. Transfection with p53 plasmid and Cytotoxicity Assay by MTT

The human full-length p53 DNA construct was synthesized by PCR amplification of the wt p53 plasmid (Invitrogen Life Technologies), using the following primer: sense 5'-TCGAATTCGCCACCATGGAGGAGCCGCAGTCAGAT-3' and antisense 5'-GCGAAT

TCTCAGT CTGAGTCAGGCCCTTCTGT-3'. The amplified full-length p53 DNA construct was inserted into a pcDNA3.1/ plasmid vector (Invitrogen Life Technologies). After verifying DNA sequence and orientation, the p53 construct was transfected into H1299 cells using the Lipofectamine LTX Reagent transfection reagent (Invitrogen Life Tech-nologies). The expression of p53 protein was confirmed by western blot anaysis. After cells were cultured for 48 hours, treated with H_2O_2(uM) for 24 hours. The cell cyto-toxicity was also assessed using a 3-[4,5-dimethylthiazol-2-yl]-2,5-dipheny-ltetrazolium bromide (MTT)-based colorimetric assay.

13. Bacterial artificial chromosome (BAC)-array comparative genomic hybridization (array-CGH)

Human fibroblast genomic DNAs derived from control-siRNA and hOGG1-siRNA transfected GM00637 were prepared by using the PUREGENE DNA Isolation kit (Gentra D5500A, Minneapolis, MN). For each CGH hybridization, we digested 2μg of genomic DNA from the reference and the corresponding experimental sample with DpnII. All digests were done for a minimum of 2 hours at 37 ^{o}C and then verified by agarose gel analysis. The samples were then filtered by using the QIAQuick PCR clean-up kit

(Quiagen, Valencia, CA). Labeling reactions were performed with 0.8 μg of purified DNA and a Bioprime labeling kit (Invitrogen) according to the manufacturer's instructions in a volume of 50 μl with a modified dNTP pool containing 120μM each of dATP, dGTP, dTTP, 60μM dCTP, and 60μM Cy5-dCTP (for the reference from control-siRNA transfected GM00637) or Cy3-dCTP (for the experimental sample from hOGG1-siRNA transfected GM00637). Experimental and reference targets for each hybridization were pooled and mixed with 50 μg of human Cot-1 DNA (Invitrogen). The target mixture was ethanol-precipitated and resuspended to a final volume of 40μl hybridization buffer. Before hybridization to the array, the hybridization mixtures were denatured at 70 ^{o}C for 15 minutes and applied to the array CGH chip slide, MacArray^{TM}Karyo 4000 (Macrogen Korea, Seoul, South Korea). Hybridization was carried out for 48 to 72 hours at 37 ^{o}C in a rotating chamber (MAUI, BioMicro Systems Inc., Salt Lake City, UT). The arrays were then disassembled in 50 % formamide, 2 X SSC at 46 ^{o}C for 15 minutes, followed by washing with 2 X SSC, 0.1 % SDS at 46 ^{o}C for 30 minutes. Slides were dried and scanned with a GenePix4000B microarray scanner (Axon Instruments-Molecular Devices, Sunnyvale, CA). Microarray images were analyzed by using Macviewer software (Macrogen). Default settings were used. Whole-genome array CGH profiles showed $\log_2$-transformed hybridization ratios of test DNA versus control-reference DNA as described in figure legend.

14. Statistical analysis

Results are expressed as mean ± standard deviation (SD). For statistical analysis, ANOVA with P values were performed for both the overall (P) and the pair-wise comparison as indicated by asterisks. Values of $P<0.05$ were considered to be significant.

15. Maintenance of Cell Lines

Human fibroblast GM00637 cells (Coriell Institute for Medical Research, Camden, NJ) were maintained in Earle's minimum essential medium supplemented with 10% fetal bovine serum, 100 units of penicillin/ml, and 100μg of streptomycin/ml (Invitrogen, Carlsbad, CA). The cells were maintained in a humidified incubator in an atmosphere containing 5 % CO2 at 37 ℃.

16. Western Blotting

The cell were washed with phosphate-buffered saline(PBS) and lysed on ice for 10 minutes in the M-PER mammalian protein Extraction Reagent (PIERCE) added protease Inhibitor Cocktail tablet (Roch). After incubation, extracts were vortexed for 5min and centrifuged at 13000rpm for 15min. The supernatant was diluted with 5X SDS-sample buffer and boiled. After cellular protein concentrations were determined using the dye-binding microassay (Bio-Rad, Hercules, CA), and 20ug of protein per lane were separated by 10% SDS-polyacrylamide gel electrophoresis (SDS-PAGE). After SDS-PAGE, the proteins were transferred onto Hybon ECL membranes (Amersham Biosciences, Piscataway, NJ). After electroblotting, the membranes were blocked by 5% skim-milk in Tris buffer saline containing 0.05% Tween-20(TBST, 10 mM Tris-HCl, pH 7.4, 150 mM NaCl, 0.1 % Tween-20) at room temperature for 2 hours. The membranes were rinsed with TBST and then incubated with appropriate primary antibodies in TBST at 4℃ overnight. All antibodies used in this study are polyclonal antibody against human MTH1 was obtained from BD Biosciences (San Diego, CA), and polyclonal antibodies against human p53, phosphorylated p53 on serine 15 and 20, cleaved caspase-3 and cleaved caspase-7 were obtained from Cell Signaling Technology (Danvers, MA). Monoclonal antibody against Noxa was produced from Calbiochem (Darmstadt, Germany) and polyclonal

antibody against γ-H2AX was obtained from Upstate (Lake placid, NY). We followed manufacturer's protocol for dilution of all primary antibodies. The membranes were then washed, incubated with the biotinylated secondary antibodies (1:4,000) in a blocking buffer for 2 hours at room temperature , and washed again. The blotted proteins were developed using an enhanced chemiluminescence detection system (iNtRON, Biotech, Seoul, Korea).

17. Semiquantative Reverse Transcriptase-Polymerase Chain Reaction.

RNA extraction was carried out using the RNA-STAT-60 according to the manufacturer's instructions (TEL-TEST, Inc., Friendswood, TX). 2 g of the total RNA was reverse-transcribed using a M-MLV cDNA synthesis system (Promega, San Luis Obispo, CA), and the reverse-transcribed DNA was subjected to PCR. The profile of the replication cycles was denaturation at 94 °C for 50 seconds, annealed at 58 °C for 50 seconds, and polymerized at 72 °C for 1 min. In each reaction, the expression of glyceraldehyde-3-phosphate dehydrogenase (GAPDH) served as the internal control. The primers used for PCR are as follows: hMTH1 forward, 5'-GTT TTA TGA GTG GAA TTA GC-3'; hMTH1 reverse, 5'-GTG GAA TTT CTT CTT GTG A-3' designed to amplify a 475-bp region; GAPDH forward, 5'-TGA CCA CAG TCC ATG CCA TC-3'; and GAPDH reverse 5'-TTA CTC CTT GGA GGC CAT GT-3' designed to amplify a 492-bp region (total number of cycles: 26). The PCR products were resolved on 1 % agarose gels, stained with ethidium bromide, and then photographed.

18. hMTH1-siRNA design, synthesis and transfection

Three target sites within human MTH1 genes were chosen from the human MTH1 mRNA sequence (Gene Bank accession no. AB025240), which was extracted from the NCBI

Entrez nucleotide database. After selection, each target site was searched with NCBI BLAST to confirm the specificity only to the human MTH1. The sequences of 21-nucleotide sense- and antisense-RNA are as follows: hMTH1-siRNA, 5'-GAA GAA AUU CCA CGG GUA CUU-3' (sense) and 5'-GUA CCC GUG GAA UUU CUU CUU-3' (antisense) for the hMTH1 gene (nt 540–560); LacZ siRNA, 5'-CGU ACG CGG AAU ACU UCG AUU-3' (sense), 5'-AAU CGA AGU AUU CCG CGU ACG UU-3' (antisense) for the LacZ gene. These siRNAs were prepared using a transcription-based method with a Silencer siRNA construction kit (Ambion, Austin, TX) according to the manufacturer's instructions. LacZ siRNA was used as the negative control. The cells were transiently transfected with the siRNA duplexes using Oligofectamine (Invitrogen). The siRNA expression vector(pSilencer hygro) for hMTH1 and a control vector were employed. The construction of siRNA-expression plasmid was base on the pSilencer hygro vector(Ambion,Texas,USA). The vector included a human U6 promoter, a hygromycin resistance gene. We purchased synthetic oligo-nucleotides(Xenotech, Korea). After anneling, DNA fragments were ligated into the pSilencer hygro. Cells were transfected with the siRNA vector by using Lipofectamine(Invitrogen. Carlsbad.CA). After transfection with the hygromycin-resistance vector, resistant colonies were grown in the presence of Hygro-mycin(100ug/ml) (Invitrogen. Carlsbad.CA).

19. Cytotoxicity Assay by trypan blue

The extent of cell death was determined by trypan blue exclusion. Cells were seeded on well plate. After 24 h, cells were treated with H_2O_2(uM). After 24 hours, The floating and trypsin-detached GM00637 cells were collected and washed once with ice-cold PBS. Trypan blue (0.2% in PBS, Invitrogen) was added to the cells. The cell counted using Cedex AS20(INNOVATIS). The cell viability was measured as a percentage of the total cell number that remained unstained.

20. Cytotoxicity Assay by MTT

The cell cytotoxicity was also assessed using a 3-[4,5-dimethylthiazol-2-yl]-2,5-diphenyltetrazolium bromide (MTT)-based colorimetric assay. Cells were seeded on well plate. After 24 h, cells were treated with H_2O_2(uM). After 24 hours, MTT(10mg/ml) was incubated with cells in a plate for 4 h at 37℃. The medium containing MTT was removed, and dimethyl sulfoxide (DMSO) was added. cells were incubated for 15min at room temperature with gentle shaking. The absorbance was read on a scanning elisa reader (BIO-TEK INSTRUMENTS,INC.) using a 540nm filter. Cell viability was calculated from relative dye intensity compared with untreated samples.

21. Flow cytometry by PI staining

The floating and trypsin-detached GM00637 cells were collected and washed once with ice-cold PBS, followed by fixing in 70% cold ethanol. The cells were then stained in PBS and PI (50 μg/ml), RNase A (50 μg/ml), and 0.05 % Triton X-100 for 45 min. The DNA content of the GM00673 cells was analyzed by fluorescent-activated cell sorting (FACSort, Becton Dickinson, Franklin Lakes, NJ). At least 10000 events were analyzed, and the percentage of cells in sub-G_1 population was calculated. Aggregates of cell debris at the origin of histogram were excluded from the sub-G_1 cells.

22. Noxa-siRNA transfection and Cytotoxicity Assay by MTT

The Noxa siRNA duplex oligoribonucleotides were purchased from Invitrogen(primar accession: NM_021127). The target sequence of siRNA for Noxa is 5'-UUGAGUAGCA CACUCGACUUCCAGC-3'(sence) and 5'-GCUGGAAGUCGAGUGUGCUAC UCAA-3'(antisence). GM00637 cells were transfected with these double-stranded siRNAs(5pmol) for 48hr by the Lipofectamine RNAiMAX method according to the manufaturer's

protocol(Invitrogen Life Technologies Carlsbad.CA). Cells were treated with H2O2(uM) for 24 hours. The cell cytotoxicity was also assessed using a 3-[4,5-dimethylthiazol-2-yl]-2,5-dipheny-ltetrazolium bromide (MTT)-based colorimetric assay.

23. p53-siRNA transfection and Cytotoxicity Assay by MTT

The Stealth TP53 RNAi was purchased from Invitrogen(TP53 Validated StealthTM RNAi DuoPak(#45-149), primar accession: NM_000546.2, coding regin: 252-1433). The target sequence of siRNA for p53 is 5'-CCAUCCACUACAACUACAUGUGUAA-3'(GC40%) and 5'-CCAGUGGUAAUCUACUGGGACGGAA-3'(GC52%). GM00637 cells were transfected with these double-stranded siRNAs(20pmol) for 48hr by the Lipofectamine RNAiMAX method according to the manufaturer's protocol(Invitrogen Life Technologies Carlsbad.CA). Cells were treated with H_2O_2(uM) for 24 hours. The cell cytotoxicity was also assessed using a 3-[4,5-dimethylthiazol-2-yl]-2,5-dipheny-ltetrazolium bromide (MTT)-based colorimetric assay.

24. Immunolocalization of phosphorylated-H2AX (H2AX).

Cells were fixed in methanol for 15 minutes at room temperature, followed by washing in phosphate buffered saline (PBS; 0.01 M, pH 7.4). They were then incubated in 10% goat serum containing 1 % bovine serum albumin for 1 hour at room temperature to reduce the binding with nonspecific antibodies. After incubation overnight at 4 ^{o}C with the rabbit derived specific anti-human ɣH2AX antibodies (1:100) (Upstate, Lake Placid, NY, USA), the immunoreactivity was detected using 2 mg/ml Alexa Fluor 488 (Molecular Probes, Eugene, OR, USA). As a control, the same cells were incubated with an isotype matched antibody using identical experimental conditions. The immunolocalization of ɣH2AX was

observed and photographed by FV300 laser microscopy (Olympus, Japan) at an excitation wavelength 488 nm.

25. Measurement of intracellular ROS by FACS

The intracellular production of ROS was assayed using the CM-H2DCFDA probe (Molecular Probes). Briefly, after addition of CM-H2DCFDA(5uM) the cells were incuvated for 15min in the dark at 37℃. CM-H2DCFDA is oxidized by ROS to the highly fluorescent CM-DCF compound. After two washes with PBS, the cells were detached by Trypsin-EDTA and immediately analyzed by flow cytometry (FACSort, Becton Dickinson, Franklin Lakes, NJ). Ten-thousand individual data points were collected for each sample.

26. Bacterial artificial chromosome (BAC)-array comparative genomic hybridization (array-CGH).

Human fibroblast genomic DNAs derived from control-siRNA and hMTH1-siRNA transfected GM00637 were prepared by using the PUREGENE DNA Isolation kit (Gentra D5500A, Minneapolis, MN). For each CGH hybridization, we digested 2μg of genomic DNA from the reference and the corresponding experimental sample with DpnII. All digests were done for a minimum of 2 hours at 37 ^{o}C and then verified by agarose gel analysis. The samples were then filtered by using the QIAQuick PCR Purification kit (Quiagen, Valencia, CA). Labeling reactions were performed with 0.8μg of purified DNA and a Bioprime Array CGH Genomic labeling kit (Invitrogen) according to the manufacturer's instructions in a volume of 50μl with a modified dNTP pool containing 120μM each of dATP, dGTP, dTTP, 60μM dCTP, and 60μM Cy5-dCTP (for the reference from control-siRNA transfected GM00637) or Cy3-dCTP (for the experimental sample

from hMTH1-siRNA transfected GM00637). Experimental and reference targets for each hybridization were pooled and mixed with 50 g of human Cot-1 DNA (Invitrogen). The target mixture was ethanol-precipitated and resuspended to a final volume of 40μl hybridization buffer. Before hybridization to the array, the hybridization mixtures were denatured at 70°C for 15 minutes and applied to the array CGH chip slide, MacArray™Karyo 4000 (Macrogen Korea, Seoul, South Korea). Hybridization was carried out for 48 to 72 hours at 37 °C in a rotating chamber (MAUI, BioMicro Systems Inc., Salt Lake City, UT). The arrays were then disassembled in 50 % formamide, 2 X SSC at 46 °C for 15 minutes, followed by washing with 2 X SSC, 0.1 % SDS at 46 °C for 30 minutes. Slides were dried and scanned with a GenePix4000B microarray scanner (Axon Instruments-Molecular Devices, Sunnyvale, CA). Microarray images were analyzed by using Macviewer software (Macrogen). Default settings were used. Whole-genome array CGH profiles showed $\log_2$-transformed hybridization ratios of test DNA versus control-reference DNA as described in figure legend.

27. Data Analysis.

The data is represented as the mean ± SD. Statistical comparisons were carried out using an unpaired t test. p values < 0.05 were considered significant.

RESULTS

I. hOGG1-deficient fibroblasts undergo p53-dependent oxidative stress-induced apoptosis.

1. Suppression of hOGG1 gene expression enhances the cytotoxic effects of H_2O_2 in human fibroblast GM00637.

Semiquantitative RT-PCR was performed using hOGG1 specific synthetic primers, as described in “Materials and Methods”, to determine if the constitutive expression of human OGG1 is specifically inhibited by hOGG1-siRNA in cultured human fibroblast GM0063 cells. Two transfectants of hOGG1-silencing GM00637 cells blocked the normal expression of hOGG1 up to 80-90%, compared to that of control-siRNA transfectants (Fig. 3A, 3C). Western blotting was also carried out to determine if the inhibition of hOGG1 mRNA corresponds to that in the hOGG1 protein level. As demonstrated in Figure 3B and 3C, hOGG1 protein expression was also 60-65% inhibited by hOGG1-siRNA transfection. In order to determine the functional significance of the inhibited hOGG1 expression, the parental-, control-siRNA and hOGG1-siRNA transfected cell lysates were prepared and examined their abilities to cleave 8-oxoG using a 21-mer oligonucleotide containing a single 8-oxoG at nucleotide 13. As shown in Figure 3D, hOGG1-siRNA transfected cells resulted in the inefficient cleavage of the 8-oxoG:C substrates compared with the parental or control-siRNA transfected cells, demonstrating that hOGG1-siRNA can cause a reduction in the hOGG1 protein level, followed by specific inhibition of the hOGG1 repair activity in human fibroblast GM00637 cells.

The effect of hOGG1 on the H_2O_2-induced cytotoxicity was next investigated in parental cells, control-siRNA and hOGG1-siRNA transfected cells. The cell viability of the

hOGG1-siRNA transfected GM00637 was significantly lower than that of the control-siRNA transfected cells and parental cells (Fig. 3E). This indicates that the inhibition of hOGG1 expression reduces the cell viability of fibroblasts in response to oxidative stress.

In order to determine if hOGG1 depletion has any effect on H_2O_2-induced apoptosis, the nuclei of GM00637 cells were stained with a propidium iodide dye for flow cytometric detection. As shown in Figure 3F, the control-siRNA transfected cells, which were treated with 0 to 60 μM H_2O_2, showed an apoptotic sub-G_1 DNA content of 4.12 % to 12.35 %. However, transfection with hOGG1-siRNA increased the proportion of apoptotic sub-G_1 DNA content. The apoptotic sub-G_1 DNA content of the hOGG1-siRNA transfected cells ranged from 4.97 % to 24.17 % at the same oxidative stress. This shows that the suppression of hOGG1 expression triggers the measured apoptosis in response to H_2O_2 in GM00637 human fibroblasts.

Figure 3.

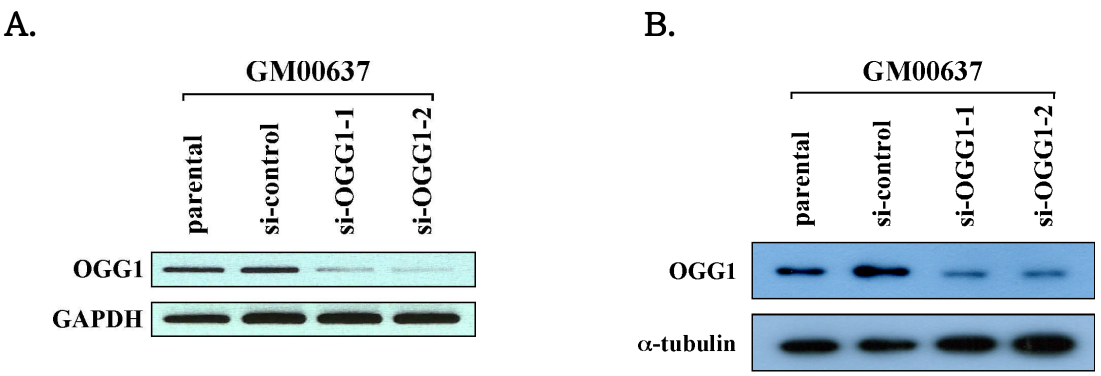

Figure 3.

C.

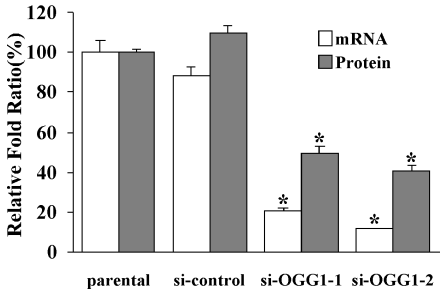

D.

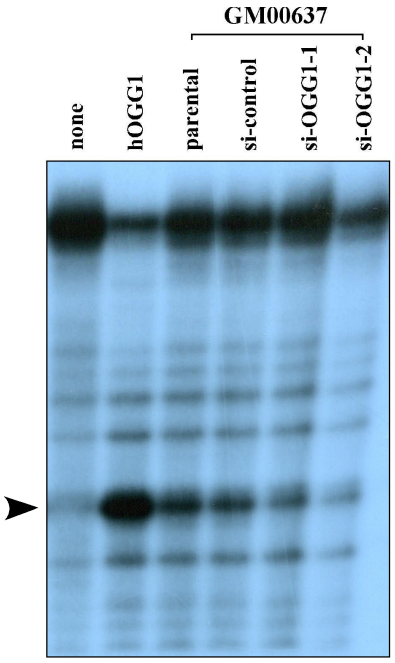

E.

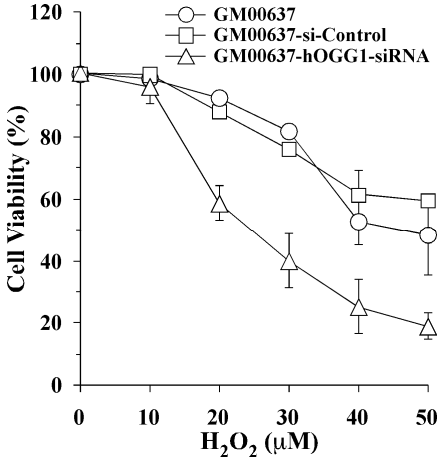

F.

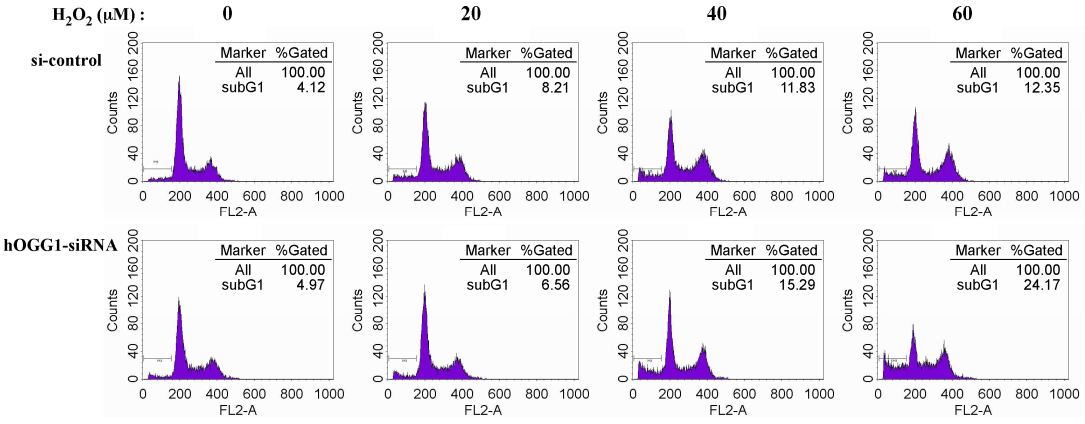

Figure 3. **Knockdown of hOGG1 expression by siRNA inference sensitizes human fibroblast GM00637 cells to H_2O_2-induced apoptosis.** The human fibroblast GM00637 cells were stably transfected with the control-siRNA and two different hOGG1-siRNA as described in "Experimental Procedures". The expression of hOGG1 was then analyzed by RT-PCR using hOGG1 specific synthetic primers (A), and by Western blot using anti-hOGG1 polyclonal antibodies (B). The data was normalized with GAPDH and a-tubulin expression, respectively. Panel C is the graphical plot based on panel A and B. All values are expressed as mean ± standard deviation (SD). Statistically significant differences in OGG1 expression were determined by the ANOVA with P values given for both the overall (P) and the pair-wise comparisons as indicated by asterisks (*, $P<0.05$). (D) The OGG1 enzyme activities were analyzed by 8-oxoG nicking assay using the parental, control-siRNA and two different hOGG1-siRNA transfected cell lysates as described in "Experimental Procedures". Purified hOGG1 and buffer alone served as positive and negative control, respectively. The arrow indicates the DNA cleavage products (13-mer). (E) Parental, control-siRNA and hOGG1-siRNA transfected cells were cultured to 70-80% confluence, and treated with the indicated concentration of H_2O_2 for one hour. The media were then changed to fresh one, and the extent of cell death was assayed by Trypan blue exclusion 24 hours after the treatment. Cell viability was determined as the percentage of total cell number that remained unstained. The values represent the means ± SD from six separate experiments. (F) Apoptotic Sub-G_1 DNA contents were estimated by FACScan analysis after treatment with the indicated H_2O_2 concentration under the same experimental condition with (E).

2. hOGG1-knockdown GM00637 cells lead to the significant increases of caspase-3 and caspase-7 activities in response to H_2O_2-oxidative stress.

The activation of caspases is one of the major processes in DNA damage-induced apoptosis. In order to understand the protective effect of hOGG1 on H_2O_2-induced apoptosis, we examined the levels of caspase-3 and caspase-7, which are the key caspases in the apoptotic pathways, by Western blotting in the control-siRNA and hOGG1-siRNA transfected GM00637 cells. There was no significant difference in the levels of the procaspase-3 and procaspase-7 between control-siRNA and hOGG1-siRNA transfected GM00637 cells (data not shown). In addition, none of the active processed products of both enzymes were detected in the control-siRNA transfected GM00637 cells up to 48 hr after the H_2O_2 treatment. On the other hand, the cleavage of procaspase-3 and procaspase-7 into the active subunit was clearly observed in the hOGG1-siRNA transfected GM00637 cells from 24 hr after H_2O_2 treatment (Fig. 4A). The observation of activated (cleaved) caspase-3 and caspase-7 is consistent with the data obtained from their enzymatic activity assay, which were performed using a Promega CaspaseGlo 3/7 kit, as described in "Materials and Methods." As demonstrated in Figure 4B, the enhanced caspase-3 and caspase-7 activity induced by H_2O_2-treatment of hOGG1-siRNA transfected cells was significantly inhibited by a treatment with caspase inhibitors. Furthermore, the level of cell viability in the hOGG1-siRNA transfected fibroblasts was almost completely reversed to those of the control-siRNA transfected cells after the treatment with caspase-3 and caspase-7 inhibitors (Fig. 4C). This indicates that the caspase-3/7 activation plays an important role in the development of H_2O_2-induced apoptosis in hOGG1-depleted human fibroblast GM00637 cells.

Figure 4.

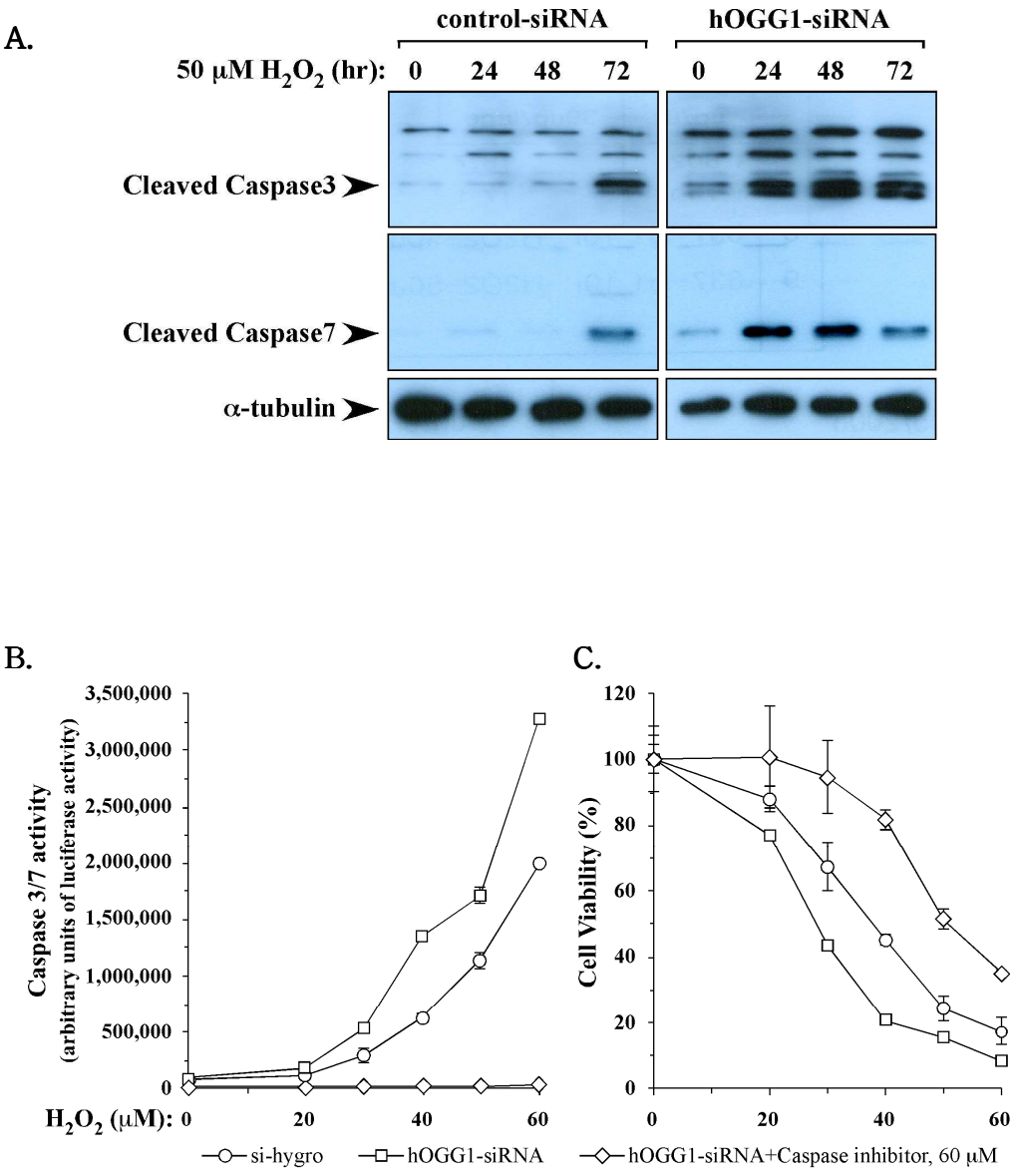
A.
control-siRNA
hOGG1-siRNA
50 μM H2O2 (hr): 0 24 48 72 0 24 48 72
Cleaved Caspase3
Cleaved Caspase7
α-tubulin
B.
Caspase 3/7 activity
(arbitrary units of luciferase activity)
3,500,000
3,000,000
2,500,000
2,000,000
1,500,000
1,000,000
500,000
0
H2O2 (μM): 0 20 40 60
si-hygro
hOGG1-siRNA
C.
Cell Viability (%)
120
100
80
60
40
20
0
0 20 40 60
hOGG1-siRNA+Caspase inhibitor, 60 μM

Figure 4. **Silencing hOGG1 triggers caspase-3 and caspase-7 activation in response to H_2O_2 in GM00637 cells.** (A) Cells were treated with 50μM H_2O_2 for one hour. The activated (cleaved) caspase-3 and caspase-7 were detected by Western blot analysis using specific antibodies for caspase-3 and caspase-7 at the indicated time-points after the H_2O_2 treatment. The data was normalized with α-tubulin expression. (B) After control-siRNA and hOGG1-siRNA transfected GM00637 cells were treated with/without 60μM caspase inhibitor and the indicated concentration of H_2O_2, caspase-3/7 activities were analyzed using Promega Caspase Glo 3/7 kit as described in "Experimental Procedures". The data was plotted as the relative units of luciferase intensity of three separate experiments. All values are expressed as mean ± SD. (C) Cell viability was determined by MTT assay kit. The Cell viability was determined after being treated with different doses of H_2O_2 under the same experimental condition with (B). All values are expressed as mean ± SD. The parental GM00637 and control-siRNA transfected cells served as experimental controls in this study.

3. Requirement of p53 activation for H_2O_2-induced cell death in hOGG1 deficient cells.

In response to a variety of death stimuli, p53 is stabilized and rapidly activated in many cell types (69). One important mechanism through which p53 promotes caspase activation is by transactivation of the proapoptotic proteins (70). In order to determine the requirement of p53 activation for H_2O_2-induced apoptosis in hOGG1-depleted cells, we investigated the activation of p53 and its downstream target protein such as p21 and Noxa in control-siRNA and hOGG1-siRNA transfected fibroblasts after a treatment with 100 μM H_2O_2. As shown in Figure 5, H_2O_2 significantly activated p53 phosphorylation (Fig. 5A) and strongly increased the expression of p21 and Noxa (Fig. 5B) in hOGG1-siRNA transfected fibroblasts in a time-course dependent manner compared with those of the control siRNA transfected cells, indicating that p53 contributes to the oxidative stress-induced cellular apoptotic responses in hOGG1-deficient GM00637 cells. Thus, we used p53-siRNA to silence p53 expression to determine the effect on H_2O_2-induced apoptosis in hOGG1-deficient cells. Expression of p53-siRNA resulted in reduced p53 levels and a concomitant decrease in p21 levels (Fig. 5C). Importantly, a decrease in p53 levels in hOGG1-deficient cells resulted in the inhibition of caspase-3 and caspase-7 cleavage in response to H_2O_2 (Fig. 5C). Consistently, determination of caspase-3 and caspase-7 enzymatic activity also gave similar results (Fig. 5D), indicating that the H_2O_2-induced caspase-3/7 activation in hOGG1-deficienct cells is reduced when p53 levels are reduced. We next examined the cell cytotoxicity in response to H_2O_2 treatment under the same experimental conditions (Fig. 5E). Significantly, p53-siRNA caused a large increase in the percentage of viable hOGG1 deficient cells in response to H_2O_2. Taken together, these data suggest that p53 contributes to the H_2O_2-induced apoptosis in hOGG1-depleted GM00637 cells.

To test again the role of p53 in the H_2O_2-mediated cell death in hOGG1-deficient cells, H1299 lung carcinoma cells (p53 null) were transfected with either control GFP-siRNA or hOGG1-siRNA, together with control-pcDNA3.1 vector or p53-pcDNA3.1 expression vector. The expression of hOGG1 was specifically down-regulated up to 25-35 %, and the p53 expression was clearly identified in H1299 p53 null cells based on these transfection (Fig. 5A). Twenty-four hours after transfection, the cells were treated with various H_2O_2 doses, and the cellular sensitivity was determined by MTT assay. As shown in Figure 6B, the hOGG1 silenced H1299 exhibited the slightly decreased cell viability to the H_2O_2 treatment compared with those of control-siRNA transfected cells. However, the cell viability of hOGG1-siRNA plus p53 expression vector transfected H1299 cells was significantly reduced up to less than 10% in response to >400 μM H_2O_2 , indicating that p53 clearly modulates cell viability in response to H_2O_2-oxidative stress in hOGG1-deficient H1299 cells.

Figure 5.

A.

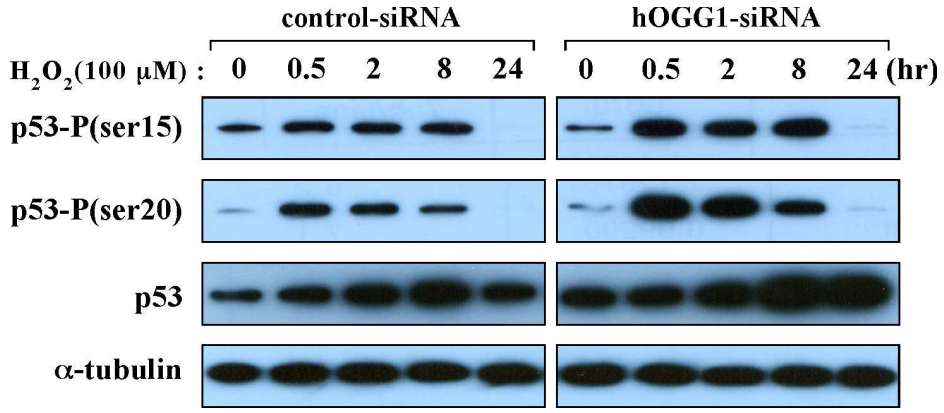

Figure 5.

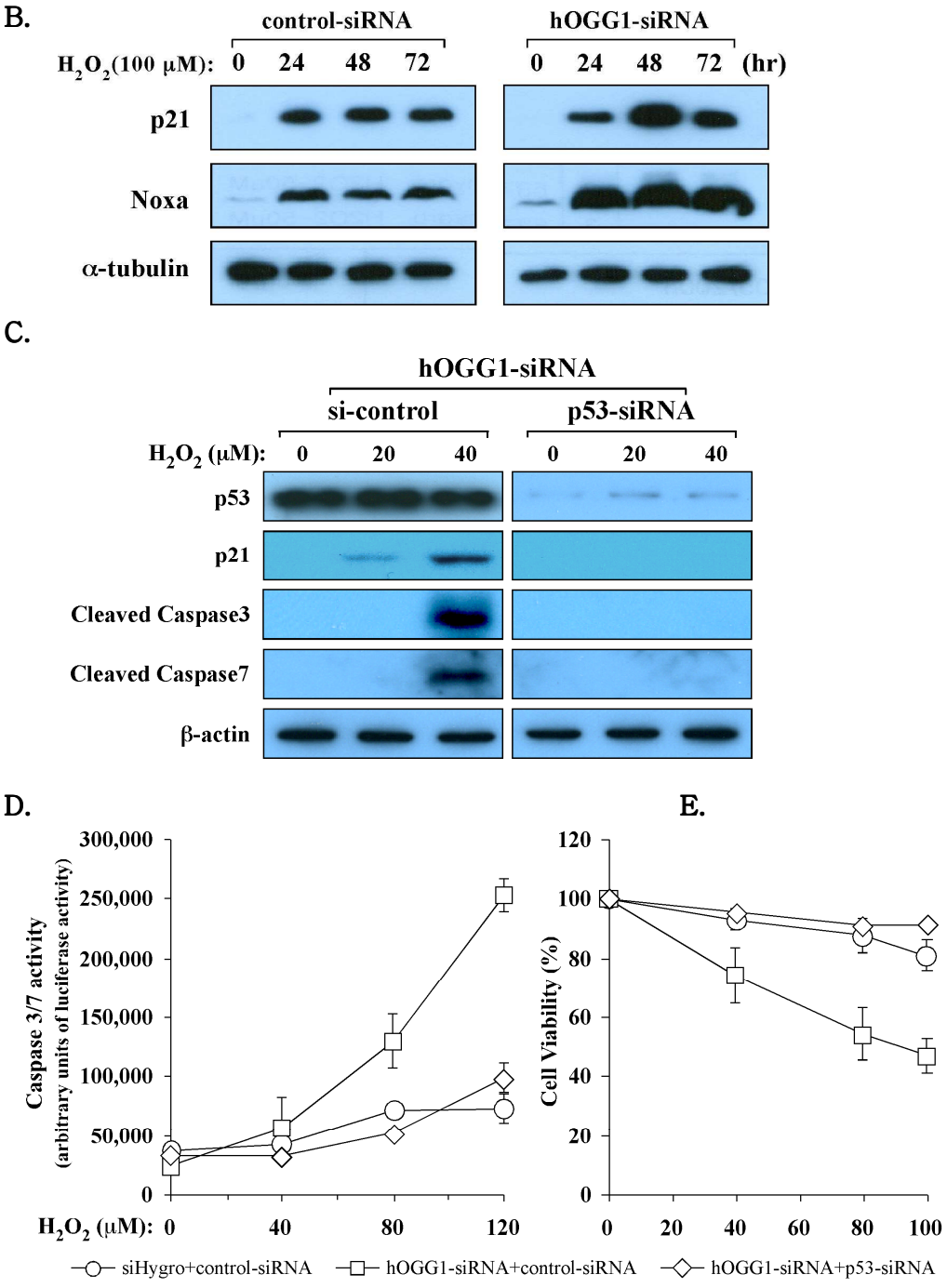
B.
control-siRNA
hOGG1-siRNA
H2O2(100 μM): 0 24 48 72 0 24 48 72 (hr)
p21
Noxa
α-tubulin
C.
hOGG1-siRNA
si-control
p53-siRNA
H2O2 (μM): 0 20 40 0 20 40
p53
p21
Cleaved Caspase3
Cleaved Caspase7
β-actin
D.
Caspase 3/7 activity
(arbitrary units of luciferase activity)
300,000
250,000
200,000
150,000
100,000
50,000
0
H2O2 (μM): 0 40 80 120
E.
Cell Viability (%)
120
100
80
60
40
20
0
0 20 40 60 80 100
siHygro+control-siRNA
hOGG1-siRNA+control-siRNA
hOGG1-siRNA+p53-siRNA

Figure 5. H_2O_2-induced changes in the expression levels of phosphorylated p53, p21 and Noxa, and significant protection by p53-siRNA against H_2O_2-induced cytotoxicity in hOGG1 silencing GM00637 cells. After control-siRNA and hOGG1-siRNA transfected GM00637 cells were treated with 100μM H_2O_2, whole cell lysates were prepared after incubation with H_2O_2 for the indicated times. Western blot analysis was carried out using specific antibodies against p53 and the phosphorylated p53 such as p53-P(ser15) and p53-P(ser20) (A), and using specific antibodies against p21 and Noxa (B). The data was normalized to α-tubulin expression. The results are representative of three independent experiments. (C) After control and hOGG1 deficient GM00637 cells were transfected with p53-siRNA, the cells were then treated with 50 μM H_2O_2 for 24 hours. Whole cell lysates were analyzed by Western blotting using specific antibodies against p53, p21 and caspase 3/7. The data were normalized with β-actin expression. (D) After hOGG1 silencing cells were transfected with control-siRNA and/or p53-siRNA, the cells were treated with the indicated H_2O_2 concentrations. Caspase-3/7 activities were analyzed by Promega Caspase Glo 3/7 kit as described in "Experimental Procedures". The data was plotted as the relative units of luciferase intensity from three separate experiments. All values are expressed as mean ± SD. (E) Cell viability was determined by MTT assay after being treated with different doses of H_2O_2 under the same experimental condition with (D). All values are expressed as mean ± SD.

Figure 6.

A.

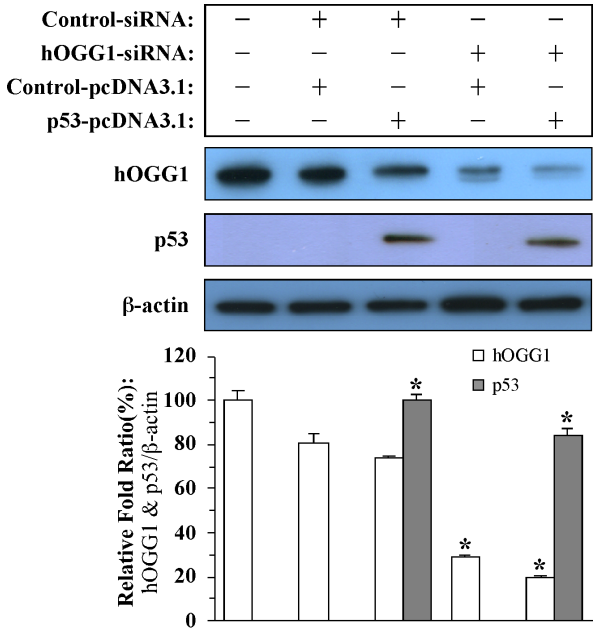

B.

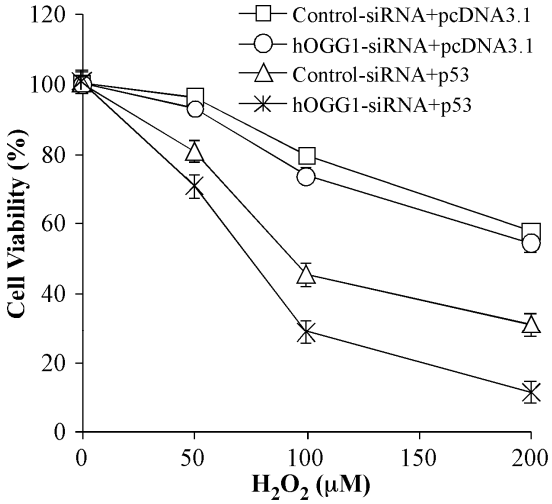

hOGG1 in H1299 cells	p53	Cell viability (%) at 100 μM H_2O_2	
Normal	p53 null	79.4	□
Blocking by siRNA	p53 null	73.6	○
Normal	Overexpression	45.2	△
Blocking by siRNA	Overexpression	28.6	✳

Figure 6. The role of p53 in H_2O_2-mediated cell death of hOGG1-deficient H1299 lung carcinoma cells (p53 null). (A) After H1299 cells were transfected with control- and/or hOGG1-siRNA together with pcDNA3.1 and/or p53-pcDNA3.1 expression vector, whole cell lysates were prepared and Western blot analysis was performed using anti-hOGG1 polyclonal antibodies and anti-p53 antibodies. The data was normalized with β-actin expression and the graphical plot based on the results from Western blot analysis was shown as mean ± SD. Statistically significant differences in the expression of hOGG1 and p53 were determined by the ANOVA with P values given for both the overall (P) and the pair-wise comparisons as indicated by asterisks (*, $P<0.05$). (B) The cells of panel A were cultured to 70-80 % confluence, and treated with the indicated concentration of H_2O_2 for one hour. The media were then changed to fresh one, and the extent of cell death was estimated with MTT assay kit as described in “Experimental Procedure”. All values are expressed as mean ± SD.

4. hOGG1 overexpression plays an important role to protect GM00637 against H_2O_2-induced apoptosis.

GM00637 cells were stably transfected with hOGG1 expression vector or the control empty vector pcDNA3.1, as described previously (71), to determine if hOGG1 overexpression suppresses H_2O_2-induced p53 phosphorylation and apoptosis. The hOGG1 expression was highly augmented in two of hOGG1 expression vector-transfectants (Fig. 7A), and their 8-oxoG cleavage enzyme activities to the 21-mer oligonucleotide containing a single 8-oxoG at nucleotide 13 were significantly increased compared with those of parental and pcDNA3.1 control vector-transfectants (Fig. 7B). The overexpression of hOGG1 decreased the level of p53-phosphorylation in response to 100 μM H_2O_2 in the overall time points (until 8 hours) (Fig. 7C). The effect of overexpressed-hOGG1 on H_2O_2-induced apoptotic responses in GM00637 cells, which had been transfected with either the hOGG1 expression vector or control pcDNA3.1, was determined by estimation of their sub-G_1 DNA contents. As shown in Figure 7D, while the control empty vector transfected cells showed an apoptotic sub-G_1 DNA content ranging from 1.21 % to 18.41 % in response to 0 to 80 μM H_2O_2, the hOGG1 overexpressed cells showed an apoptotic sub-G_1 DNA content ranging from 4.61 % to 10.10 % under the same oxidative stress, indicating that hOGG1 overexpression significantly inhibits the H_2O_2-induced apoptotic responses in GM00637 cells. Taken together, these results show that oxidative stress-induced cellular apoptotic responses are specifically inhibited by hOGG1 overexpression in GM00637 fibroblast cells.

Figure 7.

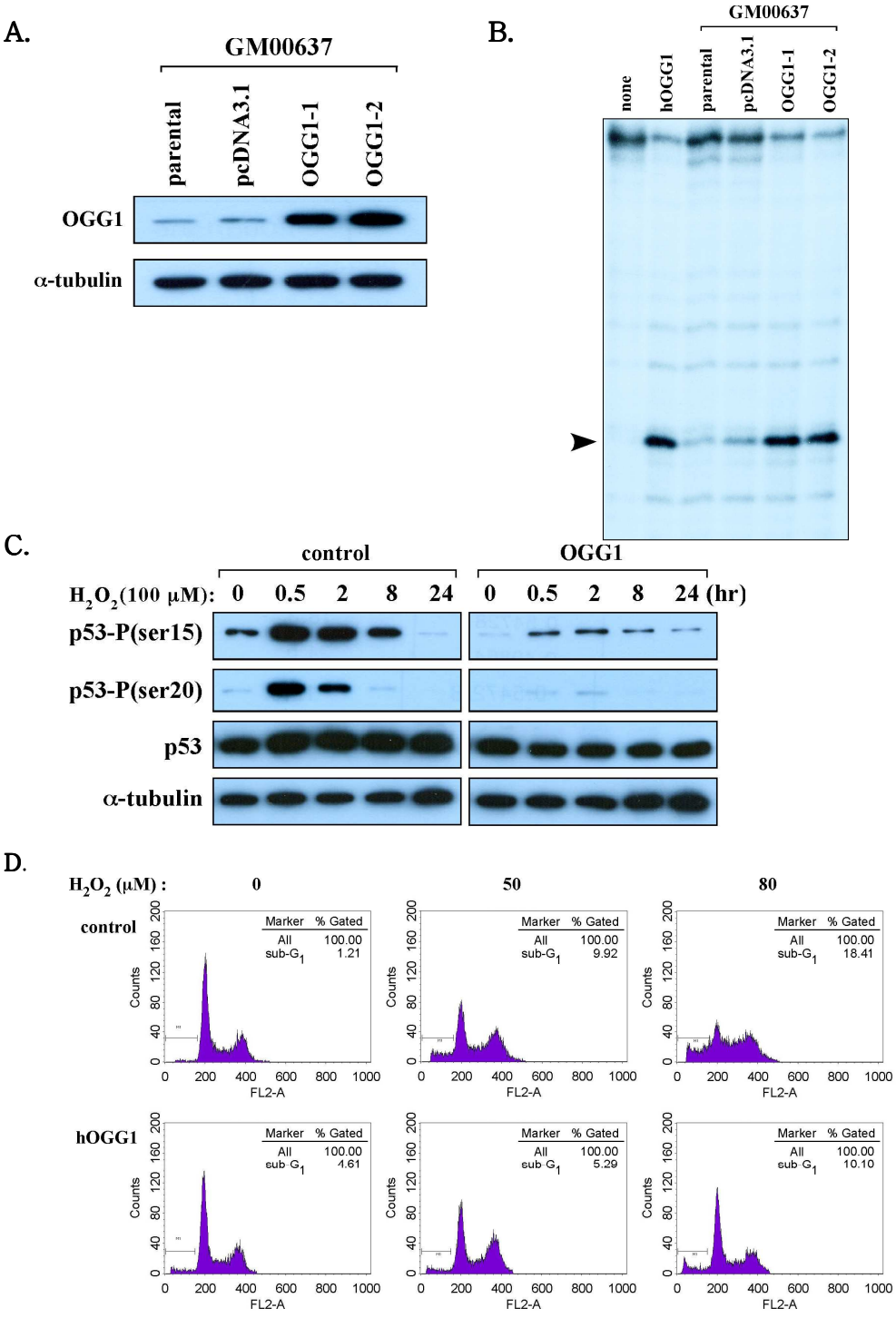
A.
GM00637
parental
pcDNA3.1
OGG1-1
OGG1-2
OGG1
α-tubulin
B.
GM00637
none
hOGG1
parental
pcDNA3.1
OGG1-1
OGG1-2
C.
control
OGG1
H2O2(100 μM): 0 0.5 2 8 24 0 0.5 2 8 24 (hr)
p53-P(ser15)
p53-P(ser20)
p53
α-tubulin
D.
H2O2 (μM) : 0 50 80
control
hOGG1
Marker % Gated
All 100.00
sub-G1 1.21
sub-G1 9.92
sub-G1 18.41
sub-G1 4.61
sub-G1 5.29
sub-G1 10.10
Counts
FL2-A

Figure 7. The overexpression of hOGG1 inhibits apoptotic cell death through p53 phosphorylation in GM00637 cells. (A) After cells were transfected with either empty vector or hOGG1 expression vector, whole cell lysates were then separated by 12 % SDS-PAGE. The expression of hOGG1 was analyzed by Western blotting using anti-hOGG1 polyclonal antibodies. The data was normalized with α-tubulin expression. (B) The OGG1 enzyme activities were analyzed by an 8-oxoG nicking assay using the parental-, empty vector transfected- and hOGG1 expression vector transfected cell lysates, as described in "Experimental Procedures". Purified hOGG1 was used as positive control. (C) After control and hOGG1-overexpressed GM00637 cells were treated with 100μM H_2O_2 for the indicated times, the level of phosphorylated p53s was examined by Western blot analysis using specific antibodies against phosphorylated p53 such as p53-P(ser15) and p53-P(ser20). The data was normalized to α-tubulin expression. This experiment is representative of three independent experiments. (D) Apoptotic sub-G_1 DNA contents were estimated by FACScan analysis using control and/or hOGG1 expression vector transfected GM00637 cells after treatment with the indicated concentration of H_2O_2 for one hour.

5. Involvement of ATM and DNA-PK in the H_2O_2-induced p53 phosphorylation of hOGG1-deficient GM00637 cells.

Several protein kinases have been identified that detect genotoxic stress and initiate signaling pathway through p53 phosphorylation at the serine or threonine residues. Among them, ATM and DNA-PK play an essential role in transmitting DNA damage signals through phosphorylation of p53. Thus, we next examined H_2O_2-induced phosphorylation of the ATM and DNA-PK in hOGG1 deficient and hOGG1 proficient cells. To determine whether these protein kinases participate in checkpoint control in response to H_2O_2-oxidative stress in hOGG1 deficient cells, we treated control-siRNA and hOGG1-siRNA transfected GM00637cells with 100 μM H_2O_2 for 0.5, 2 or 8 hours. As shown in Figure 8A, the H_2O_2 treatment caused a modest increase in ATM and DNA-PK phosphorylation in the control-siRNA transfected GM00637 cells. In contrast, the magnitude of increase in ATM and DNA-PK phosphorylation in response to H_2O_2 treatment was greater hOGG1-siRNA transfected cells. The hOGG1 defect also caused an enhanced Chk1 phosphorylation and an increased expression of Rad51 protein, which are known to be ATM downstream signal molecules, in response to H_2O_2 treatment (Fig. 8A).

To more specifically investigate whether ATM and DNA-PK activation contributes to the oxidative stress-induced p53 phosphorylation in hOGG1 deficient GM00637 cells, we pretreated control-siRNA and hOGG1-siRNA transfected cells either with caffeine, which is a potent ATM inhibitor, or wortmannin, which is a potent DNA-PK inhibitor. As shown in Figure 8B, H_2O_2-induced phosphorylation of p53-Ser15 and p53-Ser20 in hOGG1 deficient cells was significantly reduced by caffeine pretreatment, and the H_2O_2-induced phosphorylation of p53-Ser20 in hOGG1-deficient cells was markedly reduced by wortmannin pretreatment. These results suggest that enhanced p53 phosphorylation of hOGG1 deficient cells following H_2O_2 treatment was caused by an ATM and DNA-PK activation.

Figure 8.

A.

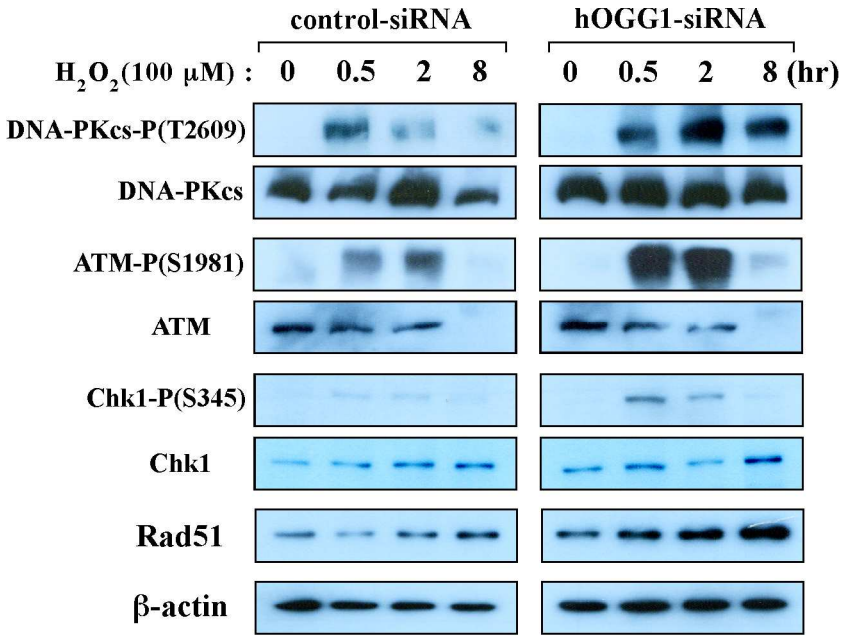
control-siRNA
hOGG1-siRNA
H_2O_2(100 μM) : 0 0.5 2 8 0 0.5 2 8 (hr)
DNA-PKcs-P(T2609)
DNA-PKcs
ATM-P(S1981)
ATM
Chk1-P(S345)
Chk1
Rad51
β-actin

B.

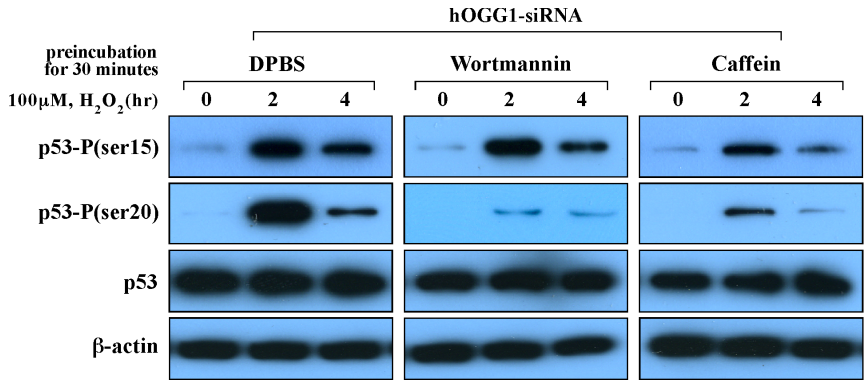
hOGG1-siRNA
preincubation for 30 minutes
DPBS
Wortmannin
Caffein
100μM, H_2O_2(hr)
0 2 4 0 2 4 0 2 4
p53-P(ser15)
p53-P(ser20)
p53
β-actin

Figure 8. The specific activation of DNA-PKcs, ATM, Chk1 and Rad51 was related with H_2O_2-induced p53 phosphorylation in hOGG1-deficient GM00637 cells. (A) After transfection with control- and/or hOGG1-siRNA, the cells were treated with 100μM H_2O_2 for the indicated times. The level of normal and phosphorylated DNA-PKcs, ATM, and Chk1 together with the expression of Rad51 was examined by Western blot analysis using each specific antibodies as described in "Experimental Procedure". (B) After hOGG1 silencing cells were pretreated either with 6mM caffeine and/or 30μM wortmannin for 30 minutes, the cells were then incubated with 100μM H_2O_2 for the indicated times. The level of phosphorylated p53s together with normal p53 was examined by Western blot analysis using specific antibodies against all related proteins. This experiment is representative of three independent experiments. All data were normalized tọ β-actin expression.

6. Array CGH characterization of the hOGG1 deficient fibroblasts following H_2O_2 treatment.

In order to identify the genetic copy number changes associated with the knockdown of hOGG1, an array comparative genome hybridization (array CGH) was performed using the genomic DNA derived from hOGG1 knockdown cells and control cells, which had been treated with 10 μM H_2O_2 for 4 weeks (Fig. 9A) and 8 weeks (Fig. 9B). The array CGH is a powerful molecular cytogenetic method, which enables genome-wide screening for copy-number losses and gains of the chromosomal parts by single hybridization (72). Currently, array-based comparative genomic hybridization (array CGH) using bacterial artificial chromosome (BAC) arrays spanning the entire human genome is used to examine genomic alterations (73). The advancements in genome-wide BAC array CGH technology have contributed to the understanding of the underlying genetic changes that correspond to disease progression. The extent and location of numerical changes in the DNA content induced by H_2O_2 in the control and hOGG1-deficient cells were examined. The H_2O_2-treated hOGG1 deficient cells showed more significantly changes in the copy number of large regions of the chromosomes, compared with the H_2O_2-treated control cells. The array CGH data provided a precise measurement of the level of gains ($\log_2$ ratio>0.225: green arrows) and losses ($\log_2$ ratio less than -0.225, red arrows) of all chromosomes. The array CGH data revealed 1q44 (gene loci of LOC339529, ZNF238 and LOC440742) and 7q36.3 (gene loci of VIPR2 and LOC442366) of chromosomal losses, and 17q11.2 (gene loci of MYO18A), 18q23 (gene locus of FLJ25715 and CTDP1) and Xq13.1 (gene loci of PJA1 and RP13-153N15.1) of chromosomal gains, respectively. These results suggest that the suppression of hOGG1 repair activity can lead to an alteration of the gene copy number in response to H_2O_2-oxidative stress.

Figure 9.

A.

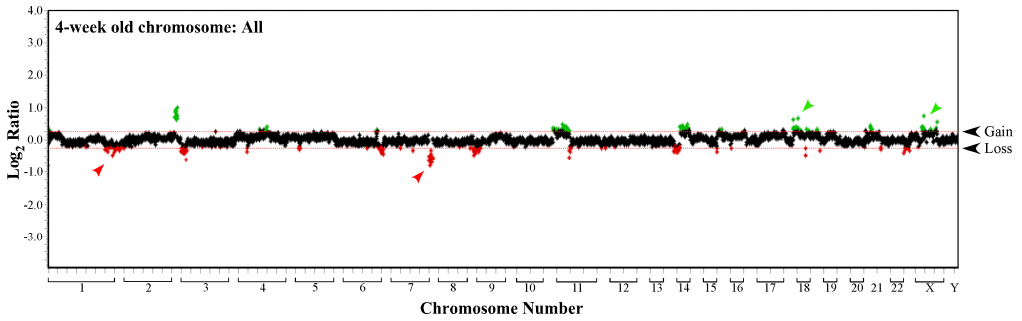

B.

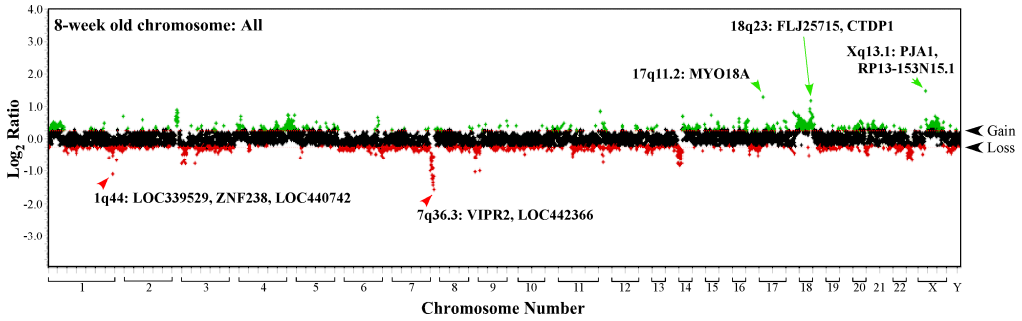

Figure 9. Array Comparative Genomic Hybridization (array CGH) of the control-siRNA and hOGG1-siRNA transfected GM00637 cells. The cells were stably transfected with control- and/or hOGG1-siRNA, and then treated with 10 mM H_2O_2 for 4 weeks (A) and 8 weeks (B). The genomic DNA was extracted and digested with DpnII, followed by random prime labeling with Cy3 for the test DNA derived from hOGG1-siRNA transfected cells and Cy5 for the reference DNA from control-siRNA transfected cells. Whole-genome array CGH profiles showed $\log_2$-transformed hybridization ratios of the test DNA versus the control-reference DNA. Representative chromosomal gains ($\log_2$ ratio>0.25: green arrows) and losses ($\log_2$ ratio less than -0.25, red arrows) are also indicated along with their chromosomal locations and candidate genes.

Figure 10.

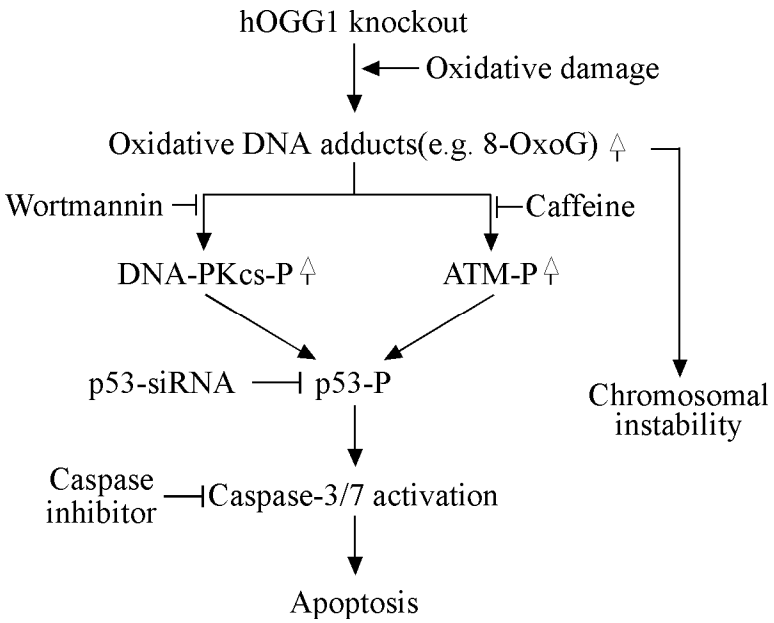

Figure 10. p53-mediated apoptotic pathway in response to H_2O_2 exposure in hOGG1 silencing GM00637 cells.

II. hMTH1 knockdown by small interfering RNA increases oxidative stress-induced cell death and chromosomal instability in human fibroblast GM00637 cells

7. The inhibition of hMTH1 expression by siRNA leads to an increase of H_2O_2-induced cytotoxicity in GM00637.

The biological role of hMTH1 in response to oxidative stress was determined using hMTH1-siRNA transfectants, which contain 21-bp hMTH1 targeting RNA duplexes to inhibit hMTH1 expression in human fibroblast GM00637 cells. The human fibroblast GM00637 cells were stably transfected with control-siRNA or hMTH1-specific siRNA. Semiquantitative RT-PCR was carried out using hMTH1 specific synthetic primers, as described in “Materials and Methods”, to determine if the constitutive expression of hMTH1 is specifically inhibited by hMTH1-siRNA in cultured human fibroblast GM00637 cells. Three different hMTH1-siRNA completely blocked the normal mRNA expression of hMTH1 in the parental GM00637 cells (Fig. 11A). Western blotting was performed to determine if the inhibition of hMTH1 mRNA corresponds to that in the hMTH1 protein level. As demonstrated in Figure 11B, hMTH1 protein expression was also specifically inhibited by hMTH1-siRNA transfection.

We next investigated the effect of hMTH1 on the H_2O_2-induced cytotoxicity of the parental cells, stable control-siRNA and hMTH1-siRNA cells. The cell viability of hMTH1-siRNA cells was significantly lower than that of either control-siRNA cells or parental cells (Fig. 12A), indicating that the inhibition of hMTH1 expression reduces the cell viability of fibroblasts in response to oxidative stress. In order to determine if hMTH1 depletion has an effect on H_2O_2-induced apoptosis, we analyzed sub-G_1 DNA contents of control-siRNA and hMTH1-siRNA stable cells by flow cytometry after staining their

nuclei with propidium iodide. As shown in Figure 12B, the control-siRNA cells, which were treated with 0 to 80 μM H_2O_2, showed apoptotic sub-G_1 DNA contents from 3.38 % to 11.96 %. However, hMTH1-siRNA increased the proportion of apoptotic sub-G_1 DNA content. The apoptotic sub-G_1 DNA contents of hMTH1-siRNA transfected cells ranged from 6.17 % to 23.94 % under similar same oxidative stress. These results suggest that the suppression of hMTH1 expression triggers apoptosis in response to H_2O_2 in human fibroblasts GM00637.

Figure 11.

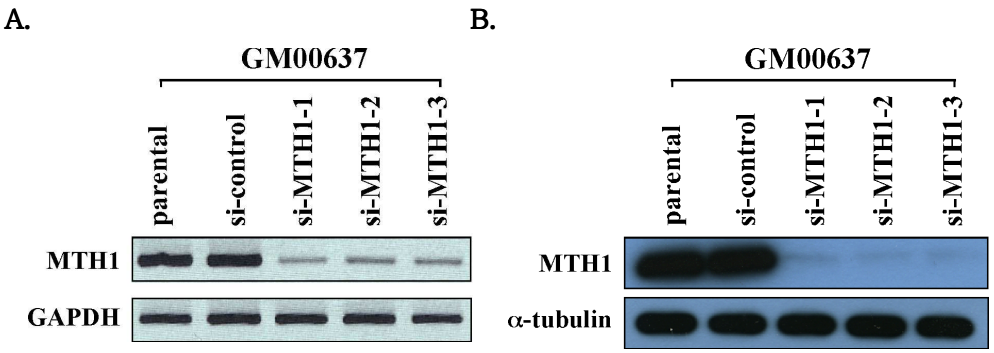

Figure 11. siRNA-mediated down-regulation of hMTH1 in human fibroblast GM00637 cells. The human fibroblast GM00637 cells were stably transfected with the control-siRNA and hMTH1-specific siRNA. The expression of hMTH1 was then analyzed by RT-PCR using hMTH1 specific synthetic primers (A), and by Western blot using anti-hMTH1 polyclonal antibodies (B). The data was normalized to GAPDH and α-tubulin, respectively.

Figure 12.

A.

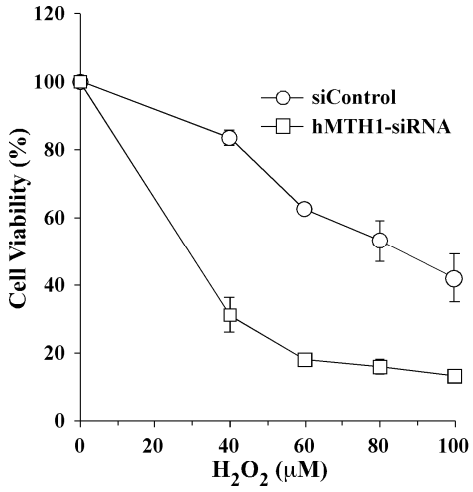
Cell Viability (%)
120
100
80
60
40
20
0
siControl
hMTH1-siRNA
0
20
40
60
80
100
H_2O_2 (μM)

B.

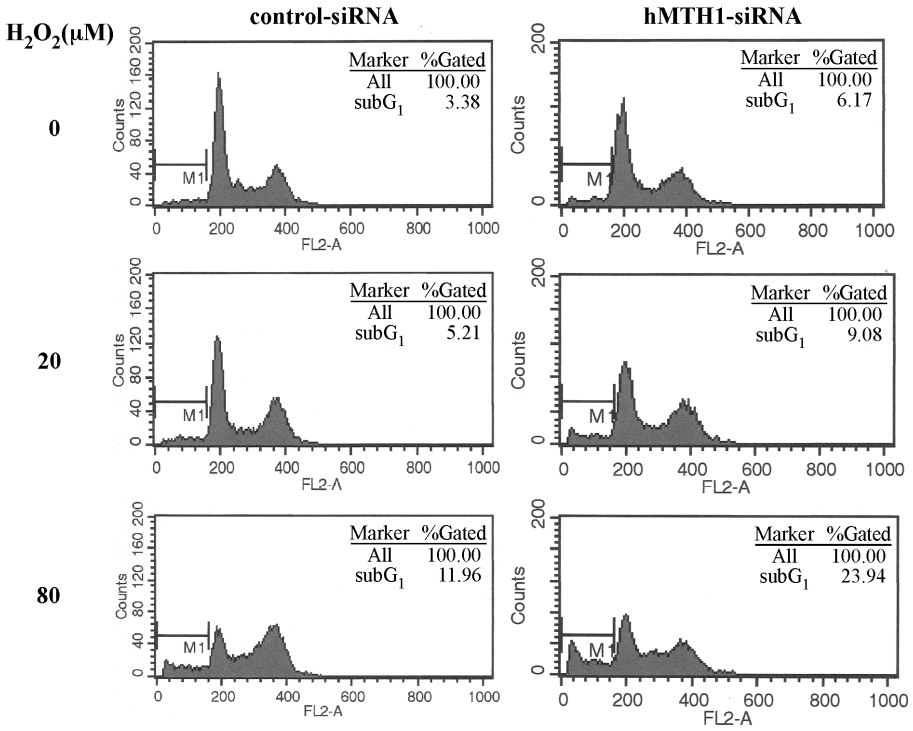
H_2O_2(μM)
control-siRNA
hMTH1-siRNA
0
20
80
Marker %Gated
All 100.00
subG1 3.38
subG1 6.17
subG1 5.21
subG1 9.08
subG1 11.96
subG1 23.94
M1
Counts
FL2-A

Figure 12. hMTH1 knockdown increases the level of H_2O_2-induced cytotoxicity in GM00637 cells. (A) The parental, control-siRNA and hMTH1-siRNA cells were cultured to 70-80% confluence, and treated with the indicated H_2O_2 concentration and the extent of cell death was measured by Trypan blue exclusion 24 hours after treatment. The cell viability was determined to be the percentage of total cell number that remained unstained. The values represent the means ± S.D. from six separate experiments. (B) The apoptotic Sub-G_1 DNA contents were estimated by FACScan analysis after being treated with the indicated H_2O_2 concentration under the same experimental condition with (A).

8. hMTH1 knockdown augments the expression of Noxa and caspase-3/7 activation, but it does not affect p53-phosphorylation in response to H_2O_2-oxidative stress.

p53 is stabilized and rapidly activated in many cell types in response to a variety of death stimuli in many cell types (118). Transactivation of proapoptotic proteins is an important mechanism through which p53 promotes caspase activation (119). In order to determine if p53 is involved in the H_2O_2-mediated apoptosis of hMTH1-depleted cells, we examined the levels of p53 phosphorylation and its downstream target proteins such as p21 and Noxa were examined in control-siRNA and hMTH1-siRNA after a treatment with 30μM H_2O_2. As shown in Figure 13A, the H_2O_2 treatment increase the expression of Noxa in hMTH1-siRNA compared to those in control-siRNA cells in a time-course dependent manner. However, the level of p53 phosphorylation such as p53-P(ser15) and p53-P(ser20) induced by the H_2O_2-oxidative stress was similar in hMTH1-siRNA and its control.

The activation of caspases is one of the major process in DNA damage-induced apoptosis. In order to understand the protective effect of hMTH1 on H_2O_2-induced apoptosis in GM00637 cells, the levels of caspase-3 and caspase-7, which are the key caspases in the apoptotic pathways, were examined by western blot analysis in control-siRNA and hMTH1-siRNA cells. As demonstrated in Figure 13B, the H_2O_2 treatment induced the cleavage of inactive 32kDa procaspase-3 into smaller detectable active forms of caspase-3 such as 14 kDa and/or 22 kDa fragments, and induced the cleavage of inactive 32 kDa procaspase-7 into detectable active forms of caspase-7 such as 26 kDa fragment. The cleavage of procaspase-3 and procaspase-7 into the active subunit was clearly observed in the hMTH1-siRNA from 24hr after H_2O_2 treatment (Fig. 13B). The observation of activated (cleaved) caspase-3 and caspase-7 is consistent with the data obtained from their enzymatic activity assay, which were performed using a Promega CaspaseGlo 3/7 kit, as described in “Materials and Methods.” As demonstrated in Figure

13C, the enhanced caspase-3 and caspase-7 activity induced by H_2O_2-treatment of hMTH1-siRNA was significantly inhibited by a treatment with caspase inhibitors. Furthermore, the level of cell viability in the hMTH1-siRNA was almost completely reversed to those of the control-siRNA transfected cells after the treatment with caspase-3 and caspase-7 inhibitors (Fig. 13C). This indicates that the caspase-3/7 activation plays an important role in the development of H_2O_2-induced apoptosis in hMTH1-depleted human fibroblast GM00637 cells.

Figure 11.

A.

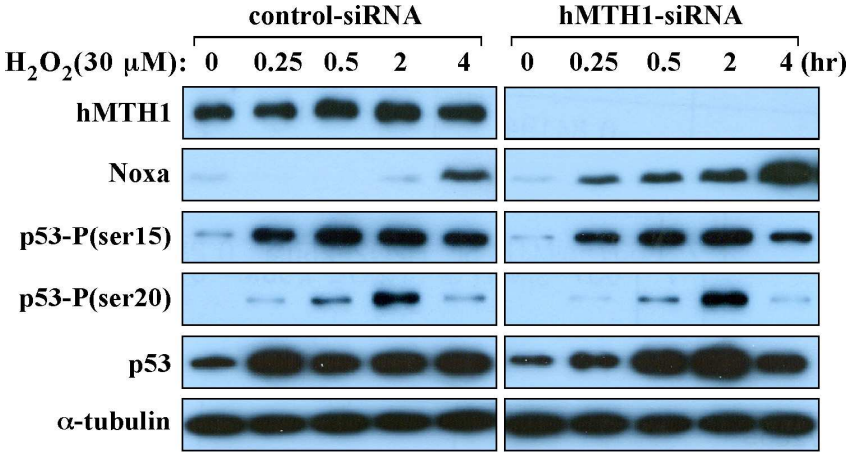

B.

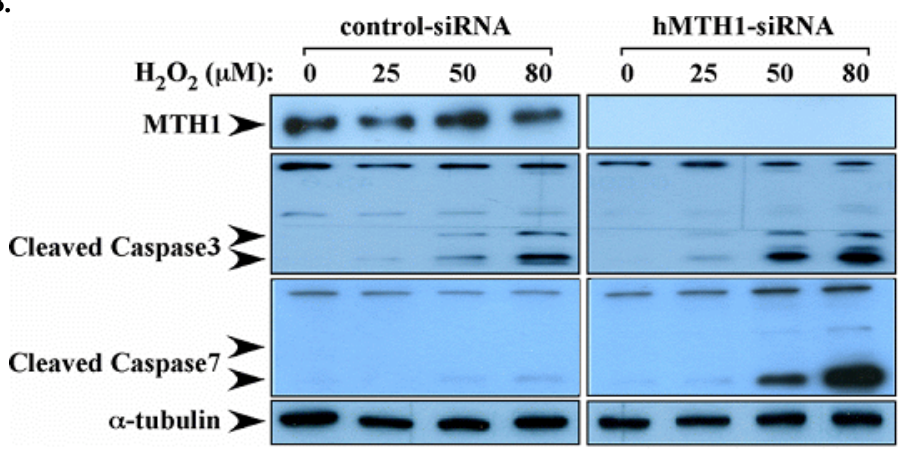

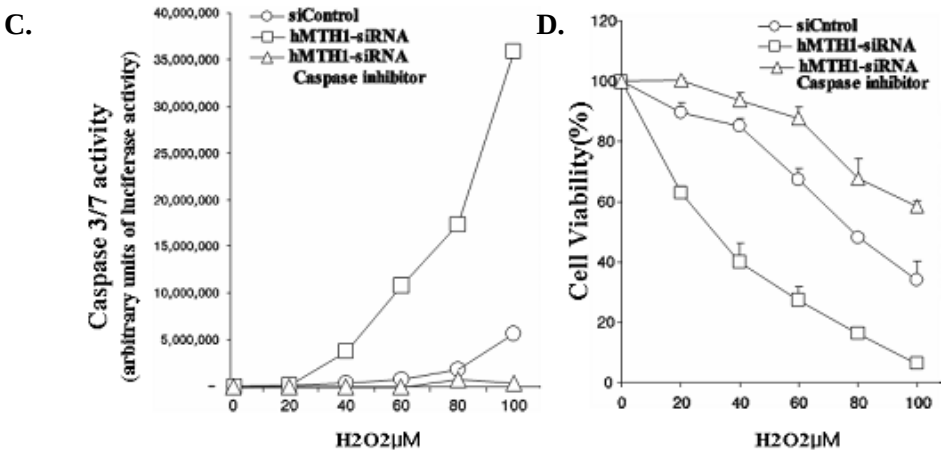

Figure 13. H_2O_2 increases the expression level of Noxa and caspase-3/7 activation, but does not affect the level of p53 phosphorylation in hMTH1-siRNA. (A) Control-siRNA and hMTH1-siRNA cells were treated with 30μM H_2O_2. The whole cell lysates were then prepared at the indicated time points, and Western blot analysis was performed using specific antibodies against hMTH1, Noxa, p53 and phosphorylated p53 such as p53-P(ser15) and p53-P(ser20). The membrane was stripped and probed with anti-α-tubulin antibody to normalize the variation in protein loading. The results are representative of three independent experiments. (B) The cells were treated with the indicated H_2O_2 concentration for one hour, and the level of activated (cleaved at arrow points) caspase 3/7 was determined by Western blot analysis using specific antibodies for caspase 3/7. The data was normalized to α-tubulin. All results are representatives from three separate experiments. (C) After control-siRNA and hMTH1-siRNA cells were treated with/without 60μM caspase inhibitor and the indicated concentration of H_2O_2, caspase-3/7 activities were analyzed using Promega Caspase Glo 3/7 kit as described in "Experimental Procedures". The data was plotted as the relative units of luciferase intensity of three separate experiments. All values are expressed as mean ± SD. (D) Cell viability was determined by MTT assay after being treated with different doses of H_2O_2 under the same experimental condition with (C). All values are expressed as mean ± SD.

9. Noxa and p53 knockdown in hMTH1 deficient cells restores the decreased cell viability in response to H_2O_2-oxidative stress.

We further investigated the role of Noxa in H_2O_2-induced cell death using hMTH1 deficient cells, which were specifically inhibited the expression of Noxa by Noxa-siRNA transfection (Fig.14A). The H_2O_2-induced expression of Noxa in hMTH1-siRNA was significantly inhibited at the level of mRNA expression (Fig. 14A) and the protein level (Fig. 14B) by Noxa-siRNA transfection. The decreased cell viability derived from hMTH1 deficient cells was restored to 80% of the normal control by the Noxa knockdown using Noxa-siRNA transfection (Fig. 14C). Therefore, these results suggest that the expression of Noxa contributes to the H_2O_2-induced cell death in hMTH1-depleted GM00637 cells.

Noxa expression pathways involved are still not completely understood. Two majar signaling pathways leading to Noxa expression have been identified. One is p53-dependent, resulting from phosphorylation of p53 at ser-15 by ATM kinase(120-122). The other is E2F1 dependent, Cyclin D: cdk4/6 mediated phosphorylation of Rb and dissociation of Rb from the Rb:E2F:DP-1 complexes(123, 124). In order to determine the requirement of p53 activation for H_2O_2-induced Noxa expression and apoptosis in hMTH1-depleted cells. we used p53-siRNA to silence p53 expression to determine the effect on H_2O_2-induced apoptosis in hMTH1-deficient cells. The H_2O_2-induced expression of Noxa in hMTH1-siRNA was inhibited at the level of protein (Fig.14B) by p53-siRNA transfection. We next examined the cell cytotoxicity in response to H_2O_2 treatment under the same experimental conditions (Fig. 14C). Significantly, p53-siRNA caused a large increase in the percentage of viable hMTH1 deficient cells in response to H_2O_2. The decreased cell viability derived from hMTH1 deficient cells was restored to 90% of the normal control by the p53 knockdown using p53-siRNA transfection (Fig. 14C). Therefore, these results suggest that the p53 contributes to the H_2O_2-induced Noxa expression and cell death in hMTH1-depleted GM00637 cells but how to expression of the Noxa protein by p53 still not know.

Figure 14.

A.

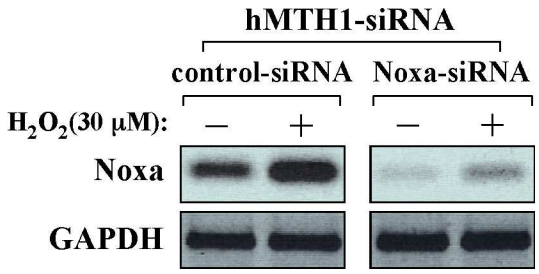

B.

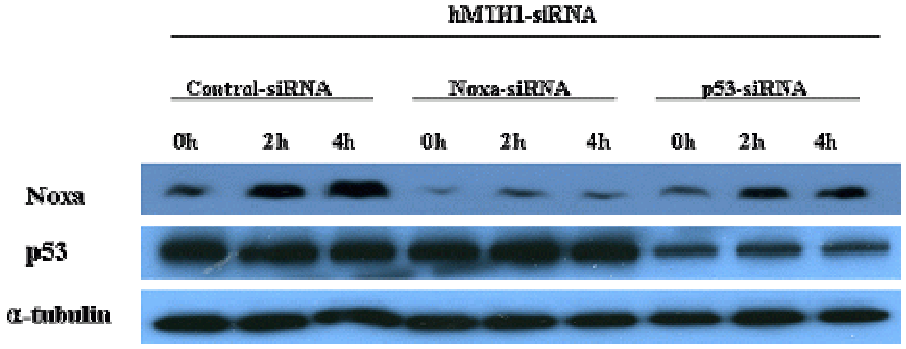

C.

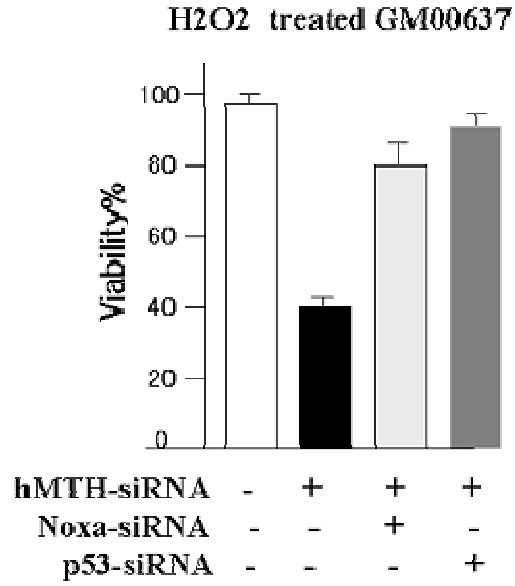

Figure 14. Noxa ans p53 siRNA provides significant protection against H_2O_2-induced cytotoxicity in hMTH1 silencing GM00637 cells. The control and hMTH1-deficient GM00637 cells were transfected with Noxa-siRNA or p53-siRNA . The cells were then treated with 30μM H_2O_2. The whole cell lysates were analyzed by comparative RT-PCR using Noxa-specific primers (A) and by Western blotting using specific antibodies against Noxa , p53 (B). The data was normalized to GAPDH and α-tubulin, respectively. This experiment is representative of three independent experiments. (C) The control and hMTH1-deficient GM00637 cells were transfected with Noxa-siRNA or p53-siRNA or control-siRNA. The cell viability after exposure to 30μM H_2O_2 was determined by MTT assay. This experiment is representative of three independent experiments. All values are expressed as mean ± SD.

10. Requirement of p53 for Noxa expression and H_2O_2-induced cell death in hMTH1 deficient cells.

In response to a variety of death stimuli, p53 is stabilized and rapidly activated in many cell types (69). One important mechanism through which p53 promotes caspase activation is by transactivation of the proapoptotic proteins (70). To test again the role of p53 in the H_2O_2-mediated cell death in hMTH1-deficient cells, H1299(p53 null) lung carcinoma cells were stably transfected with either control GFP-siRNA or hMTH1-siRNA. Semi-quantitative RT-PCR was carried out using hMTH1 specific synthetic primers, as described in "Materials and Methods", to determine if the constitutive expression of hMTH1 is specifically inhibited by hMTH1-siRNA in cultured H1299(p53 null) lung carcinoma cells. Two different hMTH1-siRNA completely blocked the normal mRNA expression of hMTH1 in the parental H1299 cells (Fig.15A). Western blotting was performed to determine if the inhibition of hMTH1 mRNA corresponds to that in the hMTH1 protein level. As demonstrated in Figure 15B, hMTH1 protein expression was also specifically inhibited by hMTH1-siRNA transfection. H1299-siGFPsiRNA and H1299-hMTH1siRNA cells were treated with different does of H_2O_2 , and the cellular sensitivity was determined by MTT assay. As shown in Figure 15C, the hMTH1 silenced H1299 exhibited the slightly decreased cell viability to the H_2O_2 treatment compared with those of GFP-siRNA cells. The p53 expression was clearly identified in H1299 p53 null cells based on these transfection (Fig.15E). Twenty-four hours after transfection, the cells were treated with various cellular sensitivity was determined by MTT assay. However, the cell viability of hMTH1-siRNA plus p53 expression vector transfected H1299 cells was significantly reduced up to less than 10% in response to >200 μM H_2O_2(Fig.15D), indicating that p53 clearly modulates cell viability in response to H_2O_2-oxidative stress in hMTH1-deficient H1299 cells. In order to determine the requirement of p53 activation for H_2O_2-induced apoptosis in hMTH1-depleted cells, we investigated the activation of p53

and its downstream target protein such as p21 and Noxa in hMTH1-siRNA transfected p53 after a treatment with 800 μM H_2O_2. As shown in Figure 15, significantly expressed p53 (Fig.15E) and strongly increased the expression of p21 and Noxa (Fig.15E) in hMTH1-siRNA transfected cells in a time-course dependent manner compared with those of the control pcdna3.1 vector transfected cells, indicating that p53 contributes to the cellular apoptotic responses in hMTH1-deficient H1299 cells.

Figure 15.

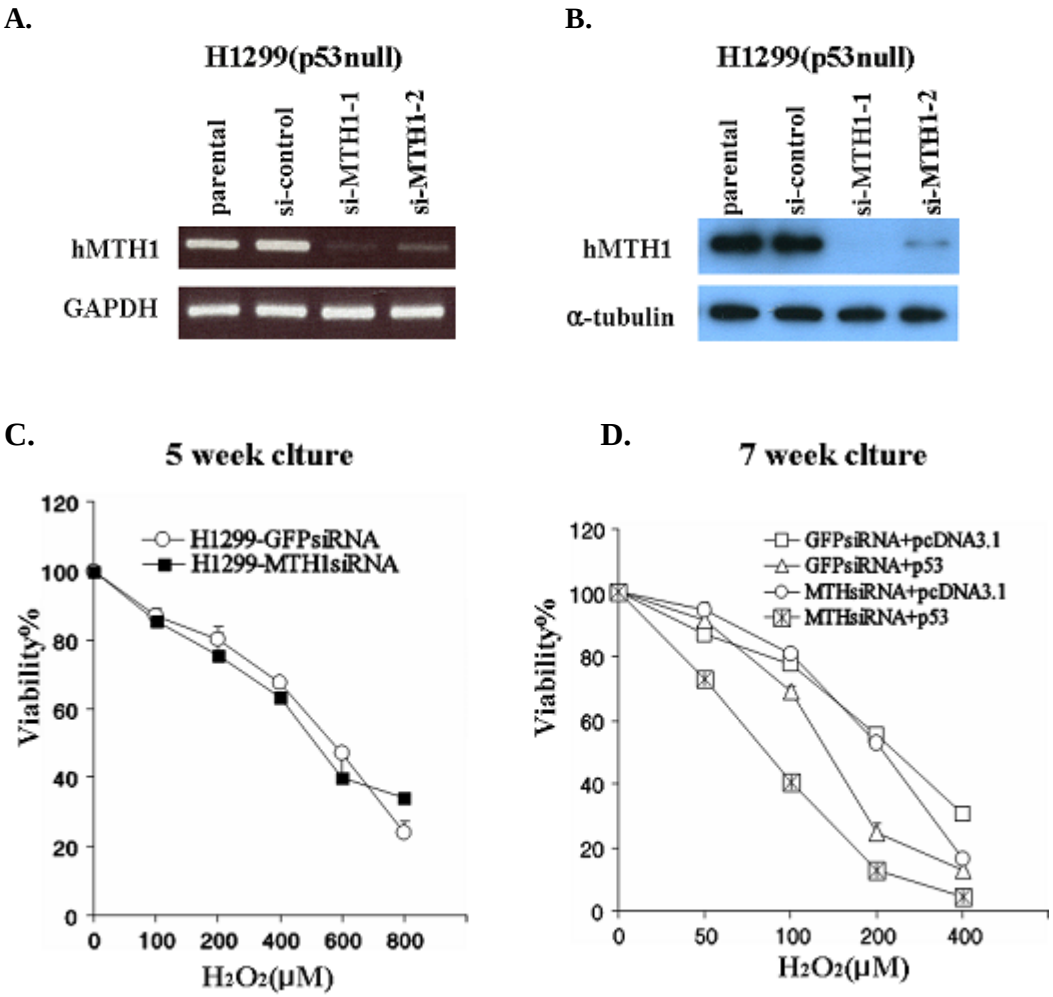

Figure 15.

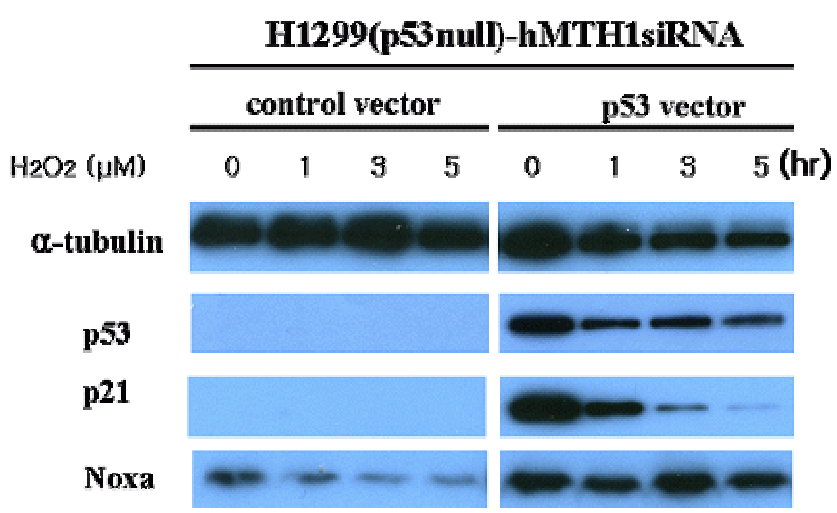

Fig 15. **The role of p53 in H_2O_2-mediated cell death of hMTH1-deficient H1299 lung carcinoma cells (p53 null).** The H1299 lung carcinoma cells were stably transfected with the control-siRNA and hMTH1-specific siRNA. The expression of hMTH1 was then analyzed by RT-PCR using hMTH1 specific synthetic primers (A), and by Western blot using anti- hMTH1 polyclonal antibodies (B). The data was normalized to GAPDH and α-tubulin, respectively. (C) The cells of panel A were cultured to 70-80 % confluence, and treated with the indicated concentration of H_2O_2 for 24hr. The cell death was estimated with MTT assay kit as described in "Experimental Procedure". (D) After the cells of panel C were transfected with pcDNA3.1 and/or p53-pcDNA3.1 expression vector, and treated with different of H_2O_2 concentrations. The cell viability was determined by MTT assay. All values are expressed as mean ± SD. (E) After the cells of panel C(H1299- hMTH1-siRNA) cells were transfected with pcDNA3.1 and/or p53-pcDNA3.1 expression vector, and treated with different of H_2O_2 800μM. The whole cell lysates were prepared and Western blot analysis was performed using anti-p53 antibodies and anti-p21 antibodies and anti-Noxa antibodies. The data was normalized with α-tubulin expression.

11. DNA damage accumulation induced intra cellular ROS and apoptosis.

DNA repair gene silencing for long-term in human cells highly sensitive, suggestive of irreversible damage following long-term DNA repair gene silencing(125). Accumulation of nuclear and mitochondrial DNA damage is though to be particularly deleterious in cells, which cannot be replaced through cell division. Base excision repair(BER) is the main pathway for the removal of small DNA base modifications, which are generated as products of normal metabolism and accumulate with age in various experimental models. (126). Several groups have documented the accumulation of oxidative DNA damage during aging in the mammalian brain (127-131) found that oxidative DNA damage accumulates preferentially in the promoter regions of several genes involved in synaptic plasticity, vesicular transport and mitochondrial function. Once DNA damage has been generated, it is the role of cellular repair systems to prevents its accumulation. However, studies have shown that aging is associated with a general reduction in DNA repair capacity. Overall nuclear and mitochondrial BER activities , measured using an in vitro uracil-initiated BER assay, were shown to gradually decline with age, reaching 80-85% lower activity in 30month old rats compared with 17day old rat. They observed a significant age dependent decrease in uracil, 8-oxoG and 5-OH-C incision activities in the mitochondria of all brain regions, whereas variable patterns of changes were seen in nuclei(132,133). mtDNA is believed to be particularly sensitive to oxidative agents due to its proximity to the inner mitochondrial membrane, where oxidants are formed, and to the lack of protective histones(134). In addition , oxidative damage to mtDNA in the heart and brain is inversely related to maximum lifespan of mammals(135,136),suggesting that accumulation of mtDNA damage plays a causative role in the various disorders that are associated with aging, cancer and neurodegeneration. That studies suggest that modifications in mtDNA repair may contribute to the accumulation of DNA damage associated with aging. It is imported to note that age-related accumulation of DNA damage

and alteration in DNA repair processes in the mammalian. To test cell senstivity in long-term cultured hMTH1-deficient cells, GM00637 cells and control-siRNA , hMTH1-sRNA cells were grown for 12weeks. The cell viability of the hMTH1-siRNA was significantly lower than that of the control-siRNA cells in not treated H_2O_2 (Fig.16A). In order to determine if hMTH1 depletion has an effect on damage accumulation-induced apoptosis, we analyzed sub-G_1 DNA contents of control-siRNA and parental cells, hMTH1-siRNA stable cells by flow cytometry after staining their nuclei with propidium iodide. As shown in Figure 16C, the control-siRNA cells and parental cells showed apoptotic sub-G_1 DNA contents 3.12 % and 3% . However, hMTH1-siRNA increased the proportion of apoptotic sub-G_1 DNA content. The apoptotic sub-G_1 DNA contents of hMTH1-siRNA cells 40.34%. These results suggest that the suppression of hMTH1 expression triggers apoptosis in response to age. This finding suggests that reduction in DNA repair capacity is related to maximum life span. In order to determine if p53 is involved in the apoptosis of hMTH1-depleted cells, we examined the levels of p53 phosphorylation were examined in parental cells and hMTH1-siRNA cells after long-term cultured. As shown in Figure 16D, the grown increase the level of p53 phosphorylation such as p53-P(ser15) and p53-P(ser37) in hMTH1-siRNA compared to those in parental cells in a time-course dependent manner. The activation of caspases is one of the major process in DNA damage-induced apoptosis. As demonstrated in Figure 16D, the grown induced the cleavage of inactive 32 kDa procaspase-7 into detectable active forms of caspase-7 such as 26 kDa fragment. The cleavage of procaspase-7 into the active subunit was clearly observed in the hMTH1-siRNA from 12weeks after grown(Fig.16D). ROS are continuously formed as consequence of normal cellular metabolism and in response to environmental factors such as UV light, ionizing radiation, heat, and pollution. This ROS production may significantly increase when cells are under metabolic stress and/or have mtDNA mutations. These endogenous ROS may damage mtDNA, leading to increased mtDNA mutations, which in turn cause malfunction of the respiratory chain components encoded by mtDNA, and thus further

increase electron leakage and ROS generation. This would result in an amplification of ROS stess and cause further damage to mtDNA and nDNA, leading to genetic instability in cells(137). Earlier studies have demonstrated that apoptotic characteristics were correlated with reactive oxygen species (ROS) production, lipid peroxidation, p53 and Noxa expression, and mitochondrial cytochrome c release following treatment of apoptosis induced agent(138). DNA damage stresses cause an increase in cellular level of ROS(139-141). P53 activation is likely involved, since p53 induces several known genes involved in ROS generation(142). We investigated the effect of DNA repair gene silencing for long-term on intracellular ROS accumulation by measuring the amount of fluorescent DCF produced from the oxidative reaction of DCF-DA. The long-term hMTH1 deficient cells(12weeks) significant increased in intracellular ROS generation compared with control-siRNA cells and parental cells(Fig 16B). p53-independent events such as NOXA expression may be involved in apoptotic processes through a complex network of p53-dependent and –independent transcriptional regulation and protein interactions. In an earlier related study, they found that the apoptotic response we reduced and delayed in p53 mutant cells compared with p53 wild-type cells(143). This may in part be due to the direct involvement of p53 as a transcription factor as well as a “damage sensor” in the regulation of cell proliferation and death. In addition, the mutant p53 cells may also exhibit so-called “gain of function” effects in apoptosis(144-146). We investigated the effect of p53 protein for long-term DNA repair gene silencing on cell viability treated with H_2O_2. The H1299 lung carcinoma and H1299-GFPsiRNA and H1299-hMTHsiRNA cells were grown for 12weeks. The cells were treated with different does of H_2O_2, and the cellular sensitivity was determined by MTT assay. The cell viability of the hMTH1-siRNA was significantly lower than that of the control-siRNA cells and parental cells(Fig. 16E). DNA repair gene silencing for long-term in human cells highly sensitive, suggestive of irreversible damage following long-term DNA repair gene silencing. Thus, we propose that there are at least two different pathways of apoptosis: one mediated through p53 activation in response to

ROS stresses and the other through p53 independent in response to DNA damage accumulation.

Figure 16.

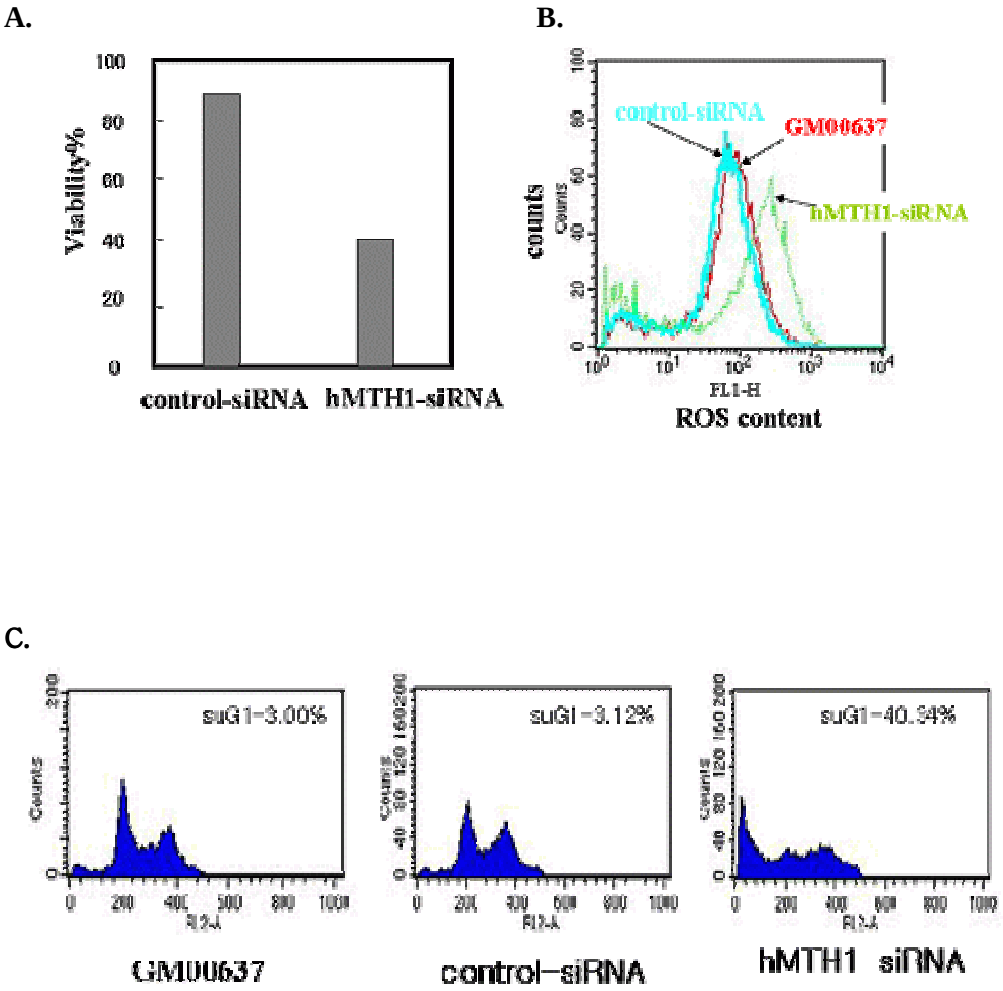

Figure 16.

D.

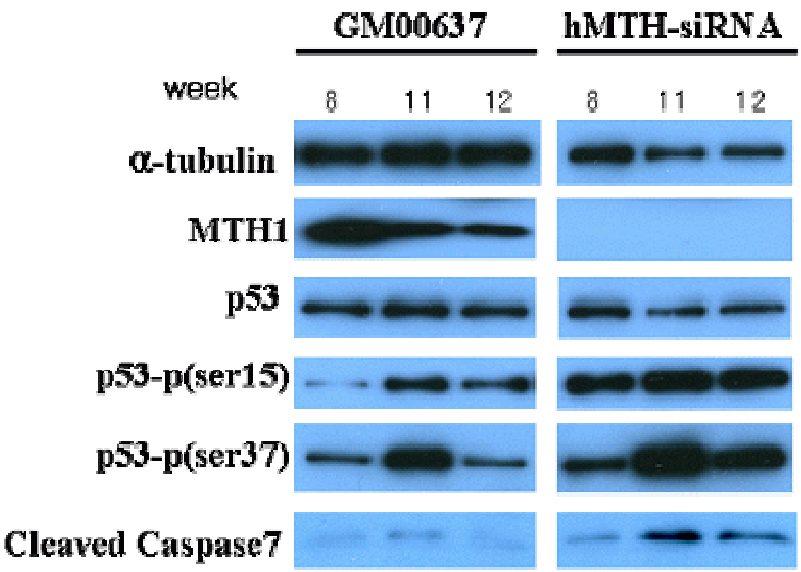
GM00637
hMTH-siRNA
week
8
11
12
8
11
12
α-tubulin
MTH1
p53
p53-p(ser15)
p53-p(ser37)
Cleaved Caspase7

E.

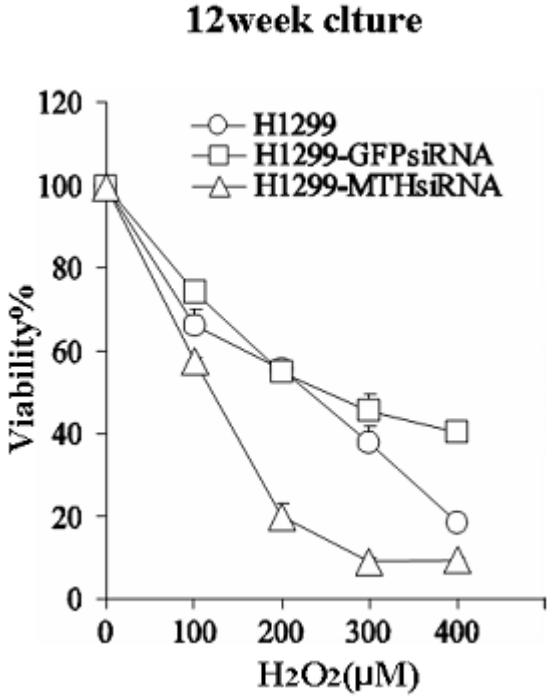
12week clture
H1299
H1299-GFPsiRNA
H1299-MTHsiRNA
Viability%
120
100
80
60
40
20
0
0
100
200
300
400
H2O2(μM)

Figure 16. Increased generation of intracellular ROS and apoptosis in long-term cultured hMTH-siRNA cells. (A) After long-term culture(12weeks) increased death of the hMTH1 deficient cells. The cell viability was measured as a percentage of the total cell number that remained unstained by trypan blue. Data represent mean ± S.D. from three separate experiments. (B) The hMTH1 deficient cells(12weeks) increased intracellular ROS generation was measured by flow cytometry analysis. Red curve, GM00637; Blue curve, control-siRNA cells; green curve, hMTH1-siRNA cells labeled with CM-DCFDA for 15min. The numbers indicate the mean ROS contents for the respective curves(displayed in log scale). (C) The apoptotic Sub-G1 DNA contents were estimated by FACScan analysis after long-term culture(12weeks). (D) Control-siRNA and hMTH1-siRNA cells were grown for 8-12weeks. The whole cell lysates were then prepared at the indicated time points, and Western blot analysis was performed using specific antibodies against hMTH1, p53, phosphorylated p53 such as p53-P(ser15) and p53-P(ser37) and caspase 3/7. The membrane was stripped and probed with anti-α-tubulin antibody to normalize the variation in protein loading. The results are representative of three independent experiments. (E) The H1299 lung carcinoma and H1299-GFPsiRNA and H1299-hMTHsiRNA cells were grown for 12weeks. The cells were cultured to 70-80 % confluence, and treated with different doses of H_2O_2 for 24hr. The cell death was estimated with MTT assay kit as described in “Experimental Procedure”. This experiment is representative of three independent experiments. All values are expressed as mean ± SD.

12. hMTH1 knockdown increases H_2O_2-induced histone H2AX phosphorylation in GM00637 cells.

In response to DNA double-stranded breaks, histone H2AX is rapidly phosphorylated by upstream kinases in the chromatin microenvironment flanking the site of DNA damage. Since phosphorylated H2AX (γ-H2AX) facilitates the focal assembly of checkpoint and DNA repair factors in many somatic cells (147), it is considered to be a sensor of DNA double strand breaks (148). We investigated the effect of hMTH1 knockdown on the formation of γ-H2AX induced by H_2O_2 in control-siRNA and/or hMTH1-siRNA transfected fibroblasts. Western blot analysis showed that the increased formation of γ-H2AX occurred in the hMTH1-siRNA transfected cells after a treatment with 25 to 80 μM H_2O_2 in a dose-dependent manner. However, there was no significant γ-H2AX increase in the control-siRNA transfected GM00637 cells (Fig.17A). Furthermore, immunofluorescent staining showed that the nuclear localization of γ-H2AX in response to 50 μM H_2O_2 was higher in hMTH1-siRNA transfected cells than in control-siRNA transfectants in a time-course dependent manner (Fig.17B). These results suggest that H_2O_2 produces DNA double strand breaks in hMTH1-deficeint GM00637 cells.

Figure 17.

A.

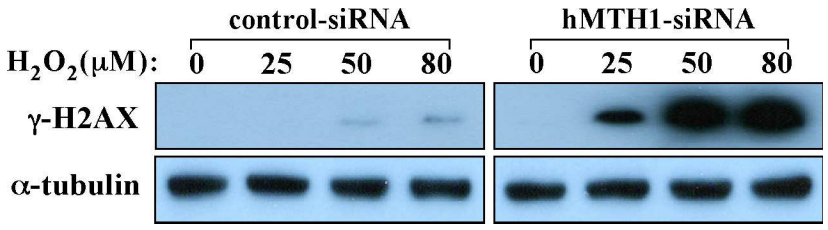

Figure 17.

B.

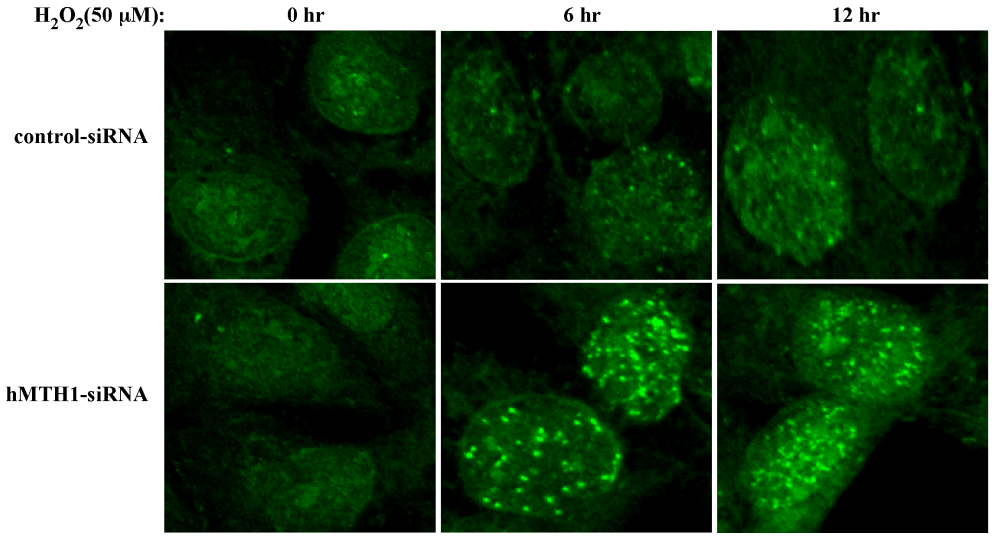

Figure 17. hMTH1 knockdown enhances H2AX phosphorylation in response to H_2O_2. (A) The control and hMTH1-deficient GM00637 cells were treated with 0 to 80 μM H_2O_2. The whole cell lysates were prepared 24 hours after H_2O_2 treatment, and Western blot analysis was performed using specific antibodies against γ-H2AX. The membrane was stripped and probed with anti-α-tubulin antibody to normalize the variation in protein loading. This experiment is representative of three independent experiments. (B) The control and hMTH1 deficient GM00637 cells were incubated with 50 μM H_2O_2 for 0, 6 and 12 hours at 37°C. The cells were then fixed and analyzed by immunofluorescent staining with anti-γ-H2AX monoclonal antibody. All results are representatives of three independent experiments.

13. Increased chromosomal instability in hMTH1-siRNA stable cells.

The chromosomal copy number changes on a genome-wide were determined by performing an array comparative genome hybridization (array CGH) using genomic DNAs derived from hMTH1-siRNA and control-siRNA cells, which were treated with 10 μM H_2O_2 for 4 weeks. The array CGH is a powerful molecular cytogenetic method that enables genome-wide screening for copy-number losses and gains of chromosomal parts through single hybridization (149). Currently, array CGH using bacterial artificial chromosome (BAC) arrays spanning the entire human genome are used to examine genomic alterations (150). The advances in genome-wide BAC array CGH technology have contributed to understanding the underlying genetic changes that correspond to disease progression. The extent and location of numerical changes in the DNA contents induced by H_2O_2 were examined in hMTH1-deficient cells and its control cells. As shown in Figure 18A, the H_2O_2-treated hMTH1 deficient cells showed significantly more changes in the copy number of large regions of chromosomes than the H_2O_2-treated control cells. The array CGH data provided a precise measurement of the level of gains ($\log_2$ ratio>0.225: green arrows) and losses ($\log_2$ ratio less than -0.225, red arrows) of all chromosomes. Based on the data, we identified the hMTH1-regulatory genome regions particularly to harbor critical cancer-related genes, such as regions with a possibly high-level amplification or high-magnitude deletion in response to H_2O_2. The array CGH data revealed 7q36.3 (gene loci of FAM62B, WDR60, LOC442366, VIPR2 and PTPRN2), 8q13.2 (gene loci of VEST1) 8q21.12 (gene loci of IL-7) and 12q21.31 (gene loci of PPFIA2) of chromosomal losses (Fig. 18B), and 14q11.2 (gene loci of RNASE11 and OR6S1), 18q12.3 (gene locus of FLJ44087) and 22q11.1 (gene loci of LOC391284, LOC400879 and LOC441969) of chromosomal gains (Fig. 18C), respectively. These results suggest that the suppression of the hMTH1 protein can lead to occur over a range of genomic instabilities in response to H_2O_2-oxidative stress.

Figure 18.

A.

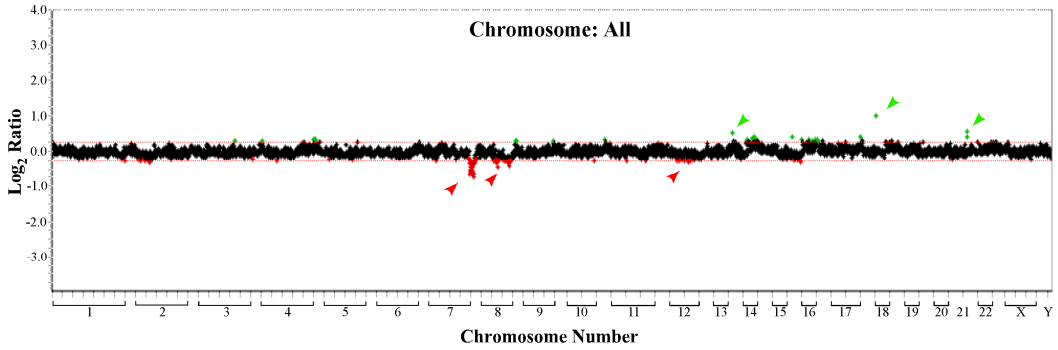

B.

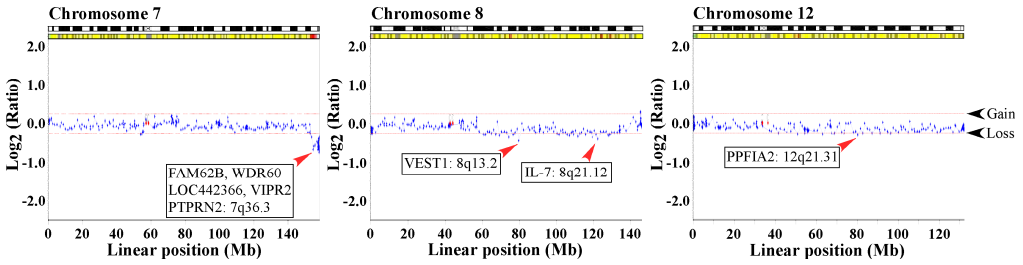

C.

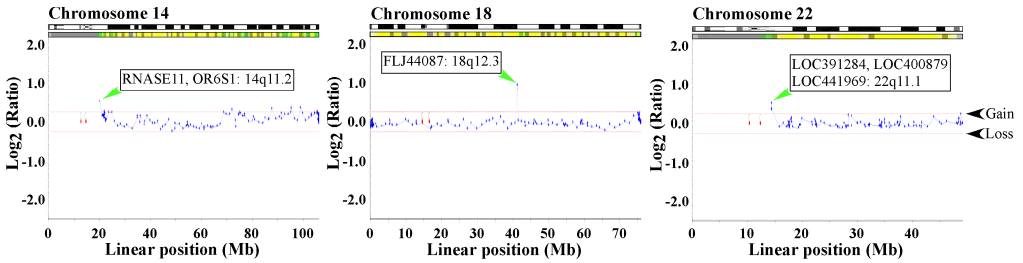

Figure 18. Array Comparative Genomic Hybridization (array CGH) of control-siRNA and hMTH1-siRNA cells. The control and hMTH1-deficient GM00637 cells were treated with 10μM H_2O_2 for 4 weeks. Their extracted genomic DNA was digested with DpnII, followed by random prime labeling with Cy3 for test DNA derived from hMTH1-siRNA transfected cells and Cy5 for the reference DNA from control-siRNA transfected cells. Whole-genome array CGH profiles showed $\log_2$-transformed hybridization ratios of test DNA versus control-reference DNA (A). Representative chromosomal losses ($\log_2$ ratio less than -0.25, red arrows) (B) and gains ($\log_2$ ratio>0.25: green arrows) (C) are also indicated. The possible critical cancer-related genes based on the chromosomal alterations are denoted by rectangles.

DISCUSSION

I. hOGG1-deficient fibroblasts undergo p53-dependent oxidative stress-induced apoptosis.

Reactive oxygen species (ROS) such as superoxide, hydroxyl radicals and hydrogen peroxide oxidize macromolecules in living cells including lipids, proteins and nucleic acids leading to various types of cellular dysfunctions including cell death and mutagenesis (74). These oxidative stresses can cause an enormous variety of natural and pathological processes such as aging, cancer, diabetes mellitus, atherosclerosis, and neurological degeneration such as Alzheimer's disease, schizophrenia, and autoimmune disorders like arthritis (63-65). Hence, understanding the mechanisms for processing oxidative DNA damage is likely to be important in elucidating the mechanisms of oxidative stress-mediated diseases. Among the many modified DNA molecules generated by oxidative stresses, 8-oxoG is the most stable product of oxidative DNA damage and appears to play a major role in mutagenesis and carcinogenesis (53). Recently, it was reported that the frequency of apoptosis and necrosis is related to the non-repair oxidative DNA adducts. For example, the expression of hOGG1 suppresses oxidative DNA damage and enhances cell survival against oxidative stress (75-77). In addition, a decrease in hOGG1 confers cellular hypersensitivity to H_2O_2 (78), and hOGG1 deficient human leukemia cells (KG-1) could be forced to undergo apoptosis by 8-hydroxyguanosine (8-OH-Gua) (79). Thus, hOGG1, a major enzyme for the repair of 8-oxoG from the cellular DNA, plays a protective role to confer a survival advantage.

In this study, we examined the role of hOGG1 in cytotoxicity of human fibroblast GM00637 cells in response to H_2O_2–oxidative stress. This was achieved by manipulating the cells' capability to perform 8-oxoG repair of free radical damages and assessing the

effects of this manipulation on the cellular survival after H_2O_2 treatment. Human fibroblast GM00637 cells, which were engineered for the RNA interference-mediated knockdown of hOGG1, lost 80 to 90% of their endogenous hOGG1 expression (Fig. 3). The siRNA-mediated inhibition of hOGG1 expression increased the cellular sensitivity to H_2O_2. Flow cytometry of PI-labeled cells was used to demonstrate a significant increase in the sub-G_1 population in hOGG1-silencing cells but not in the control-siRNA transfected cells.

Apoptosis is associated with the activation of caspases by a cytosolic multiprotein complex formed upon the release of cytochrome *c* from permeabilized mitochondria (80). This may result in the loss of the mitochondrial membrane potential or the activation of a proapoptotic protein such as Bax. The release of cytochrome *c* induces the proteolytic activation of procaspase 9 and the downstream activation of caspases-3 and caspase-7 (81). During the apoptosis induced by H_2O_2 in hOGG1-knockdown cells, H_2O_2 induces the cleavage of inactive 32 kDa procaspase-3 into smaller detectable active forms of caspase-3 such as 14 kDa and/or 22 kDa fragments, and the cleavage of inactive 32 kDa procaspase-7 into detectable active forms of caspase-7 such as the 26 kDa fragment (Fig. 4). Moreover, the caspase-3/7 inhibitor suppressed H_2O_2 induced apoptosis in hOGG1-knockdown cells. Since caspases-3 and caspase-7 are key mediators of mitochondria-induced apoptosis (82), H_2O_2 induced apoptosis in the hOGG1-depleted cells appears to be controlled by the mitochondrial apoptotic pathway. Therefore, although the direct activation of the mitochondrial proapoptotic protein and the direct loss of the mitochondria membrane potential are known to be involved in H_2O_2-induced cell death (83), the specific non-repaired oxidative DNA lesion such as 8-oxoG might play an important role in H_2O_2 induced apoptotic process in hOGG1-depleted cells.

p53 is a tumor suppressor protein that transmits the signals arising from various forms of cellular stress, including DNA damage, to the genes as well as the factors that induce cell cycle arrest and apoptosis (69, 70). p53 is not only induced by a variety of apoptotic

stimuli but the overexpression of p53 has also been demonstrated to induce apoptosis in a variety of cell types (69, 70). In this study, we investigated the role of p53 in hOGG1-depleted cells to figure out the more detailed molecular mechanisms of H_2O_2-induced apoptosis in hOGG1-depeleted cells. We found that p53 phosphorylation at serine15 and 20 was significantly induced by H_2O_2 in hOGG1-dificient GM00637 cells (Fig. 5). In addition, H_2O_2 markedly induced p21 and Noxa expression in hOGG1 deficient GM00637 cells, which are downstream targets of p53. Several p53 target mitochondrial proteins including Bax, Noxa and PUMA affect the mitochondrial membrane potential, which is an important determinant of mitochondrial apoptotic signaling (70). p53 can also directly engage in the major cellular apoptotic pathways, promoting both death receptor signaling and mitochondrial perturbations, without requiring the induction of genes (70). A close correlation between p53 phosphorylation and apoptosis prompted us to confirm the contribution of p53 to the apoptosis in hOGG1 deficient GM00637 cells. We found that the inhibition of p53 by p53-siRNA resulted in the decrease of p53 phosphorylation and caspase-3 and caspase-7 cleavage in H_2O_2-treated hOGOG1-deficient GM00637 cells (Fig. 5). Most strikingly, cell viability was markedly reduced upon treatment with H_2O_2 in hOGG1-deficient GM00637 cells. However, down-regulation of p53 by p53-siRNA in hOGG1-deficient cells resulted in the almost restoration of cell viability in response to H_2O_2, indicating that p53 plays an important role in H_2O_2-induced apoptotic cell death in hOGG1 deficient GM00637 cells. We confirmed the effect of hOGG1 on the H_2O_2-induced cell death in p53 knockout human lung carcinoma H1299 cells. The level of cell death induced by H_2O_2 was modest increased in siOGG1-deficient H1299 cells, compared to that of control H1299 cells. However, transfection of hOGG1-deficient H1299 cells with wild-type p53 resulted in the markedly increased cell death in response to H_2O_2 (Fig. 6). These results suggest that p53 is a major modulator of H_2O_2 induced cell death in hOGG1 deficient cells. Recently, Chatterjee *et al.* (84) have shown that combined suppression of hOGG1 and p53 further reduced cell viability when compared with suppression of each

gene individually . This discrepancy between the present and the previous studies may be attributable to the differences between employed cell lines. Although we focused our work on studying the role of the hOGG1 repair ability and p53 phosphorylation in cell death to H_2O_2 treatment, it is possible that many other cellular processes such as MAPK activity are also affected by the hOGG1 defect following H_2O_2 treatments, which may contribute to the increased sensitivity of the hOGG1-deficient cells to oxidative stress. Further studies need to identify these pathways and determine their roles in H_2O_2-oxidative stress-induced cellular responses in hOGG1-deficient cells.

p53 is phosphorylated at multiple sites by several different protein kinases including ATM and DNA-PK, enhancing its tetramerization, stability, and activity (69). The activation of ATM kinases, which is an important mediators of signals originating from DNA damage, is caused by ionizing irradiation and genotoxic drugs (85). DNA-PK has recently been identified as a crucial molecule activating apoptotic machinery in response to DNA damage, particularly DSBs (86). DNA-PK complex with p53 has been shown to act as a sensor of abnormal DNA structure, in which DNA-PK selectively regulates a p53-dependent apoptotic response (87). Therefore, activation of these protein kinases in H_2O_2-treated hOGG1-deficient cells would shed light on the activation of its upstream signaling molecule. To evaluate this possibility, we determined ATM and DNA-PK phosphorylation in response to H_2O_2 in hOGG1-deficient and proficient cells. The results obtained from Western blot experiments revealed that phosphorylation of ATM protein at Ser-1981 and DNA-PK protein at Tyr-2609 was significantly higher in hOGG1-deficient cells in response to H_2O_2 compared with those of hOGG1 proficient cells (Fig. 8). Additionally, the phosphorylation of Chk1 in response to H_2O_2, which has been shown to act downstream of ATM as signal transducers in DNA damage signaling (85), was also significantly increased in hOGG1-deficient cells, but H_2O_2-mediated phosphorylation of Chk1 does not significantly occur in hOGG1-proficient cells. Moreover, H_2O_2 treatment

increased the level of the Rad51 protein, which has been reported to be upregulated by post-translational modifications mediated by ATM (88), in hOGG1-deficient cells, but not in the OGG1-proficient cells. To identify the regulatory pathways of p53 activation in hOGG1-deficient GM00637 cells under our study conditions, we used caffeine, a potent inhibitor of ATM, and wortmannin, a potent inhibitor of DNA-PK. Pre-treatment with caffeine significantly abolished the increased phosphorylation of p53-Ser15 and p53-Ser20 in response to H_2O_2. In addition, wortmannin almost completely attenuated H_2O_2-induced p53-Ser20 phosphorylation in the hOGG1-deficient cells. This can be explained by the accumulation of 8-oxoG in DNA to activate ATM and DNA-PK through an yet unknown mechanism and subsequent phosphorylation of p53, thereby leading to activation of p53 apoptotic pathways.

Normally, the ATM and DNA-PK protein is activated by double stranded breaks or DNA replication arrest generated by DNA damaging treatments (85-87). In comparison, the major DNA damage generated by H_2O_2 in hOGG1-deficient cells is an oxidized purine base such as 8-oxoG DNA adducts. The mechanism that is responsible for these protein kinases activation following H_2O_2 treatment in hOGG1-deficient cells is unknown. However, ATM and DNA-PK phosphorylation in hOGG1-deficient cells following H_2O_2 treatment suggest that the accumulation of 8-oxoG can lead to multiple cycles of attempted repair and ultimately to the formation of secondary lesions such as DNA double strand breaks. It is possible that DNA nicking repair processes such as DNA glycosidase and apurinic nuclease action at lesions within the clusters of damage or closely spaced lesions on both DNA strand lead to the direct formation of DNA double strand breaks. Because 8-oxoG adducts have shown to inhibit transcription in human cells, on the other hand, the accumulation of oxidized DNA lesions may lead to transcription block and/or replication fork stalling, followed by formation of a double strand break at the site of a stalled fork (89). Taken together, activation of ATM and DNA-PK protein may represent an important

signal of H_2O_2-oxidative stress and the hOGG1 defect may enhance this signal to lead to increased p53 phosphorylation, resulting in increased apoptotic cell death (Fig. 10).

It is widely accepted that the accumulation of oxidative DNA damage over time can lead to cancer. The role of OGG1 in tumor suppression is suggested by the frequent loss of the OGG1 chromosomal locus in human lung and renal cancers, and by the significantly lower OGG1 activity in lung cancer patients (59). Yeast strains containing OGG1 mutations show a spontaneous mutator phenotype (90), and the inactivation of OGG1 gene in mice leads to the accumulation of 8-oxoG and an increase in the spontaneous mutation frequency in liver and kidney cells (91). Furthermore, knockout mice deficient in the repair of 8-oxoG have an increased rate of cancer (92). Therefore, the defect of hOGG1, that affect its repair ability, might be involved in carcinogenesis by enhancing mutation rates of the key genes, such as oncogenes or tumor suppressor genes. To detect small, high-level gains or losses that are capable of harboring or deleting specific oncogenes and tumor suppressor genes, we used the high-resolution array CGH in this study. An analysis of the overall genomic integrity revealed a significantly higher level of alteration of particular gene copy number in H_2O_2-treated hOGG1-deficient cells than in the H_2O_2-treated control cells (Fig. 9). This global difference in the genomic profiles suggests that the chronic exposure of H_2O_2 significantly affects the nature of the accumulated mutations in hOGG1 depleted GM00637 cells. The BAC array profiles of the hydrogen peroxide-treated hOGG1 knockdown cells showed chromosomal losses of LOC339529, ZNF238, LOC440742, VIPR2 and LOC442366, and chromosomal gains of MYO18A, FLJ25715, CTDP1, PJA1 and RP13-153N15.1. This suggests that hOGG1 plays an important role in maintaining the genomic stability against oxidative stress. Ongoing experiments are being carried out to determine the functionalities of those genomic target genes in hOGG1 knockdown GM00637 cells, *in vitro* and *in vivo*.

In summary, we demonstrate in this study that the down-regulation of hOGG1 expression can trigger the hydrogen peroxide-mediated apoptosis of human fibroblast GM00637 cells via the p53-dependent pathway. The hOGG1-mediated protection against oxidative stress-induced apoptosis is achieved through the negative regulation of caspase 3/7 and p53 phosphorylation. Although, the precise mechanism, whereby the inhibition of the hOGG1 repair activity affects p53 dependent apoptosis, remains to be determined, it is believed that it may be related to the shift in the balance of the damage/repair process towards the accumulation of greater oxidative DNA lesions such as 8-oxoG.. Chromosomal instability is also believed to play a critical role in tumor evolution by increasing the rate of genetic selection of cancer genes with altered DNA copy number in hOGG1-deficient cells. The future challenge is to define the target molecules that trigger the signal transduction pathways leading to oxidative stress-induced p53 activation in hOGG1- deficient cells and to define the biological significance of these activated stress-signaling pathways. Studies focusing on these biochemical steps would extend our understanding of the oxidative DNA damage signaling cascades stimulated by ROS during normal metabolic and pathological processes.

II. hMTH1 knockdown by small interfering RNA increases oxidative stress-induced cell death and chromosomal instability in human fibroblast GM00637 cells

Recently, the frequency of apoptosis and necrosis was reported to be related with the non-repair oxidative DNA adducts (112-117, 151-153). For example, hOGG1 overexpression enhances the repair of oxidative lesions in the cellular DNA and increases the cellular survival against oxidative stress (151-153). On the other hand, hOGG1 deficient cells show hypersensitivity to H_2O_2 (154). 8-OH-Gua is involved in the development of apoptosis in hOGG1-deficient cells, and an increase in 8-OH-Gua accumulation is related to cell death (116). Furthermore, MTH1-null mouse embryo fibroblasts are highly susceptible to cell dysfunction and death caused by H_2O_2 exposure with the morphological features of pyknosis and the accumulation of electron dense deposits in the mitochondria (112). All of the H_2O_2-induced alterations observed in MTH-null mouse embryo fibroblast were effectively suppressed by the expression of wild-type hMTH1. The MTH1 also protects the dopamine neurons from oxidative damage (114). Therefore, the accumulation of oxidative DNA lesions might play an important role in oxidative stress induced cell death.

In this study, we investigated the role of hMTH1 in cytotoxicity of human fibroblast GM00637 cells in response to free radical damage such as hydrogen peroxide. It was achieved by manipulating the cells' capability to perform the repair of oxidized purine nucleoside triphosphate and assessing the effects of this manipulation on the cellular survival after H_2O_2 treatment. Human fibroblast GM00637 cells, which were engineered for the RNA interference-mediated knockdown of hMTH11, lost 90 to 95% of their endogenous hMTH1 expression (Fig.1). The siRNA-mediated inhibition of hMTH1

expression increased the cellular sensitivity to H_2O_2. Flow cytometry of PI-labeled cells was used to demonstrate a significant increase in the subG_1 population in hMTH1-silencing cells but not in the control-siRNA transfected cells (Fig. 2).

Many DNA-damaging agents have been shown to induce apoptosis through p53-dependent mechanism (155). In general, the p53 protein is a tumor suppressor protein that transmits the signals arising from various forms of cellular stress, including DNA damage, to genes as well as the factors that induce cell cycle arrest and apoptosis (156). It has also been reported that the phosphorylation of p53 at Ser-15 and Ser-20 increase in response to DNA damaging agents (157,158). Thus, we investigated in this study the role of p53 in the hMTH1-mediated cellular response to H_2O_2 and its molecular mechanism related with cell death caused by H_2O_2-induced oxidative DNA damage in hMTH1-depeleted cells. Although the H_2O_2-oxidative stress induced p53 phosphorylation at Ser-15 and Ser-20, the level of p53 phosphorylation was similar in hMTH1-dificient cells and control cells, indicating that p53 may not be an important mediator of H_2O_2-induced cell death in hMTH1-depeleted cells. The activation of caspases is one of the major process in DNA damage-induced apoptosis. we clearly observed cleavage of procaspase-7 into the active subunit was clearly observed in the hMTH1 deficient cells after H_2O_2 treatment (Fig. 13B). These results are different from the previous reported that caspases do not contribute to the oxidative stress-induced cell death in MTH1 null mice (112). These differences may be due to cell or tissue specificity.

Most importantly, the expression level of Noxa, proapoptotic BH3-only family member, was significantly increased in hMTH1-deficent cells after H_2O_2 exposure in this study. Noxa is commonly described as a p53 target gene and is a key mediator of p53 dependent apoptosis (159-160). The p53 response elements are present in the Noxa promoter and are up-regulated by p53 (159). However, the up-regulation of Noxa has also been described by p53-independent mechanisms, and Noxa can directly activate apoptotic pathway (163-166).

In this study, we confirmed the contribution of Noxa to the H_2O_2-induced cell death in hMTH1-deficient cells. The level of Noxa inhibition by siRNA was quite good with a knockdown of 85 to 90% after the treatment of H_2O_2, which resulted in protection of cell death induced by H_2O_2 in hMTH1-deficient cells. These results indicate that Noxa may be an important modulator of H_2O_2-induce cell death in hMTH1 deficient cells. We also p53 inhibition by siRNA, which resulted in protection of cell death induced by H_2O_2 in hMTH1-deficient cells and in slight inhibition of Noxa expression. Therefore, these results suggest that the p53 contributes to the H_2O_2-induced Noxa expression and cell death in hMTH1-depleted GM00637 cells but how to expression of the Noxa protein by p53 still not know. Although detailed mechanism of Noxa induction by H_2O_2 in hMTH1 deficient cells is not completely understood, it may be related to the shift in the balance between oxidative damage and repair process towards the accumulation of oxidized purine triphosphate such as 8-oxo-dGTP.

DNA repair gene silencing for long-term in human cells highly sensitive, suggestive of irreversible damage following long-term DNA repair gene silencing(125). Accumulation of nuclear and mitochondrial DNA damage is though to be particularly deleterious in cells, which cannot be replaced through cell division. Several groups have documented the accumulation of oxidative DNA damage during aging in the mammalian brain (127-131) Once DNA damage has been generated, it is the role of cellular repair systems to prevents its accumulation. However, studies have shown that aging is associated with a general reduction in DNA repair capacity. Overall nuclear and mitochondrial BER activities , were shown to gradually decline with age, reaching 80-85% lower activity in old rats compared with young rat. Oxidative damage to mtDNA in the heart and brain is inversely related to maximum lifespan of mammals(135,136), suggesting that accumulation of mtDNA damage plays a causative role in the various disorders that are associated with aging, cancer and neurodegeneration. That studies suggest that modifications in mtDNA repair

may contribute to the accumulation of DNA damage associated with aging. It is imported to note that age-related accumulation of DNA damage and alteration in DNA repair processes in the mammalian. To test cell senstivity in long-term cultured hMTH1-deficient cells were grown for 12weeks. The cell viability of the hMTH1-siRNA was significantly lower than that of the control-siRNA cells in not treated H_2O_2 (Fig. 16A). As shown in Figure 16C the hMTH1 deficient cells increased the proportion of apoptotic sub-G_1 DNA content 40.34%. These results suggest that the suppression of hMTH1 expression triggers apoptosis in response to age. This finding suggests that reduction in DNA repair capacity is significantly decreased maximum life span.

ROS are continuously formed as consequence of normal cellular metabolism and in response to environmental factors such as UV light, ionizing radiation, heat, and pollution. This ROS production may significantly increase when cells are under metabolic stress and/or have mtDNA mutations. The superoxide radicals generated in mitochondria may cause damage not only to mtDNA, but also to nuclear DNA(nDNA) by their conversion to hydrogen peroxide, which is relatively stable and able to travel to the nucleus. These endogenous ROS may damage mtDNA, leading to increased mtDNA mutations, which in turn cause malfunction of the respiratory chain components encoded by mtDNA, and thus further increase electron leakage and ROS generation. This would result in an amplification of ROS stress and cause further damage to mtDNA and nDNA, leading to genetic instability in cells(137). We investigated the effect of DNA repair gene silencing for long-term on intracellular ROS accumulation. As shown in Fig.16B, hMTH1- deficient cells increase of ROS production. Earlier studies have demonstrated that apoptotic characteristics were correlated with reactive oxygen species(ROS) production, lipid peroxidation, p53 and Noxa expression, and mitochondrial cytochrome c release following treatment of apoptosis induced agent(138). DNA damage stresses cause an increase in cellular level of ROS(139-141). P53 activation is likely involved, since p53 induces

several known genes involved in ROS generation(142). This results suggest that irreversible damage following modification in DNA repair may contribute to increase in cellular level of ROS. Accumulative evidence indicated that ROS may play a role as trigger or signaling molecules in p53 modulated apoptosis as reviewed by Carmody and Cotter(167). However, hMTH1-deficient cells highly sensitive treated H_2O_2. This cell death is p53-independent events. Thus, we propose that there are at least two different pathways of apoptosis: one mediated through p53 activation in response to ROS stresses and the other through p53 independent in response to DNA damage accumulation.

H2AX, a variant form of histone H2A, is rapidly phosphorylated at serine 139 in response to DNA double strand break inducing agents (148). Phosphorylated histone H2AX, which is designated γ-H2AX, forms distinct nuclear foci at or near the DSB sites, and is considered to be important role for mediating DNA damage-related cellular responses (147). In this study, we demonstrated that hMTH1-deficient GM00637 cells contained significantly higher γ-H2AX levels than normal control cells after H_2O_2 treatment, suggesting that H_2O_2 produces DNA double strand breaks in hMTH1-deficeint GM00637 cells. hMTH1 hydrolyzes oxidized purine nucleotides 8-oxodGTP, 2-OH-dATP or their ribo-forms to their monophosphates (103). Unrepaired oxidized purines in hMTH1-deficient cells cause the accumulation of oxidized DNA adducts (106), which can lead to multiple cycles of attempted repair and ultimately to the formation of secondary lesions such as DNA double strand breaks. However, the mechanisms by which oxidized purines induce this DNA damage response are unknown at this point. It is possible that DNA nicking repair processes such as DNA glycosidase and apurinic nuclease action at lesions within the clusters of damage or closely spaced lesions on both DNA strand lead to the direct formation of DNA double strand breaks. On the other hand, the accumulation of oxidized DNA lesions may lead to replication fork stalling and/or collapse, and formation of a double strand break at the site of a stalled fork, followed by the onset of homologous

recombination.

It is widely accepted that the accumulation of oxidative DNA damage promotes mutagenesis, which can lead to cancer (168). The role of MTH1 in tumor suppression has been suggested from mice lacking the Mth1 gene, which show an increased spontaneous mutation rate as well as an increased incidence of spontaneous carcinogenesis in liver, lung and stomach (106). Moreover, hMTH1 expression in mismatch-deficient mouse embryo fibroblasts efficiently suppresses the increased spontaneous mutagenesis (169). Therefore, defects in hMTH1 that affect its repair ability may be involved in carcinogenesis by enhancing the rate of mutation of the key genes, such as oncogenes or tumor suppressor genes. The technique of CGH was used for the genome-wide characterization of the genetic imbalances present in this study. The key biological value of high-resolution array CGH lies in its ability to detect small, high-level gains that can harbor specific oncogenes and tumor suppressor genes (149,150). The H_2O_2-treated hMTH1-deficient GM00637 cells were subjected to array-CGH analysis. An analysis of the overall genomic integrity, as measured by the loss and gain of the DNA copy number, revealed a significantly higher level of alterations of a particular gene copy number in H_2O_2-treated hMTH1 deficient cells than in H_2O_2-treated control cells. This global difference in the genomic profiles indicates that the chronic exposure to H_2O_2 significantly affects the nature of the accumulated mutations in hMTH1 depleted GM00637 cells. It is believed that chromosomal instability plays an important role in tumor evolution by increasing the rate of the genetic selection of cancer genes with altered DNA copy number (170). The biological significance of the genomic target genes in hMTH1-deficient cells after oxidative stress is currently under investigation.

In summary, we demonstrate in this study that the down-regulation of hMTH1 expression can trigger H_2O_2-mediated cell death via Noxa-dependent pathway, and increase the γ-H2AX foci in response to H_2O_2. Although the precise mechanism how the

suppression of hMTH1 expression affects this DNA damage response remains to be determined, it may be related to the accumulation of oxidized purine triphosphate. The BAC array CGH showed significant H_2O_2-associated differences between the hMTH1 deficient and proficient cells in terms of the overall genome-wide degree of amplifications and deletions reflected in the width of data ranges for the array CGH signals. The accumulation of oxidative DNA lesions in proliferating cells is believed to promote mutagenesis and chromosomal instability, which is the initial step for the development of cancer. On the other hand, the accumulation of oxidative DNA lesions in non-proliferating neurons promotes cell death resulting in neurodegeneration. Further studies will be required to define the target molecule that trigger the signal transduction pathways leading to oxidative stress induced Noxa expression in hMTH1 deficient cells and to define the biological significance of these activated stress-signaling pathways. Studies focusing on these biochemical steps would extend our understanding of the important role of hMTH1 in preventing the development of cancer and the progression of neurodegenerative diseases.

REFERENCES

1. M.Pinak, 8-oxoguanine lesioned B-DNA molecule complexed with repair enzyme hOGG1: a molecular dynamics study, J.Comput.Chem.24 (2003) 898-907
2. M.Pinak Electrostatic energy analysis of 8-oxoguanine DNA lesionmolecular dynamics study, J.Comput. Biol.Chem.27 (2003) 431-441
3. H.J.Einolf, F. P. Guengerich, Fidelity of nucleotide insertion at 8-oxo7-,8-dihydroguanine by mammalian DNA polymerase delta. Steady-state and pre-state kinetic analysis, J. Bio . Chem.276 (2001) 3764-3771
4. Y. Zhang, F. Yuan, X. Wu, O. Rechkoblit, J.S. Taylor, N.E. Geacintov, Z. Wang, Error-prone lesion bypass by human DNA polymerase eta, Nucleic Acids Res. 28 (2000) 4717-4724
5. J.P.Radicella, C. Baikalov, W.M. Luther, J.H. Chiang, Y.F. Wei, J.H.Miller, Cloning and characterization of hOGG1, a human homolog of the OGG1 gene of Saccharomyces cerevisiae, Pro. Natl. Acad. Sci. USA 94 (1997) 8010-8015
6. M.M. Slupska, C. Baikalov, W.M. Luther, J.H. Chiang, Y.F. Wei,J.H. Miller, Cloning and sequencing a human homolog (hMYH) of the Escherichia coli mutY gene whose function is required for the repair of oxidative DNA damage, J.Bacteriol. 178 (1996) 3885-3892.
7. M. Furuichi, M.C. Yoshida, H. Oda, T. Tajiri, Y.Nakabeppu, T. Tsuzuki, M. Sekiguchi, Genomic structure and chromosome location of the human mutT homologue gene MTH1 encoding 8-oxo-dGTPase for prevention of A:T to C:G transversion, Genomics 24 (1994) 485-490
8. Ames,B.N., Shigenaga, M.K., and Hangen, T,M,(1993) Proc.Natl.Acad.Aci.U.S.A. 90,7915-7922

9. Berlett,B., and Stadtman, E.R.(1997) J.Biol.Chem. 272,20313-20336)

10. Effect of mitochondrial electron transport chain inhibitors on superoxide radical generation in rat hippocampal and striatal slices. Antioxid. Redox Signal. 3, 1099-1104

11. Mitochodrial superoxide radical formation is controlled by electron bifurcation to the high and low potential pathway. Free Radic. Res. 36, 381-387).

12. The mitochondrial generation of hydrogen peroxide: general properties and effect of hyperbaric oxygen. Biochem.J. 134, 707-716

13. Superoxide radical and superoxide dismutases. Annu. Rev. Biochem. 64,97-112

14. Oxidants in mitochondria: from physiology to diseases. Biochim. Biophys. Acta 1271, 67-74.

15. Free Radical in Biology and Medicine, 3rd ed. Oxford University Press Inc., Neww York, NY, U.S.A

16. The superoxide-generating NADPH oxidase: structural aspects and activation mechanism. Cell Mol. Life Sci. 59, 1428-1459

17. NADPH oxidase and the respiratory burst. Semin. Cell Biol. 6, 357-365

18. Endogenous DNA damage as related to cancer ad aging. Mutant. Res. 214, 41- 46

19. Chemical determination of free radical- induced damage to DNA. Free Rad. Biol. Med. 10, 225-242

20. DNA adducts of chemical carcinogens. Carcinogenesis 16, 437-441

21. Structural origins of bulky oxidative DNA adducts (type III-compounds) as deduced of oxidation of oligonucleotides of known sequence. Chem. Res. Toxicol. 9, 247-254

22. Generation of putative intrastrand cross-links and strand breaks in DNA by transition metal ion-mediated oxygen radical attack. Chem. Res. Toxicol. 10, 393-400

23. Misreading of DNA templates in containing 8-hydroxydeoxyguanosine at the modified base and at the adjacent residues. Nature 327, 77-79

24. Insertion of specific bases during DNA synthesis past the oxidation-damaged base 8-oxodG. Nature 349, 431- 434

25. Mitochondrial DNA alterations in cancer. Caner Invest. 20, 557-569

26. The contribution of endogenous sources of DNA damage to the multiple mutations in cancer. Mutat. Res. 477, 7-21

27. Fridovich, E.(1998)J.Exp.Biol.201,1203-1209

28. Davies,K.J(1999)IUBMB Life 48, 41-47).

29. Wiese,A.G.,Pacifici.R.E., and Davies,K.J(1995) Arch.Biochem.Biophys. 318,231-240

30. Yakes,F.M., and Van Houten,B.(1997) Proc.Natl.Acad.Sci.U.S.A. 94,514-519

31. Salazer,J.J., and Van Houten,B.(1997) Mutat. Res. 385, 139-149

32. Chen,Q.,and Ames,B.N.(1994) Proc.Natl.Acad.Sci.U.S.A. 91,4130-4134,

33. . Chen,Q.M.,(2000) Ann. N. Y. Acad. Sci.908,111-125

34. Frippiat, C., Chen,Q. M., Zdanov, S., Magalhaes, J.P., Remacle, J., and Toussaint, O.(2001) J.Biol. Chem. 276, 2531-2537

35. Chen, Q. M., Bartholomew, J.C., Campisi, C., Acosta, M., Reagan, J.D., Ames, B.N. (1998) Biochem.J.332,43-50

36. Carwford, D.R., Schools, G. P., and Davies, K. J. (1996) Arch. Biochem. Biophys. 329, 137-144

37 . Chen, Q., Liu, B., and Merrett, J. B.(2000) Biochem. J. 347, 543-551

38. Bladier, C., Wolvetang, E. J., Hutchinson, P., de Haam, J. B., and Kola, I. (1997) Cell Growth Differ. 8, 589-598

39. Graziewicz, M.A., Day, B. J., and Copeland, W. C. (2002) Nucleic Acids Res. 30, 2817-2824

40. Sensitization to death receptor cytotoxicity by inhibition of fas-associated death domain protein (FADD)/caspase signaling. Requirement of cell cycle progression. J.Biol.Chem. 275,24670-24678

41. The cellular response to p53: the decision between life and death. Oncogene 18,6145-6157

42. Post-translational modifications and activation of p53 by genotoxic stresses. Eur.J.Biochem. 268, 2764-2772

43. Bcl-xL and E1B-19K proteins inhibit p53-induced irreversible grwth arrest and senescence by preventing reactive oxygen species-dependent p38 activation. J.Biol.Chem. 279, 17765-17771

44. Reactive oxygen species are downstream mediators of p53-dependent apoptosis. Proc. Natl. Acad. Sci. USA 93, 11848-11852

45. Dinstinct ROS and biochemical profiles in cells undergoing DNA damage-induced senescence and apoptosis. Mechanisms of Ageing and Development 126 (2005) 580-590

46. DNA repair, mitochondria, and neurodegeneration Neuroscience(2006)

47. Oxidants, antioxidants, and the degenerative diseases of aging. Pro Natl Acad Sci USA 90:7915-7922

48. Oxidative damage to mitochondrial DNA is inversely related to maximum life span in the heart and brain of mammals. FASEB J 14:312-318

49. Age-related base excision repair activity in mouse brain and liver nuclear extracts. J Gerontol A Biol Sci Med Sci 58:205-211.

50. Mitochondrial and nuclear DNA-repair capacity of various brain regions in mouse is altered in an age-dependent manner. Neurobiol Aging 27: 1129-1136

51. Eyfjord JE, Bodvarsdottir SK. Genomic instability and cancer: networks involved in response to DNA damage. Mutat Res 2005;592(1-2):18-28.

52. Ide H, Kotera M. Human DNA glycosylases involved in the repair of oxidatively damaged DNA. Biol Pharm Bull 2004;27(4):480-5.

53. Fortini P, Pascucci B, Parlanti E, D'Errico M, Simonelli V, Dogliotti E. 8-Oxoguanine DNA damage: at the crossroad of alternative repair pathways. Mutat Res 2003;531(1-2):127-39.

54. Sancar A, Lindsey-Boltz LA, Unsal-Kacmaz K, Linn S. Molecular mechanisms of mammalian DNA repair and the DNA damage checkpoints. Annu Rev Biochem 2004;73:39-85.

55. Norbury CJ, Hickson ID. Cellular responses to DNA damage. Annu Rev Pharmacol Toxicol 2001;41:367-401.

56. Mitra S, Boldogh I, Izumi T, Hazra TK. Complexities of the DNA base excision repair pathway for repair of oxidative DNA damage. Environ Mol Mutagen 2001;38(2-3):180-90.

57. Barnes DE, Lindahl T. Repair and genetic consequences of endogenous DNA base damage in mammalian cells. Annu Rev Genet 2004;38:445-76.

58. Shibutani S, Takeshita M, Grollman AP. Insertion of specific bases during DNA synthesis past the oxidation-damaged base 8-oxodG. Nature 1991;349(6308):431-4.

59. Boiteux S, Radicella JP. The human OGG1 gene: structure, functions, and its implication in the process of carcinogenesis. Arch Biochem Biophys 2000;377(1):1-8.

60. Nakabeppu Y, Tsuchimoto D, Furuichi M, Sakumi K. The defense mechanisms in mammalian cells against oxidative damage in nucleic acids and their involvement in the suppression of mutagenesis and cell death. Free Radic Res 2004;38(5):423-9.
61. Bohr VA. Repair of oxidative DNA damage in nuclear and mitochondrial DNA, and some changes with aging in mammalian cells. Free Radic Biol Med 2002;32(9):804-12.
62. Fan CY, Liu KL, Huang HY, et al. Frequent allelic imbalance and loss of protein expression of the DNA repair gene hOGG1 in head and neck squamous cell carcinoma. Lab Invest 2001;81(10):1429-38.
63. Cardozo-Pelaez F, Cox DP, Bolin C. Lack of the DNA repair enzyme OGG1 sensitizes dopamine neurons to manganese toxicity during development. Gene Expr 2005;12(4-6):315-23.
64. Iida T, Furuta A, Nishioka K, Nakabeppu Y, Iwaki T. Expression of 8-oxoguanine DNA glycosylase is reduced and associated with neurofibrillary tangles in Alzheimer's disease brain. Acta Neuropathol (Berl) 2002;103(1):20-5.
65. Kikuchi H, Furuta A, Nishioka K, Suzuki SO, Nakabeppu Y, Iwaki T. Impairment of mitochondrial DNA repair enzymes against accumulation of 8-oxo-guanine in the spinal motor neurons of amyotrophic lateral sclerosis. Acta Neuropathol (Berl) 2002;103(4):408-14.
66. Harrison JF, Hollensworth SB, Spitz DR, Copeland WC, Wilson GL, LeDoux SP. Oxidative stress-induced apoptosis in neurons correlates with mitochondrial DNA base excision repair pathway imbalance. Nucleic Acids Res 2005;33(14):4660-71.
67. Mambo E, Nyaga SG, Bohr VA, Evans MK. Defective repair of 8-hydroxyguanine in mitochondria of MCF-7 and MDA-MB-468 human breast cancer cell lines. Cancer research 2002;62(5):1349-55.
68. Hyun JW, Jung YC, Kim HS, et al. 8-hydroxydeoxyguanosine causes death of human leukemia cells deficient in 8-oxoguanine glycosylase 1 activity by inducing

apoptosis. Mol Cancer Res 2003;1(4):290-9.

69. Lavin MF, Gueven N. The complexity of p53 stabilization and activation. Cell Death Differ 2006;13(6):941-50.

70. Haupt S, Berger M, Goldberg Z, Haupt Y. Apoptosis - the p53 network. J Cell Sci 2003;116(Pt 20):4077-85.

71. Lee MR, Kim SH, Cho HJ, et al. Transcription factors NF-YA regulate the induction of human OGG1 following DNA-alkylating agent methylmethane sulfonate (MMS) treatment. The Journal of biological chemistry 2004;279(11):9857-66.

72. Kallioniemi A, Kallioniemi OP, Sudar D, et al. Comparative genomic hybridization for molecular cytogenetic analysis of solid tumors. Science 1992;258(5083):818-21.

73. Wolf M, Mousses S, Hautaniemi S, et al. High-resolution analysis of gene copy number alterations in human prostate cancer using CGH on cDNA microarrays: impact of copy number on gene expression. Neoplasia 2004;6(3):240-7.

74. Klaunig JE, Kamendulis LM. The role of oxidative stress in carcinogenesis. Annu Rev Pharmacol Toxicol 2004;44:239-67.

75. Dobson AW, Xu Y, Kelley MR, LeDoux SP, Wilson GL. Enhanced mitochondrial DNA repair and cellular survival after oxidative stress by targeting the human 8-oxoguanine glycosylase repair enzyme to mitochondria. The Journal of biological chemistry 2000;275(48):37518-23.

76. Wu M, He YH, Kobune M, Xu Y, Kelley MR, Martin WJ, 2nd. Protection of human lung cells against hyperoxia using the DNA base excision repair genes hOgg1 and Fpg. Am J Respir Crit Care Med 2002;166(2):192-9.

77. Kannan S, Pang H, Foster DC, Rao Z, Wu M. Human 8-oxoguanine DNA glycosylase increases resistance to hyperoxic cytotoxicity in lung epithelial cells and involvement with altered MAPK activity. Cell Death Differ 2006;13(2):311-23.

78. Yang N, Chaudhry MA, Wallace SS. Base excision repair by hNTH1 and hOGG1: a two edged sword in the processing of DNA damage in gamma-irradiated human

cells. DNA Repair (Amst) 2006;5(1):43-51.

79. Hyun JW, Choi JY, Zeng HH, et al. Leukemic cell line, KG-1 has a functional loss of hOGG1 enzyme due to a point mutation and 8-hydroxydeoxyguanosine can kill KG-1. Oncogene 2000;19(39):4476-9.

80. Garrido C, Galluzzi L, Brunet M, Puig PE, Didelot C, Kroemer G. Mechanisms of cytochrome c release from mitochondria. Cell Death Differ 2006;13(9):1423-33.

81. Norbury CJ, Zhivotovsky B. DNA damage-induced apoptosis. Oncogene 2004;23(16):2797-808.

82. Lakhani SA, Masud A, Kuida K, et al. Caspases 3 and 7: key mediators of mitochondrial events of apoptosis. Science 2006;311(5762):847-51.

83. Ricci JE, Gottlieb RA, Green DR. Caspase-mediated loss of mitochondrial function and generation of reactive oxygen species during apoptosis. J Cell Biol 2003;160(1):65-75.

84. Chatterjee A, Mambo E, Osada M, Upadhyay S, Sidransky D. The effect of p53-RNAi and p53 knockout on human 8-oxoguanine DNA glycosylase (hOgg1) activity. Faseb J 2006;20(1):112-4.

85. Shiloh Y. ATM and ATR: networking cellular responses to DNA damage. Current opinion in genetics & development 2001;11(1):71-7.

86. Collis SJ, DeWeese TL, Jeggo PA, Parker AR. The life and death of DNA-PK. Oncogene 2005;24(6):949-61.

87. Achanta G, Pelicano H, Feng L, Plunkett W, Huang P. Interaction of p53 and DNA-PK in response to nucleoside analogues: potential role as a sensor complex for DNA damage. Cancer research 2001;61(24):8723-9.

88. Daboussi F, Dumay A, Delacote F, Lopez BS. DNA double-strand break repair signalling: the case of RAD51 post-translational regulation. Cellular signalling 2002;14(12):969-75.

89. Kuzminov A. Single-strand interruptions in replicating chromosomes cause double-

strand breaks. Proceedings of the National Academy of Sciences of the United States of America 2001;98(15):8241-6.

90. Thomas D, Scot AD, Barbey R, Padula M, Boiteux S. Inactivation of OGG1 increases the incidence of G. C-->T. A transversions in Saccharomyces cerevisiae: evidence for endogenous oxidative damage to DNA in eukaryotic cells. Mol Gen Genet 1997;254(2):171-8.

91. Klungland A, Rosewell I, Hollenbach S, et al. Accumulation of premutagenic DNA lesions in mice defective in removal of oxidative base damage. Proceedings of the National Academy of Sciences of the United States of America 1999;96(23):13300-5.

92. Kunisada M, Sakumi K, Tominaga Y, et al. 8-Oxoguanine formation induced by chronic UVB exposure makes Ogg1 knockout mice susceptible to skin carcinogenesis. Cancer research 2005;65(14):6006-10.

93. Barnes DE, Lindahl T. Repair and genetic consequences of endogenous DNA base damage in mammalian cells. Annu Rev Genet 2004;38:445-76.

94. Fortini P, Pascucci B, Parlanti E, D'Errico M, Simonelli V, Dogliotti E. 8-Oxoguanine DNA damage: at the crossroad of alternative repair pathways. Mutat Res 2003;531:127-39.

95. Tajiri T, Maki H, Sekiguchi M. Functional cooperation of MutT, MutM and MutY proteins in preventing mutations caused by spontaneous oxidation of guanine nucleotide in Escherichia coli. Mutat Res 1995;336:257-67.

96. Kamiya H, Kasai H. Formation of 2-hydroxydeoxyadenosine triphosphate, an oxidatively damaged nucleotide, and its incorporation by DNA polymerases. Steady-state kinetics of the incorporation. J Biol Chem 1995;270:19446-50.

97. Maki H, Sekiguchi M. MutT protein specifically hydrolyses a potent mutagenic substrate for DNA synthesis. Nature 1992;355:273-5.

98. Shibutani S, Takeshita M, Grollman AP. Insertion of specific bases during DNA synthesis past the oxidation-damaged base 8-oxodG. Nature 1991;349: 431-4.

99. Tchou J, Grollman AP. Repair of DNA containing the oxidatively-damaged base, 8-oxoguanine. Mutat Res 1993;299:277-87.

100. Nakabeppu Y, Tsuchimoto D, Furuichi M, Sakumi K. The defense mechanisms in mammalian cells against oxidative damage in nucleic acids and their involvement in the suppression of mutagenesis and cell death. Free Radic Res 2004;38:423-9.

101. Bohr VA. Repair of oxidative DNA damage in nuclear and mitochondrial DNA, and some changes with aging in mammalian cells. Free Radic Biol Med 2002;32:804-12.

102. Furuichi M, Yoshida MC, Oda H, et al. Genomic structure and chromosome location of the human mutT homologue gene MTH1 encoding 8-oxo-dGTPase for prevention of A:T to C:G transversion. Genomics 1994;24:485-90.

103. Fujikawa K, Kamiya H, Yakushiji H, Nakabeppu Y, Kasai H. Human MTH1 protein hydrolyzes the oxidized ribonucleotide, 2-hydroxy-ATP. Nucleic Acids Res 2001;29:449-54.

104. Yanofsky C, Cox EC, Horn V. The unusual mutagenic specificity of an E. Coli mutator gene. Proc Natl Acad Sci U S A 1966;55:274-81.

105. Sakumi K, Furuichi M, Tsuzuki T, et al. Cloning and expression of cDNA for a human enzyme that hydrolyzes 8-oxo-dGTP, a mutagenic substrate for DNA synthesis. J Biol Chem 1993;268:23524-30.

106. Tsuzuki T, Egashira A, Igarashi H, et al. Spontaneous tumorigenesis in mice defective in the MTH1 gene encoding 8-oxo-dGTPase. Proc Natl Acad Sci U S A 2001;98:11456-11461.

107. Zhang J, Perry G., Smith MA, et al. Parkinson's disease is associated with oxidative damage to cytoplasmic DNA and RNA in substantia nigra neurons. Am J Pathol 1999;154:1423-9.

108. Nunomura A, Perry G., Aliev G., et al. Oxidative damage is the earliest event in Alzheimer disease. J Neuropathol Exp Neurol 2001;60:759-67.

109. Kikuchi H, Furuta A, Nishioka K, Suzuki SO, Nakabeppu Y, Iwaki, T. Impairment

of mitochondrial DNA repair enzymes against accumulation of 8-oxo-guanine in the spinal motor neurons of amyotrophic lateral sclerosis. Acta Neuropathol (Berl) 2002;103:408-14.

110. Shimura-Miura H, Hattori N, Kang D, Miyako K, Nakabeppu Y, Mizuno Y. Increased 8-oxo-dGTPase in the mitochondria of substantia nigral neurons in Parkinson's disease. Ann Neurol 1999;46:920-4.
111. Furuta A, Iida T, Nakabeppu Y, Iwaki T. Expression of hMTH1 in the hippocampi of control and Alzheimer's disease. Neuroreport 2001;12:2895-9.
112. Yoshimura D Sakumi K, Ohno M, et al. An oxidized purine nucleoside triphosphatase, MTH1, suppresses cell death caused by oxidative stress. J Biol Chem 2003;278:37965-73.
113. Nakabeppu Y, Kajitani K, Sakamoto K, Yamaguchi H, Tsuchimoto D. MTH1, an oxidized purine nucleoside triphosphatase, prevents the cytotoxicity and neurotoxicity of oxidized purine nucleotides. DNA Repair (Amst) 2006;5:761-72.
114. Yamaguchi H, Kajitani K, Dan Y, et al. MTH1, an oxidized purine nucleoside triphosphatase, protects the dopamine neurons from oxidative damage in nucleic acids caused by 1-methyl-4-phenyl-1,2,3,6-tetrahydropyridine. Cell Death Differ 2006;13:551-63.
115. Dobson AW, Grishko V, LeDoux SP, Kelley MR, Wilson GL, Gillespie MN. Enhanced mtDNA repair capacity protects pulmonary artery endothelial cells from oxidant-mediated death. Am J Physiol Lung Cell Mol Physiol 2002;283:L205-10.
116. Hyun JW, Jung YC, Kim HS, et al. 8-hydroxydeoxyguanosine causes death of human leukemia cells deficient in 8-oxoguanine glycosylase 1 activity by inducing apoptosis. Mol Cancer Res 2003;1:290-9.
117. Harrison JF, Hollensworth SB, Spitz DR, Copeland WC, Wilson GL, LeDoux SP. Oxidative stress-induced apoptosis in neurons correlates with mitochondrial DNA base excision repair pathway imbalance. Nucleic Acids Res 2005;33:4660-71.

118. Lavin MF, Gueven N. The complexity of p53 stabilization and activation. Cell Death Differ 2006;13:941-50.

119. Haupt S, Berger M, Goldberg Z, Haupt Y. Apoptosis - the p53 network. J Cell Sci 2003;116:4077-85.

120. The Molecular Mechanism of Noxa-induced Mitochondrial Dysfuntion in p53-Mediated Cell Death The Journal of Biological Chemistry Vol.278,No. 48, November 28, 48292-48299, 2003

121. Apototic Signaling Pathways Induced by Nitric Oxide in Human Lymphoblastoid Cells Expressing Wild-Type or Mutant p53 Cancer research 64,3022-3029, May 1, 2004

122. Nitric Oxide Inhibition of Homocysteine-induced Human Endothelial Cell Apoptosis by Down-regulation of p53-dependent Noxa Expression through the Formation of S-Nitrosohomocysteine The Journal of Biological Chemistry Vol.280,No. 7, February18, 5781-5788, 2005)

123. Up-regulation of Bcl-2 homology 3 (BH3)-only proteins by E2F1 mediates apoptosis J Biol Cheem 2004 Mar 5;279(10):8627-34. Epub 2003 Dec 18.

124. p53-independent NOXA induction overcomes apoptotic resistance of malignant melanomas Molecular Cancer Therapeutics 895, August 2004

125. Development of New EBV-Based Vector for Stable Expression of Small interfering RNA to Mimick Human Syndromes: Application to NER Gene Dilencing Mol Cancer Res 2005; 3(9) September 2005

126. Death signal-induced location of p53 protein to mitochondria. A potential role in apoptotic signaling. J Biol Chem 275: 16202-16212

127. DNA repair, mitochondria, and neurodegeneration Neuroscience(2006))

128. Changes of 8-hydroxydeoxyguanosine levels in rat organ DNA during the aging process. J environ pathol Toxicol Oncol 11: 139-143, 1992

129. Non-linear accumulation of 8-hydrosy-2'-deoxyguanosine, a marker of oxidized DNA damage, during aging. Mutat Res 316:277-285

130. 8-hydroxyguanine levels in nuclear DNA and its repair acticity in rat organs associated with age. J Gerontol A Biol Sci Med Sci 51: B303-B307

131. Age and organ dependent spontaneous generation of nuclear 8-hydroxydeoxyguanosine in male Fischer 344 rats. Lab invest 80:249-261

132. Does oxidative damage to DNA increase with age? Proc Natl Acad Sci USA 98:10469-10474

133. Age-related base excision repair activity in mouse brain and liver nuclear extracts. J Gerontol A Biol Sci Med Sci 58:205-211.)

134. Mitochondrial and nuclear DNA-repair capacity of various brain regions in mouse is altered in an age-dependent manner. Neurobiol Aging 27: 1129-1136)

135. Oxidants, antioxidants, and the degenerative diseases of aging. Pro Natl Acad Sci USA 90:7915-7922).

136. Oxidative damage to mitochondrial DNA is inversely related to maximum life span in the heart and brain of mammals. FASEB J 14:312-318

137. ROS stress in cancer cells and therapeutic implications. Drug Resist Updat 7: 97-110

138. Nittric oxide inhibition of Homocysteine-induced Human Endothelial Cell Apotosis by Down-regulation of p53-dependent Noxa Expression through the Formation of S-Nitrosohomocysteine Journal of biological chemistry vol. 280;18 :5781-5788, 2005

139. Oxidative stress as a mediator of apoptosis. Immunol. Today 15,7-10

140. Reactive oxygen species and programmed cell death. Trends Biochem. Sci. 21, 83-86

141. A model for p53-induced apoptosis. Nature389, 300-305).

142. Nitric oxide-induced genotoxicity, mitochondrial damage, and apoptosis in human lymphoblastoid cells expressing wild-type and mutant p53 Proc Natl Acad Sci USA 2002;99: 10364-9

143. Oncogenic mutations of the p53 tumor suppressor: the demons of the guardian of the genome. Cancer Res 2000;60:6788-93

144. P53 has a direct apoptogenic role at the mitochondria Mol Cell 11 : 577-590

145. Direct activation of Bax by p53mediates mitochondrial membrane permeabilization and apoptosis. Science 303: 1010-1014

146. In vivo mitochondrial p53 translocation triggers a rapid first wave of cell death in response to DNA damage that can precede p53 target gene activation. Mol Cell Biol 24: 6728-6741

147. Fernandez-Capetillo O, Chen HT, Celeste A, et al. DNA damage-induced G2-M checkpoint activation by histone H2AX and 53BP1. Nat Cell Biol 2002;4:993-7.

148. Rogakou EP, Pilch DR, Orr AH, Ivanova VS, Bonner WM. DNA double-stranded breaks induce histone H2AX phosphorylation on serine 139. J Biol Chem 1998;273:5858-68.

149. Holzmann K, Kohlhammer H, Schwaenen C, et al. Genomic DNA-chip hybridization reveals a higher incidence of genomic amplifications in pancreatic cancer than conventional comparative genomic hybridization and leads to the identification of novel candidate genes. Cancer Res 2004;64:4428-33.

150. Clark J, Edwards S, Feber A, et al. Genome-wide screening for complete genetic

loss in prostate cancer by comparative hybridization onto cDNA microarrays. Oncogene 2003;22:1247-52.

151. Kobune M, Xu Y, Baum C, Kelley MR, Williams DA. Retrovirus-mediated expression of the base excision repair proteins, formamidopyrimidine DNA glycosylase or human oxoguanine DNA glycosylase, protects hematopoietic cells from N,N',N''-triethylenethiophosphoramide (thioTEPA)-induced toxicity in vitro and in vivo. Cancer Res 2001;61:5116-25.
152. Wu M, He YH, Kobune M, Xu Y, Kelley MR, Martin WJ. 2nd Protection of human lung cells against hyperoxia using the DNA base excision repair genes hOgg1 and Fpg. Am J Respir Crit Care Med 2002;166:192-9.
153. Kannan S, Pang H, Foster DC, Rao Z, Wu M. Human 8-oxoguanine DNA glycosylase increases resistance to hyperoxic cytotoxicity in lung epithelial cells and involvement with altered MAPK activity. Cell Death Differ 2006;13:311-23.
154. Yang N, Chaudhry MA, Wallace SS. Base excision repair by hNTH1 and hOGG1: a two edged sword in the processing of DNA damage in gamma-irradiated human cells. DNA Repair (Amst) 2006;5:43-51.
155. Sionov RV, Haupt Y. The cellular response to p53: the decision between life and death. Oncogene 1999;18:6145-57.
156. Vogelstein B, Lane D, Levine AJ. Surfing the p53 network. Nature 2000;408:307-10.
157. Chehab NH, Malikzay A, Stavridi ES, Halazonetis TD. Phosphorylation of Ser-20 mediates stabilization of human p53 in response to DNA damage. Proc Natl Acad Sci U S A 1999;96:13777-82.
158. She QB, Chen N, Dong Z. ERKs and p38 kinase phosphorylate p53 protein at serine 15 in response to UV radiation. J Biol Chem 2000;275:20444-9.
159. Oda E, Ohki R, Murasawa H, et al. Noxa, a BH3-only member of the Bcl-2 family and candidate mediator of p53-induced apoptosis. Science 2000;288:1053-8.
160. Shibue T, Takeda K, Oda E, et al. Integral role of Noxa in p53-mediated apoptotic

response. Genes Dev 2003;17:2233-8.

161. Seo YW, Shin JN, Ko KH, et al. The molecular mechanism of Noxa-induced mitochondrial dysfunction in p53-mediated cell death. J Biol Chem 2003;278:48292-9.

162. Yakovlev AG, Di Giovanni S, Wang G, Liu W, Stoica B, Faden AI. BOK and NOXA are essential mediators of p53-dependent apoptosis. J Biol Chem 2004;279:28367-74.

163. Qin JZ, Stennett L, Bacon P, et al. p53-independent NOXA induction overcomes apoptotic resistance of malignant melanomas. Mol Cancer Ther 2004;3:895-902.

164. Hershko T, Ginsberg D. Up-regulation of Bcl-2 homology 3 (BH3)-only proteins by E2F1 mediates apoptosis. J Biol Chem 2004;279:8627-34.

165. Kim JY, Ahn HJ, Ryu JH, Suk K, Park JH. BH3-only protein Noxa is a mediator of hypoxic cell death induced by hypoxia-inducible factor 1alpha. J Exp Med 2004;199:113-24.

166. Jullig M, Zhang WV, Ferreira A, Stott NS. MG132 induced apoptosis is associated with p53-independent induction of pro-apoptotic Noxa and transcriptional activity of beta-catenin. Apoptosis 2006;11:627-41.

167. Signalling apoptosis: a radical approach, Redox Rep. 6 (2) (2001) 77-90

168. Ames BN, Shigenaga MK, Hagen TM. Oxidants, antioxidants, and the degenerative diseases of aging. Proc Natl Acad Sci U S A 1993;90:7915-22.

169. Russo MT, Blasi MF, Chiera F, et al.The oxidized deoxynucleoside triphosphate pool is a significant contributor to genetic instability in mismatch repair-deficient cells. Mol Cell Biol 2004;24:465-74.

170. Anderson GR, Stoler DL, Brenner BM. Cancer: the evolved consequence of a destabilized genome. Bioessays 2001;23:1037-46.

<국문초록>

DNA 수복효소가 산화성 스트레스에 의한 세포 사멸사에 미치는 영향

윤 차 경
지도교수 : 유 호 진
조선대학교 대학원 생물신소재학과

본 연구는 8-oxoguanine DNA glycosylase(hOGG1)와 human 8-oxo-dGTPase(MutT) homologue1(hMTH1)의 발현 억제가 산화성 스트레스에 의한 세포 사멸사에 미치는 영향에 관한 것이다.

hOGG1 은 세포 내 돌연변이체인 8-oxoG 를 제거하는 효소이다. Small interfering RNA (siRNA)를 사용하여 hOGG1 의 효소 기능을 억제한 섬유아세포(fibroblast GM00637)에서는 H_2O_2 관련 세포사멸이 증가한다. 이러한 세포 사멸은 p53 과 관련된 세포 사멸사 경로(apoptotic pathway)를 통한 것이다. 또한 hOGG1 의 효소기능이 억제된 세포는 유전적 불안정성도 증가한다. 세포내 hOGG1 의 활성이 저하되더라도 p53 기능이 억제된 경우에는 같은 농도의 H_2O_2 를 처리하였어도 세포사멸(apoptosis)이 나타나지 않았다. hOGG1 의 활성이 억제된 세포에서는 H_2O_2 를 처리 하였을 때 p21, Noxa, caspase-3/7 의 활성이 증가하였지만 p53 기능을 siRNA 로 억제 하였을 때는 이러한 단백질의 활성이 증가하지 않으면서 세포 생존율이 증가하였다. p53 유전자가 발현되지 않는 세포인 H1299 에서 hOGG1 의 효소 활성을 siRNA 로 억제하고 p53 을

과발현 시켰을 때, H_2O_2에 대한 세포 생존율은 p53 이 없을 때보다 감소하였다. 섬유아세포 GM00637 에서 hOGG1 효소 활성을 증가시키면, hOGG1 이 정상적으로 발현되고 있을 때와 비교하여, 같은 농도의 H_2O_2 를 처리하였을 경우 세포 생존율이 증가하고 p53 활성이 감소하였다. 이러한 결과는 hOGG1 이 H_2O_2 가 유발하는 산화적 스트레스에 대항하여 유전적인 안정성을 증가시킴으로 p53 이 매개하는 세포사멸로부터 세포를 보호하는 역할을 함을 시사한다.

hMTH1 활성이 억제된 세포는 정상적인 세포에 비해서 H_2O_2 관련 세포사멸(apoptosis)이 증가하게 되는데, 이러한 세포사멸은 p53 단백질이 매개하는 신호전달이 활성화된 결과이다. hMTH1 활성이 억제된 세포에서는 H_2O_2 에 의한 Noxa 단백질의 발현과 H2AX 단백질의 인산화(γ-H2AX)가 증가한다. Noxa 와 p53 이 기능을 하지 못하게 되면, hMTH1 이 억제된 세포는 같은 농도의 H_2O_2 에서도 정상 세포에 비해 세포사멸이 감소한다. hMTH1 활성이 억제된 세포에서 H_2O_2 관련 세포사멸의 증가는, p53 단백질의 인산화로 인한 Noxa 단백질의 과발현에 의한 것으로 추측된다. 또한 hMTH1-siRNA 로 hMTH1 단백질의 발현을 억제시킨 세포에서 H_2O_2 에 의한 유전인자의 불안정성이 증가되는 것을 확인하였다. hMTH 의 활성이 억제된 세포를 120 일간 키웠을 때, 외부 자극 없이도 세포 내에서 발생하는 reactive oxygen species (ROS)가 증가하고 이와 동시에 p53 이 매개하는 세포사멸(apoptosis)이 진행됨을 관찰하였다. 이러한 현상은 오랜 기간 동안 세포내 DNA 손상이 복구 되지 못하고 축적된 결과로 추측된다. 이러한 연구 결과를 종합해 볼 때 hMTH1 은 H_2O_2 와 같은 산화성 스트레스에 의한 DNA 손상을 제거함으로써 유전인자의 안정성을 유지하고 세포사멸로부터 세포를 보호하는 중요한 역할을 하고 있는 것으로 사료된다.

저작물 이용 허락서

학 과	생물신소재학과	학 번	20047472	과 정	박 사
성 명	한글 : 윤 차 경 한문 : 尹 次 慶 영문 : Youn Cha-Kyung				
주 소	광주광역시 북구 두암동 408-35번지				
연락처	E-MAIL : threefold@hanmail.net				
논문제목	한글: DNA 수복효소가 산화성 스트레스에 의한 세포 사멸사에 미치는 영향 영문: The effect of DNA repair system on the oxidative stress-mediated apoptosis.				

본인이 저작한 위의 저작물에 대하여 다음과 같은 조건아래 조선대학교가 저작물을 이용할 수 있도록 허락하고 동의합니다.

- 다 음 -

1. 저작물의 DB구축 및 인터넷을 포함한 정보통신망에의 공개를 위한 저작물의 복제, 기억장치에의 저장, 전송 등을 허락함
2. 위의 목적을 위하여 필요한 범위 내에서의 편집·형식상의 변경을 허락함. 다만, 저작물의 내용변경은 금지함.
3. 배포·전송된 저작물의 영리적 목적을 위한 복제, 저장, 전송 등은 금지함.
4. 저작물에 대한 이용기간은 5년으로 하고, 기간종료 3개월 이내에 별도의 의사표시가 없을 경우에는 저작물의 이용기간을 계속 연장함.
5. 해당 저작물의 저작권을 타인에게 양도하거나 또는 출판을 허락을 하였을 경우에는 1개월 이내에 대학에 이를 통보함.
6. 조선대학교는 저작물의 이용허락 이후 해당 저작물로 인하여 발생하는 타인에 의한 권리 침해에 대하여 일체의 법적 책임을 지지 않음
7. 소속대학의 협정기관에 저작물의 제공 및 인터넷 등 정보통신망을 이용한 저작물의 전송·출력을 허락함.

동의여부 : 동의(0) 반대( )

2007년 2 월 일

저작자: 윤 차 경 (서명 또는 인)

조선대학교 총장 귀하

ACKNOWLEDGEMENTS

I am especially grateful to principal supervisor, Ho Jin You, provided for me with this especial opportunity and support. I am thankful to Prof. In-Youb Chang, Peter I. Song, Ae Ran Moon.

This study was supported by Hyun-Ju Cho, Soo-Hyun Kim, Seung Hee Song, Jin-Hee Kim, Mi-Hwa Kim, Do Yung Lee, Soo-Mi Lee , Na-Hee Kim. I am really grateful to the members of the Korean DNA Repair Research Center.

6 년 동안 공부한 결과로 이제야 박사과정을 졸업하게 되지만 배우고 공부한 것보다 앞으로 배우고 공부해야 할 것들이 더 많다는 것을 스스로에게 일깨우고 있습니다.

“ 이제 끝나냐?” 하시는 엄마께 “ 엄마! 이제 시작이야!” 라는 말과 감사의 마음을 전합니다. 엄마 사랑해!! 우리 식구들 지금까지 사람구실 잘 못했는데 앞으로 쪼금 할께요.

서로를 힘들게도 하고, 서로 위로도 하면서 지내왔던 KDRRC 실험실 식구들에게 감사 드리며, 여기서 끝이 아니기에 앞으로도 즐거운 생활을 함께 했으면 합니다.

힘든 생활에 위로가 되어준 효진, 수연, 명섭, 영철, 지연, 선아, 경희, 영화…이름을 다 적을 수 없는 친구들 탱큐 베리 감사!! 애경언니 집에 꼭 놀러 갈께요!! 고마워요!

사랑하는 사람!! 고마워!!

윤 차 경